High Temperature Proton Conducting Materials and Fluorescent-Labeled Polymers for Sensor Applications

HIGH TEMPERATURE PROTON CONDUCTING MATERIALS AND FLUORESCENT-LABELED POLYMERS FOR SENSOR APPLICATIONS

A Dissertation Presented

by

SURANGKHANA MARTWISET

Submitted to the Graduate School of the
University of Massachusetts Amherst in partial fulfillment
of the requirements for the degree of

DOCTOR OF PHILOSOPHY

September 2009

Polymer Science and Engineering

HIGH TEMPERATURE PROTON CONDUCTING MATERIALS AND FLUORESCENT-LABELED POLYMERS FOR SENSOR APPLICATIONS

A Dissertation Presented

by

SURANGKHANA MARTWISET

Approved as to style and content by:

_____

E. Bryan Coughlin, Chair

_____

Todd Emrick, Member

_____

Mark T. Tuominen, Member

_____

Shaw Ling Hsu, Department Head
Polymer Science and Engineering

DEDICATION

To my beloved parents and sister

ACKNOWLEDGEMENTS

I would like to thank Prof. Bryan Coughlin for giving me the guidance over the past 5 years. Thanks for being patient, listening, and allowing me to work on several areas of interest. The assistance in my career preparation is also very much appreciated. I would like to extend my gratitude to Prof. Mark Tuominen for insightful discussions on the fuel cell project. Thanks to Prof. Todd Emrick for participating as a committee member and providing invaluable suggestions.

I also would like to thank all of my collaborators. As a polymer chemist, working with Prof. Maria Santore, Prof. Jeffrey Davis and their groups on the sensor project taught me to view problems from a different angle. It has also been my privilege to work with the fuel cell team, Sergio, Rich, Makoto, Shilpi, Ozgur, Xinyu, Mike, Craig and Chandra. I just cannot thank you all enough for the help and efforts. I also appreciate the help with press-molding and a mechanical study by Deepak, Naveen and Kate. I am grateful for all the instrumental help from Dr. Stephen Eyles, Dr. Weiguo Hu and John Domian.

Thanks to past and present Coughlin group members. Special thanks to Gregoire for showing me the necessary synthetic skills when I first joined the group. Thanks to Gunjan for a friendship and thoughtful comments on various projects. Thanks to Ranga and Bon-cheol for cheering me up on bad days in the lab. I also want to thank Chris for proof reading many of my writings. It has always been fun being around Tarik, Jen, Nui, Brad, Yoan, Justin, Liz, Kathy and Tsung Han.

Thanks to all PSE faculty members and staffs for transferring the knowledge and keeping things running smooth. I also would like to thank Prof. Donald Cotter for giving me an opportunity to do research when I was at Mount Holyoke College. Thanks to Prof. Wei Chen for introducing me to polymers and PSE. Thanks for the encouragement and the assistance throughout the years. A financial support for the undergraduate and graduate work from the Royal Thai Government is gratefully acknowledged.

Last but not least, I would like to thank my family and friends. This accomplishment wouldn't be possible without your love and support.

ABSTRACT

HIGH TEMPERATURE PROTON CONDUCTING MATERIALS,
AND FLUORESCENT-LABELED POLYMERS FOR SENSOR APPLICATIONS

September 2009

SURANGKHANA MARTWISET, B.A., MOUNT HOLYOKE COLLEGE

M.S., UNIVERSITY OF MASSACHUSETTS AMHERST

Ph.D., UNIVERSITY OF MASSACHUSETTS AMHERST

Directed by: Professor E. Bryan Coughlin

The majority of this dissertation focuses on proton conducting materials that could be used at high operating temperatures. Higher operating temperatures are desirable as they will increase fuel cell efficiency, reduce cost, and simplify the heat management system. The factors governing proton conduction including segmental mobility, protogenic group identity, and charge carrier density were investigated on a variety of polymers containing 1*H*-1,2,3-triazole moieties. Proton conductivity measurements were made using AC impedance spectroscopy. Random copolymers and terpolymers of triazole-containing acrylates and poly(ethylene glycol)methyl ether acrylate (PEGMEA) have been synthesized. Conductivity increased with increasing degree of PEG incorporation until reaching a maximum at 30% mole PEGMEA. In comparison to benzimidazole-functionalized polyacrylate with 35% mole PEGMEA, the triazole analog showed a higher proton conductivity, and a less pronounced conductivity temperature dependence. Further increases in conductivity was achieved through the addition of trifluoroacetic acid. To study the effect of charge carrier density on proton conduction,

polyacrylates containing a different number of triazole groups per repeat unit were synthesized. The result showed that introduction of more than one triazole per repeat unit did not result in an increase in conductivity as there was an accompanying increase in T_g. To improve the thermal and mechanical properties, triazole groups were tethered to a higher T_g backbone polymer, polynorbornene. Introduction of polyhedral oligomeric silsesquioxane (POSS) into triazole-functionalized polynorbornene was also investigated.

In a parallel set of investigations, poly(2-(dimethylamino)ethyl methacrylate), PDMAEMA, and copolymers of DMAEMA and methyl methacrylate (PDMAEMA-co-PMMA) were synthesized via atom transfer radical polymerization (ATRP). Fluorescently-labeled PDMAEMAs were synthesized using fluorescent ATRP initiators to ensure the presence of one dye molecule on every polymer chain. PDMAEMAs and PDMAEMA-co-PMMA with different molecular weights have been deposited onto a negatively-charged silica surface via controlled flow deposition. The results show that the polymer deposition rate depends on molecular weight, and is inversely proportional to molecular weight. A preliminary adhesion study of 1-μm negatively charged silica spheres onto these functionalized surfaces indicates that by varying the molecular weight, the adhesion threshold can be changed. System modeling is being conducted to support experimental observations.

TABLE OF CONTENTS

LIST OF TABLES

LIST OF FIGURES

LIST OF SCHEMES

LIST OF ABBREVIATIONS

AFC	Alkaline fuel cells
AFM	Atomic force microscopy
AIBN	2,2′-Azobis(2-methylpropionitrile)
AMBIB	9-Anthracenemethyl-2-bromoisobutyrate
AMP	Azidomethyl pivalate
ATR	Attenuated total reflectance
ATRP	Atom transfer radical polymerization
CD_3OD	Methanol-d_4
$CDCl_3$	Chloroform-*d*
CuBr	Copper(I) bromide
$CuSO_4.5H_2O$	Copper(II) sulfate
Da	Daltons
DCC	*N,N′*-Dicyclohexylcarbodiimide
DCM	Dichloromethane
DMA	Dynamic mechanical analysis
DMAC	Dimethylacetamide
DMAP	4-(Dimethylamino)pyridine
DMF	Dimethylformamide
DMFC	Direct methanol fuel cells
DMSO	Dimethyl sulfoxide
DMSO-d_6	Dimethyl sulfoxide-d_6

DNA	Deoxyribonucleic acid
DSC	Differential scanning calorimetry
EI-HRMS	Electron impact high resolution mass spectrometry
EtOAc	Ethyl acetate
EW	Equivalent weight
FAB-HRMS	Fast atom bombardment high resolution mass spectrometry
FTIR	Fourier transform infrared
GPC	Gel permeation chromatograhpy
HMTETA	1,1,4,7,10,10-Hexamethyltriethylenetetramine
HPA	Heteropolyacid
MCFC	Molten carbonate fuel cells
NaH	Sodium hydride
NaOH	Sodium hydroxide
NB-POSS	NorbornenylethylIsobutyl POSS®
NMR	Nuclear magnetic resonance
p-TsCl	*p*-Toluenesulfonyl chloride
PAFC	Phosphoric acid fuel cells
PCR	Polymerase chain reaction
PDI	Polydispersity index
PDMAEMA	Poly(2-(dimethylamino)ethyl methacrylate)
PEEK	Poly(arylene ether ether ketone)
PEGME	Poly(ethylene glycol)methyl ether
PEGMEA	Poly(ethylene glycol)methyl ether acrylate

PEMFC	Polymer electrolyte membrane fuel cells
PEMs	Polyelectrolyte membranes
PEO	Poly(ethylene oxide)
PMMA	Poly(methyl methacrylate)
POM	Polyoxometalates
POM	Pivaloyloxymethyl
POSS	Polyhedral oligomeric silsesquioxane
PS	Polystyrene
PSS	Polystyrene sulfonic acid
PWA	Phosphotungstic acid
SANS	Small-angle neutron scattering
SAXS	Small-angle X-ray scattering
SEBS	Styrene-ethylene-butylene-styrene
SOFC	Solid oxide fuel cells
T	Temperature
t-BuOH	*t*-Butanol
TEA	Triethylamine
TFA	Trifluoroacetic acid
TFE	Tetrafluoroethylene
T_g	Glass transition temperature
TGA	Thermogravimetric analysis
TIRF	Total internal reflectance fluorescence
UV-Vis	Ultra-violet-visible spectroscopy

VTF	Vogel-Tamman-Fulcher
WAXD	Wide-angle X-ray diffraction

CHAPTER 1

INTRODUCTION

1.1 Fuel cells

The decreasing supply of fossil fuels and the increase in greenhouse gas emissions have led to a large number of investigations into the development of alternative, environmental friendly sources of energy in the last few years. Some of the most promising and reliable sources of alternative energy are fuel cells. Fuel cells convert chemical energy into electrical energy. Fuel cells consist of an anode, a cathode, and an electrolyte between the electrodes. Unlike batteries, the fuel and oxidant are supplied from an external source. Fuel cells can also have parts to feed the device with reactants as well as a battery to supply energy for start-up.[1] Fuel cells are not electrically recharged, rather the tank is refilled with fuel after use. Hydrogen gas has been considered as the fuel of choice as water is generated as the exhaust product. Other fuels can be converted to hydrogen for use in a fuel cell.

There are several varieties of fuel cells, which are classified by the type of electrolyte they contain. The six major types are alkaline fuel cells (AFC), polymer electrolyte membrane fuel cells (PEMFC), direct methanol fuel cells (DMFC), phosphoric acid fuel cells (PAFC), molten carbonate fuel cells (MCFC), and solid oxide fuel cells (SOFC). Table 1.1 summarizes the typical characteristics of these various fuel cell systems. Fuel cells can be used as highly efficient and non-polluting power sources. In addition, they are quiet and safe in operation with low levels of maintenance required.

Table 1.1. Fuel cell characteristics.[1]

Type	Anode feed	Cathode feed	Electrolyte	Operating temp.
AFC	H_2	O_2 or air	aq. KOH	ambient-90 °C
PEMFC	H_2	O_2 or air	acidic polymer	ambient-90 °C
DMFC	methanol or methanol-water	O_2 or air	acidic polymer	60-90 °C
PAFC	H_2	O_2 or air	phosphoric acid	200 °C
MCFC	H_2 or natural gas	O_2 or air	molten Li_2CO_3	550 °C
SOFC	gasoline or natural gas	O_2 or air	stabilized yttria	900 °C

1.2 PEMFCs

In a typical PEMFC, the electrodes are formed as a thin layer on each side of a proton-conducting membrane typically consisting of a copolymer of tetrafluoroethylene and a fluorinated monomer with a pendant sulfonic acid group. Hydration of the membrane leads to dissociation and solvation of the proton from the sulfonic acid groups on the polymer. The solvated protons are mobile within the polymer matrix and provide electrolyte conductivity. A good polyelectrolyte membrane should have low permeability to oxygen and hydrogen (to prevent crossover) for high coulombic efficiency. A common configuration for a PEMFC is shown in Figure 1.1. At the anode, H_2 is catalytically dissociated into H^+ and electrons. While electrons travel from anode to cathode, producing an electrical current, protons (or solvated hydronium ions) diffuse through a polymer electrolyte membrane. At the cathode, water is formed from a combination of $2H^+$ and $2e^-$, and half a mole of oxygen obtained from air.

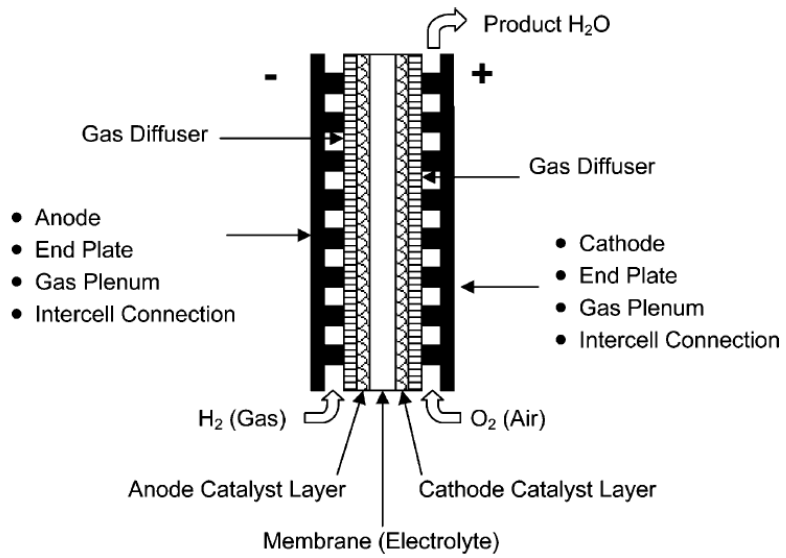

Figure 1.1. Schematic of a PEMFC (image from Ref.1).

The PEMFC is an attractive power source for vehicles and portable electronic devices due to its high power density and relatively low operating temperature. Other advantages of PEMFCs over other types of fuel cells are their nonvolatile electrolytes and efficient energy conversion. In order to obtain high performance, the polymer electrolyte membrane should have high proton conductivity, low electron conductivity, low permeability to fuel and oxidant, low water transport, oxidative stability, hydrolytic stability, good mechanical properties, low cost, and the capability for easy fabrication. The current conductivity goal for proton conducting membranes set by the U.S. Department of Energy is 0.1 S/cm at 120 ºC and 50% relative humidity.[2]

1.2.1 Hydrated operating condition

1.2.1.1 Nafion and other poly(perfluorosulfonic acid) membranes

The current polyelectrolyte membranes (PEMs) used are generally based on hydrated sulfonated polymers. Among these, perfluorosulfonic acid membranes, such as

Nafion®, have drawn much interest because of their chemical and electrochemical stability. Nafion was developed in the late 1960s by Dupont (structure shown in Figure 1.2). Nafion is prepared by the free radical initiated copolymerization of tetrafluoroethylene (TFE) and a perfluorovinyl ether containing a sulfonyl fluoride. There are three common types of Nafion, 112, 115, and 117. The designation 117 refers to a film having 1100 equivalent weight (EW), the number of grams of dry Nafion per mole of sulfonic acid groups when the material is in the acid form, and a thickness of 0.007 in. The molecular weight of these polymers with high EW cannot be determined by common methods such as light scattering and gel permeation chromatography as they do not form true solutions. The only molecular weight range mentioned in the literature is between 10^5 and 10^6 Da.[3] Similar perfluorinated ionomers have been developed by the Asahi Chemical Company (Aciplex®), the Asahi Glass Company (Flemion®), and Dow Chemical Company. These structures are also shown in Figure 1.2.

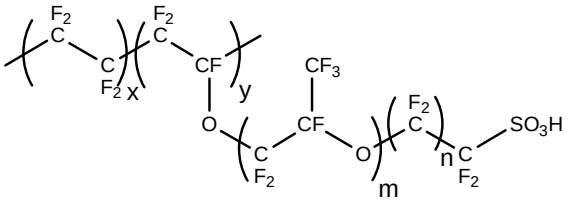

Nafion®: m≥1, n=2, x=5-13.5, y=1000
Aciplex® : m=0-3, n=2-5, x=1.5-14
Flemion® : m=0 or 1, n=1-5
Dow Mem : m=0, n=2, x=3.6-10, y=1000

Figure 1.2. Structures of commercially available poly(perfluorosulfonic acid).

The proton transport of hydrated Nafion is dominated by a vehicular mechanism, where protons diffuse through the material. The morphology of Nafion is not well defined due to the random structure and the organization of the crystalline and ionic domains of the copolymer. A number of studies using small-angle X-ray scattering (SAXS), wide-angle X-ray diffraction (WAXD),[4-8] small-angle neutron scattering

(SANS),[9, 10] and atomic force microscopy (AFM) have been conducted to develop an understanding of the morphology of Nafion. Gierke *et al.* proposed a model based on SAXS observations hypothesizing that clusters of sulfonate groups are organized as inverted micelles, connected by 1-nm-diameter channels (Figure 1.3, left).[3-5, 11] Although this model is the most popular, the presence of elongated structures was reported from the SAXS studies by a number of other groups.[12-14] Recently, Schmidt-Rohr and Chen proposed a new structure of the Nafion ionomer (Figure 1.3, right). Using a new calculation method on previously reported SAXS data, they suggested that hydrated Nafion consists of long parallel water channels in cylindrical inverted micelles.[15] The water channels are packed randomly, surrounded by the ionic side groups with the polymer backbones on the outside.

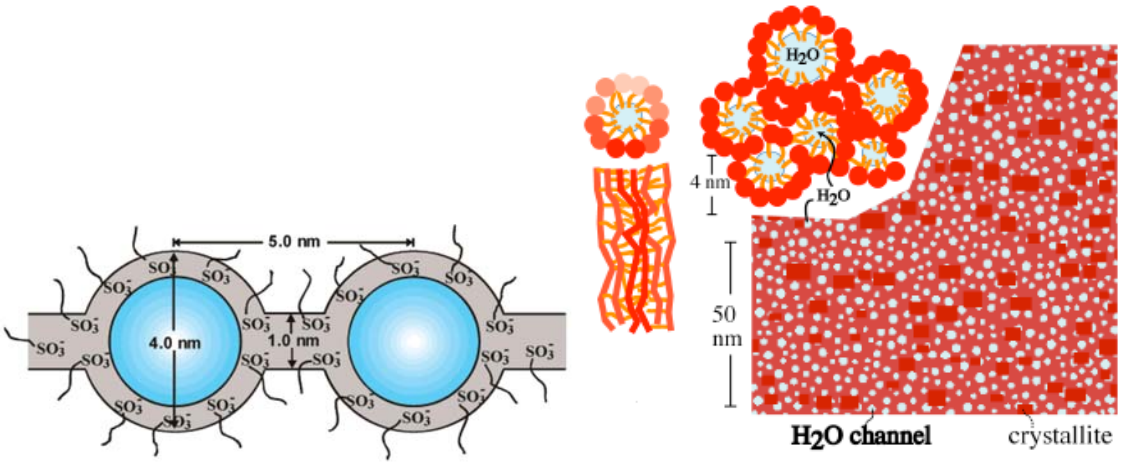

Figure 1.3. Gierke's model (left, image from Ref.11), and Schmidt-Rohr's model (right, image from Ref.15) of hydrated Nafion.

1.2.1.2 Sulfonated hydrocarbon polymers

Due to the cost of perfluoroether comonomers and the safety concerns of tetrafluoroethylene in the synthesis of poly(perfluorosulfonic acids),[2] a variety of alternative sulfonated hydrocarbon polymers have been reported.[16-19] Two commercially

available styrene-based polymers are BAM® from Ballard Advanced Materials Corporation, and sulfonated styrene-ethylene-butylene-styrene (SEBS) membrane from Dais Analytic (Figure 1.4). The main drawback of SEBS is the poor oxidative stability due to its aliphatic character.[20] Poly(arylene ether) materials such as poly(arylene ether ether ketone) (PEEK), poly(arylene ether sulfone), and their derivatives have been widely studied due to their availability and oxidative and hydrolytic stabilities. Introduction of sulfonic groups to the polymers have been conducted by both post-polymerization modification, using concentrated sulfuric acid, fuming sulfuric acid, chlorosulfonic acid,[21] or sulfur trioxide,[22] and direct copolymerization of sulfonated monomers.[23] Sulfonated five-and six-membered ring polyimides have also been investigated. The naphthalenic polyimides are more stable than the phthalic polyimides, which undergo hydrolysis, in a fuel cell environment.[24] Other high performance polymeric backbones that have been investigated include poly(phenylquinoxaline),[25] poly(2,6-dimethyl-1,4-phenylene oxide),[26] poly(4-phenoxybenzoyl-1,4-phenylene),[27] poly(phthalazinone ether ketone),[28] and polyphosphazene.[29, 30]

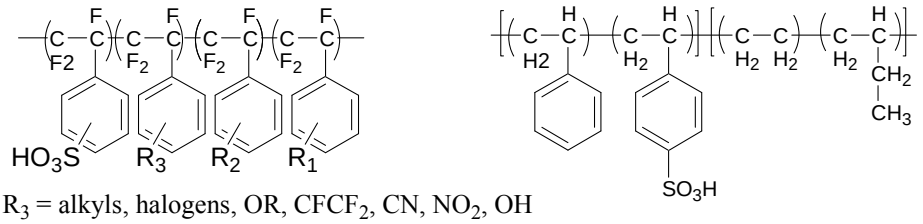

R_1, R_2, R_3 = alkyls, halogens, OR, $CFCF_2$, CN, NO_2, OH

Figure 1.4. Chemical structures of BAM (left) and SEBS (right).

Kreuer *et al.* has compared the hydrated structure of sulfonated poly(ether ketone) to that of Nafion.[31] Sufonated poly(ether ketone) was described as having narrower

channels, more branches with dead ends, larger inter-sulfonate group separation, and more hydrophobic-hydrophilic interface area than Nafion (Figure 1.5). These differences could be attributed to the less hydrophobic backbone, the lower acidity of the sulfonic acid group ($pK_a \sim -1$ vs. $pK_a \sim -6$), and the less flexible backbone of sulfonated poly(ether ketone).

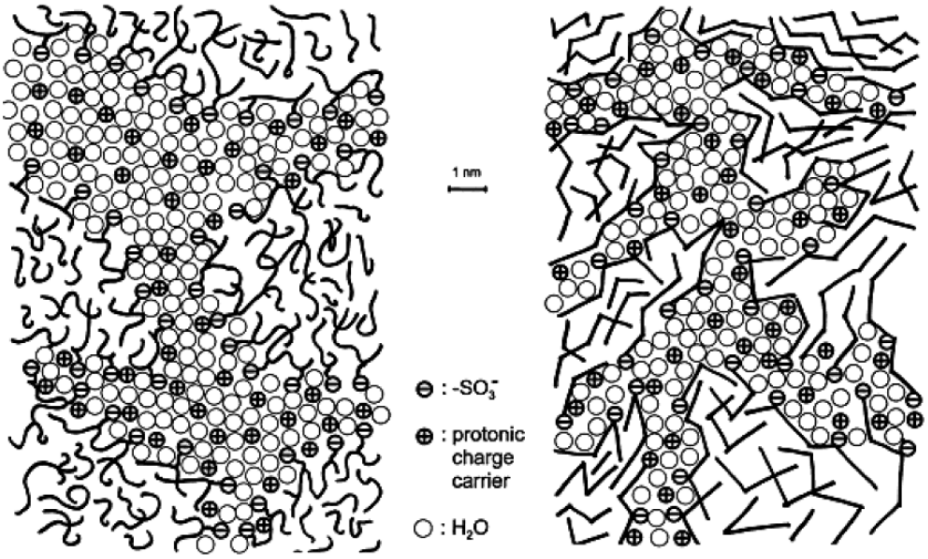

Nafion	**Sulfonated poly(ether ketone)**
wide channels	narrow channels
more separated	less separated
less branched	highly branched
good connectivity	dead-end channels
small sulfonate group separation	large sulfonate group separation
pKa ~ -6	pKa ~ -1

Figure 1.5. Hydrated structures of Nafion and sulfonated poly(ether ketone) (image from Ref. 31).

1.2.1.3 Other proton conducting moieties

Phosphonic acid has been reported as an alternative proton conducting moiety. Although phosphonic acid containing polymers are more chemically and thermally stable relative to sulfonic acid containing polymers,[32] they are not well studied due to limited

synthetic procedures. Based on a study on model oligomeric compounds containing phosphonic acid and sulfonic acid as protogenic groups, the phosphonic acid-tethered oligomer showed a higher proton conductivity at intermediate temperatures under low humidity.[33] The good proton donor and accepter properties, and the high dielectric constant of phosphonic acid lead to high degrees of self-dissociation and high proton conductivity. Phosphonic acid groups have also been tethered to several polymeric backbones including poly(arylene ether),[32, 34, 35] poly(phosphazene),[36] poly(vinylbenzyl chloride),[37] and oligosiloxane.[38]

Heteropolyacids (HPAs) are the most attractive inorganic modifiers in sulfonated polymer composites, because these inorganic materials have been demonstrated to be highly conductive and thermally stable. They can also be dissolved in polar solvents such as dimethylformamide (DMF), dimethylacetamide (DMAC), etc.[39] The heteropolyacid $H_3PW_{12}O_{40}$ (12-phosphotungstic acid, PWA) is a Keggin-type ion. Its primary structure, as shown in Figure 1.6, is characterized by units in which a central phosphorus atom, in a tetrahedral coordination environment, is surrounded by 12 edge-sharing metal-oxygen octahedral (WO_6). The negative charge of this structure is neutralized in the acidic form by three protons.[40] HPAs are known to have different hydrated structures that depend on their environment,[41] and the proton conductivity of these structures is very different. For example, proton conductivity of phosphotungstic acid (PWA) decreases from 1.8×10^{-2} S/cm to 6×10^{-5} S/cm when the number of hydrated water molecules decreases from 29 to 6.

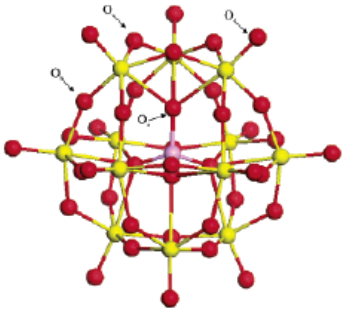

Figure 1.6. Structure of phosphotungstic acid (image from Ref. 41).

1.2.2 Anhydrous operating condition

One of the main hurdles for the widespread utilization of PEMFC power sources is the need for better performing and more cost effective membranes.[42-44] Most current research efforts have focused on systems relying on water as the media for proton transport. This limits the operating temperature to ~100 °C.[2, 43, 44] However, there are many advantages in developing PEMFC's capable of operating at temperatures close to 200 °C. Operating at such temperatures increases the efficiency of the fuel cell by increasing the kinetics of the redox reaction, and by improving the tolerance of the system for CO, which is present in hydrogen fuel refined from hydrocarbons. Running the cell at high temperatures will also reduce the overall cost by decreasing the platinum loading required in the electrodes, as well as simplify the overall heat management of the device.[45]

1.2.2.1 Phosphotungstic acid and phosphoric acid

The proton conduction of PWA at high temperature under anhydrous conditions was first reported by Yamada *et al*.[40] A composite material of PWA and polystyrene

sulfonic acid (PSS) showed a proton conductivity of 1 x 10^{-2} S/cm at 180 ºC. The proposed proton conducting mechanism of the PWA-encapsulated material is shown in Figure 1.7. Proton conduction starts at the interface between PWA and PSS, which are a Bronsted acid and base, respectively. The jump of protons from PWA to $–SO_3H$ in PSS form the protonated sulfonic groups. The transport of proton can then occur from the protonated to the nonprotonated sulfonic acid group in PSS. Recently, a heteropolyacid liquid salt, produced by the partially replacement of protons with polyethylene glycol containing quaternary ammonium cation showed proton conductivity 4 orders of magnitude higher than that of its solid analog under anhydrous condition.[46] The smaller, more mobile protons, compared to the bulky polyoxometalates (POM) clusters and quaternary ammonium counteractions, were postulated to account for the increase in conductivity.

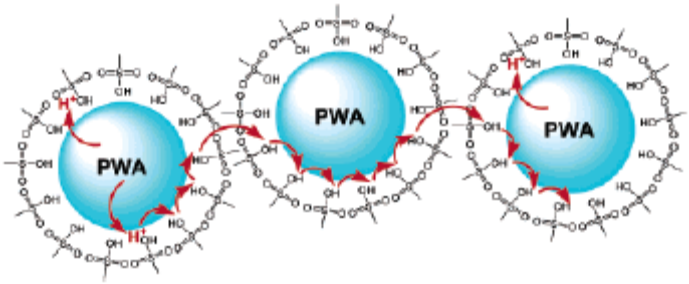

Figure 1.7. Proton conduction of PWA-encapsulated material (image from Ref. 40).

Besides heteropolyacids, there have been a few reports of proton conducting systems capable of operating efficiently at temperatures above 100 °C. For example, phosphoric acid has been blended with a variety or polymers including polyethylene glycol,[47, 48] poly(ethylenimine),[49, 50] Nylon,[51] and polybenzimidazole.[16, 52, 53] Although these phosphoric acid-based membranes show promising conductivities, their drawbacks

include the lack of stability, the inhomogeneity, and the loss of acid from the polymer membranes due to leaching.

1.2.2.1 Heterocycles

An attractive alternative approach, using amphoteric nitrogen containing heterocycles as the proton conducting species, has been proposed by Kreuer.[54, 55] As amphoteric nitrogen-based heterocycles, such as imidazole, pyrazole and benzimidazole, showed dynamic hydrogen bonding and proton transport mechanisms similar to water,[56, 57] they were studied as proton solvents in PEMFCs.[58, 59]

1.2.2.1.1 Tethering to oligomers

Although these heterocycles have been shown to provide comparable proton conductivities to that of hydrated polymers, they will gradually leach out of the membrane, resulting in a continuous decrease in proton conductivity. To overcome this problem, the heterocycles have been immobilized as oligomers and polymers. Immobilization of the heterocycles limits the translational motion of the rings; therefore, proton transport relies solely on a structure diffusion mechanism, where protons are transferred via the formation and breaking of hydrogen bonds between heterocycles (Figure 1.8).[57, 60] This proton hopping process is also known as the Grotthuss mechanism.[61, 62]

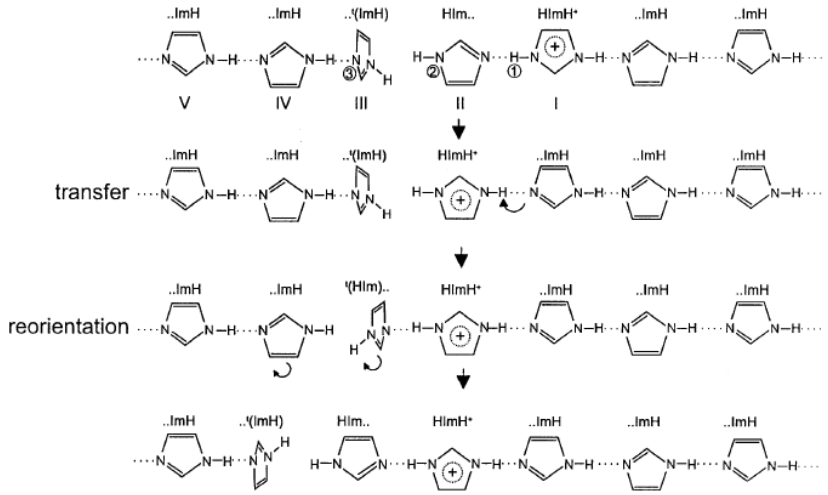

Figure 1.8. Complex network of hydrogen bonds (image from Ref. 57).

Previously reported oligomers with pendant heterocycles are listed in Table 1.2. Persson *et al*. have studied benzimidazole-tethered ethylene oxide oligomers.[63] The conductivity of the oligomer with a long tether length (Bimi-10EO, n=10) was higher than that of a short one (Bimi-2EO, n=2) in the temperature range studied, very likely because of the larger amorphous content, and higher segmental mobility of the long tether length oligomer. Imidazole-terminated ethylene oxide oligomers have also been studied by Schuster *et al.*[64, 65] At high temperature, the conductivity of the oligomers Imi-2/3/5 increases with decreasing tether length. However, the trend reverses at lower temperatures. Tether length reduction results in increased T_g, and the conductivity displays an increase in temperature dependence. Although Imi-5/2 has almost identical density to that of imidazole and free volume compared to Imi-5, the conductivity of Imi-5/2 increases by 0.5 order of magnitude. In imidazole containing materials, T_g is thought to be more influential on proton conductivity than the density of imidazole moieties. Imidazole tethered cyclic siloxanes have also been reported.[66] The highest conductivity in

these materials was observed in a structure with the longest tether length and the lowest T_g.

Table 1.2. Oligomers containing heterocycles and proton conductivities.

Structure	Nomenclature	T_g	Log σ(S/cm)[a]		Ref.
		(°C)	10 °C	100 °C	
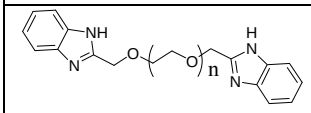	Bimi-2EO (n=2) Bimi-10EO (n=10)	- -30	-11.7 -8.3	-7.5 -4.3	63
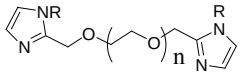	R= H Imi-2 (n=2) Imi-3 (n=3) Imi-5 (n=5) R= CH_3 MeImi-2 (n=2)	 -8 -14 -24 -48	 -9.1 -8.3 -8.0 -6.9	 -4.4 -4.7 -5.1 -5.5	64, 65
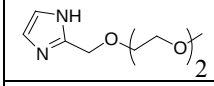	Imi-5/2	-67	-5.5	-4.4	65
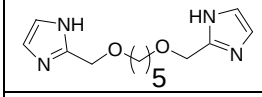	Imi-C2	-5	NA	-4.2	65
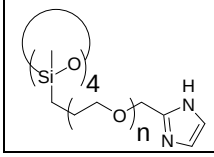	CimSs (n=1) CimSl (n=2)	9 -1	-11.0 -8.6	-4.5 -3.9	66

[a] Conductivities in numbers were obtained from reported plots. NA = not available

1.2.2.1.2 Tethering to polymers

Further studies using benzimidazole and imidazole as the proton conducting groups in polymeric systems have revealed that proton conductivity depends on the local mobility of the heterocycles and the effective concentration of mobile protons within the polymer matrix. Persson *et al.* have reported ABA triblock copolymers having a

poly(ethylene oxide) (PEO) backbone with benzimidazole-tethered end blocks.[67] The proton conductivity was found to be favored by both a high segmental mobility and a high benzimidazole content. The same research group also reported the proton conductivity of comb-like poly(styrene-*g*-PEO) with benzimidazole pendant groups.[68] This work also confirmed the importance of a high segmental mobility. A maximum conductivity of 6.6 μS/cm was reached at 160 °C under anhydrous conditions. Similarly, imidazole has also been tethered to a number polymeric backbones. The highest proton conductivity was observed for a low T_g polysiloxane with the longest tether.[66] In addition, imidazole tethered to polystyrene by alkyl lengths was reported by Herz and coworkers.[69] At low temperatures, polystyrene with a shorter spacer length and a lower T_g showed the highest conductivity, while the conductivity at high temperatures was highest in the polymer with a longer spacer length. These observations again point out two predominant factors, segmental mobility and charge carrier density, which govern the overall proton conduction. To further increase the conductivity, the mobile proton concentration is increased by adding varying amounts of acid to protonate the heterocyclic nitrogens has also been investigated.[16, 65]

Liu and coworkers have observed a pronounced increase in the conductivity of vinyl heterocycle polymers when the heterocyclic group is changed from imidazole to triazole.[70] This is thought to be attributed to both a reduction in the pK_a of the ring and to reduced conformational changes needed for conduction in triazoles relative to imidazoles.[71] A recent report by Subbaraman *et al.* further supports the importance of proton affinity (pK_a) in facilitating proton conduction in amphoteric heterocyclic systems.[72] The validity of the report on the conductivity of polyvinyl triazole has recently

been called into question. An approximately 4 orders of magnitude drop in conductivity was observed by our group. In our results, polyvinyl triazole and polyvinyl imidazole display similar conductivities.[73] However, 1,2,3-triazole is still preferred as a protogenic group because of its better electrochemical stability relative to imidazole.

1.2.3 Click chemistry

In addition to the electrochemical stability of triazole, the ease of synthesis through the copper catalyzed alkyne-azide coupling, click chemistry, makes triazole attractive. Click chemistry was introduced by K. B. Sharpless in 2001. The term "click chemistry" is defined as a reaction that is "modular, wide in scope, give very high yields, generates only inoffensive byproducts that can be removed by nonchromatographic methods, and be stereospecific."[74] Examples of this reaction include cycloadditions of unsaturated species, nucleophilic substitution chemistry, carbonyl chemistry of the non-aldol type, and additions to carbon-carbon multiple bonds. Among those, the Huisgen 1,3-dipolar cycloaddition of alkynes to azides to form 1,4-disubstituted 1,2,3-triazoles is often referred to simply as the *Click* reaction (Scheme 1.1). The copper(I)-catalyzed reaction is mild and very efficient, requiring no protecting groups, and requiring no purification in many cases.[75]

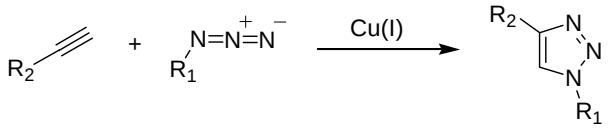

Scheme 1.1. Huisgen 1,3-dipolar cycloaddition.

Himo *et al*. proposed a mechanism of Huisgen 1,3-cycloaddition based on experimental and computational observations of the reaction of methyl azide and propyne, among others.[76] As shown in Scheme 1.2, the catalytic cycle starts with the coordination of the alkyne **1.1** to the Cu(I) species to yield acetylide **1.2**. The azide then replaces one of the ligands and binds to the copper atom, forming intermediate **1.3**, following the attack of the distal nitrogen to the C-2 carbon of the acetylide. As the barrier of ring contraction of the six-membered copper(III) metallacycle **1.4** is very low, **1.5** is formed. Finally, the triazole product is obtained from proteolysis of **1.5**.

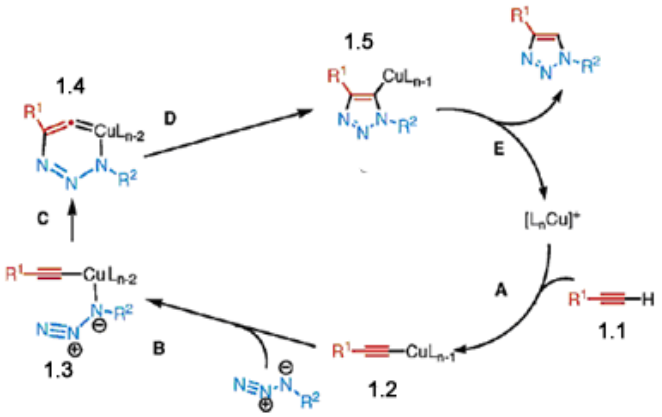

Scheme 1.2. Proposed click reaction mechanism (image from Ref. 76).

1.3 Outline of the dissertation

This thesis will focus on determining and understanding the factors governing proton transport in heterocyclic proton conducting systems, which include protogenic group identity, mobility and charge carrier density. In Chapter 2, the effect of segmental mobility is studied. Polyacrylates with tethered 1,2,3-triazole motifs and varying degrees of poly(ethylene glycol)methyl ether acrylate (PEGMEA) incorporation, to tune the glass transition temperature, are investigated. The obtained polymers are then compared with

the benzimidazole analogs. Doping the 1,2,3-triazole-based polymers with a strong acid is also explored. Chapter 3 studies the effect of charge carrier density on proton conductivity by introducing multiple triazoles per repeat unit. A membrane with good thermal and mechanical properties is introduced in Chapter 4, through the use of polynorbornenes and hybrid organic-inorganic materials containing triazole pendants. Chapter 5 summarizes the projects and outlines possible extensions.

In a parallel set of investigations, Chapter 6 studies the effect of patchy size of polycations, and the effect of charge density on the adhesion of 1 μm silica particles . Poly(2-(dimethylamino)ethyl methacrylate), PDMAEMA, and copolymers of DMAEMA and methyl methacrylate (PDMAEMA-co-PMMA) are synthesized via atom transfer radical polymerization (ATRP), and deposited onto a negatively-charged silica surface to provide patchy surfaces. Preliminary results from the adhesion study are discussed.

1.4 References

1. Whittingham, M. S.; Savinell, R. F.; Zawodzinski, T. *Chemical Reviews* **2004,** 104, (10), 4243-4244.

2. Hickner, M. A.; Ghassemi, H.; Kim, Y. S.; Einsla, B. R.; McGrath, J. E. *Chemical Reviews* **2004,** 104, (10), 4587-4611.

3. Mauritz, K. A.; Moore, R. B. *Chemical Reviews* **2004,** 104, (10), 4535-4585.

4. Hsu, W. Y.; Gierke, T. D. *Journal of Membrane Science* **1983,** 13, (3), 307-326.

5. Gierke, T. D.; Munn, G. E.; Wilson, F. C. *Journal of Polymer Science, Part B: Polymer Physics* **1981,** 19, (11), 1687-1704.

6. Hsu, W. Y.; Gierke, T. D. *Macromolecules* **1982,** 15, (1), 101-105.

7. Gierke, T. D.; Munn, G. E.; Wilson, F. C. *ACS Symposium Series* **1982,** 180, 195-216.

8. Fujimura, M.; Hashimoto, T.; Kawai, H. *Macromolecules* **1981,** 14, (5), 1309-1315.

9. Roche, E. J.; Pineri, M.; Duplessix, R.; Levelut, A. M. *Journal of Polymer Science, Part B: Polymer Physics* **1981,** 19, (1), 1-11.

10. Roche, E. J.; Pineri, M.; Duplessix, R. *Journal of Polymer Science, Part B: Polymer Physics* **1982,** 20, (1), 107-116.

11. Gierke, T. D.; Hsu, W. Y. *ACS Symposium Series* **1982,** 180, 283-307.

12. Londono, J. D.; Davidson, R. V.; Mazur, S. *Abstracts of Papers of the American Chemical Society* **2001,** 222, 14-PMSE.

13. Van der Heijden, P. C.; Rubatat, L.; Diat, O. *Macromolecules* **2004,** 37, (14), 5327-5336.

14. Page, K. A.; Landis, F. A.; Phillips, A. K.; Moore, R. B. *Macromolecules* **2006,** 39, (11), 3939-3946.

15. Schmidt-Rohr, K.; Chen, Q. *Nature Materials* **2008,** 7, (1), 75-83.

16. Wei, J.; Stone, C.; Steck, A. E., of Ballard Power Systems, Inc., June 6, 1995; U.S. Patent 5,422,411.

17. Serpico, J. M.; Ehrenberg, S. G.; Fontanella, J. J.; Jiao, X.; Perahia, D.; McGrady, K. A.; Sanders, E. H.; Kellogg, G. E.; Wnek, G. E. *Macromolecules* **2002,** 35, (15), 5916-5921.

18. Ding, J. F.; Chuy, C.; Holdcroft, S. *Chemistry of Materials* **2001,** 13, (7), 2231-2233.

19. Chuy, C.; Ding, J. F.; Swanson, E.; Holdcroft, S.; Horsfall, J.; Lovell, K. V. *Journal of the Electrochemical Society* **2003,** 150, (5), E271-E279.

20. Hodgdon, R. B. *Journal of Polymer Science, Part A: Polymer Chemistry* **1968,** 6, (1PA1), 711-717.

21. Kerres, J. A. *Journal of Membrane Science* **2001,** 185, (1), 3-27.

22. Noshay, A.; Robeson, L. M. *Journal of Applied Polymer Science* **1976,** 20, (7), 1885-1903.

23. Wang, F.; Hickner, M.; Kim, Y. S.; Zawodzinski, T. A.; McGrath, J. E. *Journal of Membrane Science* **2002,** 197, (1-2), 231-242.

24. Savadogo, O. *Journal of New Materials for Electrochemical Systems* **1998,** 1, (1), 47-66.

25. Kopitzke, R. W.; Linkous, C. A.; Nelson, G. L. *Journal of Polymer Science Part A-Polymer Chemistry* **1998,** 36, (7), 1197-1199.

26. Kruczek, B.; Matsuura, T. *Journal of Membrane Science* **1998,** 146, (2), 263-275.

27. Kobayashi, T.; Rikukawa, M.; Sanui, K.; Ogata, N. *Solid State Ionics* **1998,** 106, (3-4), 219-225.

28. Gao, Y.; Robertson, G. P.; Guiver, M. D.; Jian, X. G. *Journal of Polymer Science Part A-Polymer Chemistry* **2003,** 41, (4), 497-507.

29. Wycisk, R.; Pintauro, P. N. *Journal of Membrane Science* **1996,** 119, (1), 155-160.

30. Guo, Q. H.; Pintauro, P. N.; Tang, H.; O'Connor, S. *Journal of Membrane Science* **1999,** 154, (2), 175-181.

31. Kreuer, K. D., Technology and Applications. John Wiley & Sons Ltd: Chichester, U.K., **2003**; Vol. 3.

32. Miyatake, K.; Hay, A. S. *Journal of Polymer Science, Part A: Polymer Chemistry* **2001,** 39, (21), 3770-3779.

33. Schuster, M.; Rager, T.; Noda, A.; Kreuer, K. D.; Maier, J. *Fuel Cells* **2005,** 5, (3), 355-365.

34. Miyatake, K.; Hay, A. S. *Journal of Polymer Science, Part A: Polymer Chemistry* **2001,** 39, (11), 1854-1859.

35. Meng, Y. Z.; Tjong, S. C.; Hay, A. S.; Wang, S. J. *European Polymer Journal* **2003,** 39, (3), 627-631.

36. Allcock, H. R.; Hofmann, M. A.; Ambler, C. M.; Lvov, S. N.; Zhou, X. Y. Y.; Chalkova, E.; Weston, J. *Journal of Membrane Science* **2002,** 201, (1-2), 47-54.

37. Schmidt-Naake, G.; Bohme, M.; Cabrera, A. *Chemical Engineering and Technology* **2005,** 28, (6), 720-724.

38. Steininger, H.; Schuster, M.; Kreuer, K. D.; Maier, J. *Solid State Ionics* **2006,** 177, (26-32), 2457-2462.

39. Li, X. F.; Xu, D.; Zhang, G.; Wang, Z.; Zhao, C. J.; Na, H. *Journal of Applied Polymer Science* **2007,** 103, (6), 4020-4026.

40. Yamada, M.; Honma, I. *Journal of Physical Chemistry B* **2006,** 110, (41), 20486-20490.

41. Janik, M. J.; Davis, R. J.; Neurock, M. *Journal of Physical Chemistry B* **2004,** 108, (33), 12292-12300.

42. Steele, B. C. H.; Heinzel, A. *Nature* **2001,** 414, (6861), 345-352.

43. Rikukawa, M.; Sanui, K. *Progress in Polymer Science* **2000,** 25, (10), 1463-1502.

44. Rusanov, A. L., Likhatchev, D.Y., Mullen, K. *Russian Chem. Rev.* **2002,** 71, (9), 761-774.

45. Lecolley, F.; Waterson, C.; Carmichael, A. J.; Mantovani, G.; Harrisson, S.; Chappell, H.; Limer, A.; Williams, P.; Ohno, K.; Haddleton, D. M. *Journal of Materials Chemistry* **2003,** 13, (11), 2689-2695.

46. Bourlinos, A. B.; Raman, K.; Herrera, R.; Zhang, Q.; Archer, L. A.; Giannelis, E. P. *Journal of the American Chemical Society* **2004,** 126, (47), 15358-15359.

47. Donoso, P.; Gorecki, W.; Berthier, C.; Defendini, F.; Poinsignon, C.; Armand, M. B. *Solid State Ionics* **1988,** 28, 969-974.

48. Przyluski, J.; Dabrowska, A.; Stys, S.; Wieczorek, W. *Solid State Ionics* **1993,** 60, (1-3), 141-146.

49. Daniel, M. F.; Desbat, B.; Cruege, F.; Trinquet, O.; Lassegues, J. C. *Solid State Ionics* **1988,** 28, 637-641.

50. Tanaka, R.; Yammoto, H.; Kawamura, S.; Iwase, T. *Electrochimica Acta* **1995,** 40, (13-14), 2421-2424.

51. Grondin, J.; Rodriquez, D.; Lassegues, J. C. *Solid State Ionics* **1995,** 77, 70-75.

52. Wainright, J. S.; Wang, J. T.; Weng, D.; Savinell, R. F.; Litt, M. *Journal of the Electrochemical Society* **1995,** 142, (7), L121-L123.

53. Bouchet, R.; Miller, S.; Duclot, M.; Souquet, J. L. *Solid State Ionics* **2001,** 145, (1-4), 69-78.

54. Kreuer, K. D. *Solid State Ionics* **1997,** 94, (1-4), 55-62.

55. Kreuer, K. D., Fuchs, A., Ise, M., Spatch, M., Maier, J. *Electrochimica Acta* **1998,** 43, 1281.

56. Kreuer, K. D.; Paddison, S. J.; Spohr, E.; Schuster, M. *Chemical Reviews* **2004,** 104, (10), 4637-4678.

57. Munch, W.; Kreuer, K. D.; Silvestri, W.; Maier, J.; Seifert, G. *Solid State Ionics* **2001,** 145, (1-4), 437-443.

58. Schuster, M. E.; Meyer, W. H. *Annual Review of Materials Research* **2003,** 33, 233-261.

59. Borup, R.; Meyers, J.; Pivovar, B.; Kim, Y. S.; Mukundan, R.; Garland, N.; Myers, D.; Wilson, M.; Garzon, F.; Wood, D.; Zelenay, P.; More, K.; Stroh, K.; Zawodzinski, T.; Boncella, J.; McGrath, J. E.; Inaba, M.; Miyatake, K.; Hori, M.; Ota, K.; Ogumi, Z.; Miyata, S.; Nishikata, A.; Siroma, Z.; Uchimoto, Y.; Yasuda, K.; Kimijima, K. I.; Iwashita, N. *Chemical Reviews* **2007,** 107, (10), 3904-3951.

60. Goward, G. R.; Schuster, M. F. H.; Sebastiani, D.; Schnell, I.; Spiess, H. W. *Journal of Physical Chemistry B* **2002,** 106, (36), 9322-9334.

61. Agmon, N. *Chemical Physics Letters* **1995,** 244, (5-6), 456-462.

62. Kreuer, K. D. *Chemistry of Materials* **1996,** 8, (3), 610-641.

63. Persson, J. C.; Jannasch, P. *Chemistry of Materials* **2003,** 15, (16), 3044-3045.

64. Schuster, M.; Meyer, W. H.; Wegner, G.; Herz, H. G.; Ise, M.; Schuster, M.; Kreuer, K. D.; Maier, J. *Solid State Ionics* **2001,** 145, (1-4), 85-92.

65. Schuster, M. F. H.; Meyer, W. H.; Schuster, M.; Kreuer, K. D. *Chemistry of Materials* **2004,** 16, (2), 329-337.

66. Scharfenberger, G.; Meyer, W. H.; Wegner, G.; Schuster, M.; Kreuer, K. D.; Maier, J. *Fuel Cells* **2006,** 6, (3-4), 237-250.

67. Persson, J. C.; Jannasch, P. *Chemistry of Materials* **2006,** 18, (13), 3096-3102.

68. Persson, J. C.; Jannasch, P. *Solid State Ionics* **2006,** 177, (7-8), 653-658.

69. Herz, H. G.; Kreuer, K. D.; Maier, J.; Scharfenberger, G.; Schuster, M. F. H.; Meyer, W. H. *Electrochimica Acta* **2003,** 48, (14-16), 2165-2171.

70. Zhou, Z.; Li, S. W.; Zhang, Y. L.; Liu, M. L.; Li, W. *Journal of the American Chemical Society* **2005,** 127, (31), 10824-10825.

71. Zhou, Z.; Liu, R.; Wang, J. H.; Li, S. W.; Liu, M. L.; Bredas, J. L. *Journal of Physical Chemistry A* **2006,** 110, (7), 2322-2324.

72. Subbaraman, R., Ghassemi, H., Zawodzinski, T.A. *Journal of the American Chemical Society* **2007,** 129, (8), 2238-2239.

73. Sanghi, S.; Coughlin, E. B. *Private communication.*

74. Kolb, H. C.; Finn, M. G.; Sharpless, K. B. *Angewandte Chemie, International Edition in English* **2001,** 40, (11), 2004-2021.

75. Rostovtsev, V. V.; Green, L. G.; Fokin, V. V.; Sharpless, K. B. *Angewandte Chemie, International Edition in English* **2002,** 41, (14), 2596-2599.

76. Himo, F.; Lovell, T.; Hilgraf, R.; Rostovtsev, V. V.; Noodleman, L.; Sharpless, K. B.; Fokin, V. V. *Journal of the American Chemical Society.* **2005,** 127, (1), 210-216.

CHAPTER 2

INTRINSICALLY CONDUCTING POLYMERS AND COPOLYMERS CONTAINING TRIAZOLE MOIETIES

2.1 Introduction

Previous work in our group systematically studied the effect of polymer backbone mobility on proton conductivity.[1, 2] The results from that study confirmed that proton conductivity increases as the glass transition of the backbone decreases. A natural extension of this work is the combination of a low T_g backbone with a smaller, more mobile, weakly basic heterocyclic motif, such as 1,2,3-triazole to increase the proton mobility within the resulting polymer membrane. Furthermore, the optimum combination of plasticizing and charge carrier groups that maximize backbone mobility and proton transport remains an open question. Therefore preparing a series of copolymers with an increasing proportion of plasticizing side chains would allow for probing the influence of inert flexible groups on proton conductivity while confirming the positive effect of substituting benzimidazole by 1,2,3-triazole as the proton carrier.

This chapter reports the synthesis and characterization of polyacrylates with tethered 1,2,3-triazole motifs and varying degrees of poly(ethylene glycol)methyl ether acrylate (PEGMEA) incorporation to tune the glass transition temperature of the resulting materials. Doping the 1,2,3-triazole-based polymers with the strong acid trifluoroacetic acid (TFA) was also studied. Polyacrylates were chosen as a model system in this study because of the ability to quickly and simply modify the structure of the copolymers to examine structural factors and to provide direct analogs to benzimidazole materials previously investigated in our laboratory.

2.2 Experimental

2.2.1 Materials

5-hexyn-1-ol, acryloyl chloride, triethylamine, copper(II) sulfate ($CuSO_4.5H_2O$), sodium ascorbate, *t*-butanol (*t*-BuOH), poly(ethylene glycol) methyl ether acrylate (PEGMEA) (M_n ~454 g/mol), and trifluoroacetic acid (TFA) were purchased from Sigma-Aldrich and used as received. 2,2′-Azobis(2-methylpropionitrile) (AIBN) was purchased from Sigma-Aldrich, and was recrystallized from methanol before use. Azidomethyl pivalate was prepared as reported in the literature.[3]

2.2.2 Instrumentation

^{1}H-NMR (300 MHz) and ^{13}C-NMR (75 MHz) spectra were obtained on a Bruker DPX-300 NMR Spectrometer with the samples dissolved in either chloroform-*d* or dimethyl sulfoxide-d_6 (DMSO-d_6). Molecular weight and polydispersity index were measured by gel permeation chromatograhpy (GPC) in DMF at 50 ºC with a flow rate of 1 mL/min on systems equipped with two-column sets (from Polymer Laboratories), and refractive index detectors (HP 1047A). Poly(methyl methacrylate) standards were used for molecular weight calibration. Thermogravimetric analysis (TGA) was carried out using a TA Instruments TGA 2950 thermogravimetric analyzer with a heating rate of 10 ºC/min from room temperature to 700 ºC under air purge. Glass transition temperatures were obtained by differential scanning calorimetry (DSC) using a TA instruments Dupont DSC 2910. Samples, approximately 3-5 mg, were used with a heating rate of 10 ºC/min from -100 ºC to 180 ºC under a flow of nitrogen (50 mL/min). Electrochemical impedance data was obtained using a Solartron 1287 potentiostat/1252A frequency

response analyzer in the 0.1 Hz–300 kHz range.[2] The polymers were pressed between two gold coated blocking electrodes followed by an application of 100 mV excitation voltage with a logarithmic frequency sweep from $3x10^5$ Hz to $1x10^{-1}$ Hz. Resistance values were taken at the minimum imaginary response in a Z' vs. Z'' plot to determine conductivity in the low frequency limit.

2.2.3 Monomer synthesis

5-hexyn-1-acrylate, 2.1. To dichloromethane (DCM, 90 mL) in a 250 mL round bottom flask was added 5-hexyn-1-ol (5.0 mL, 54.48 mmol) and triethylamine (6.12 mL, 83.82 mmol). The resulting solution was cooled in an ice bath, and acryloyl chloride (6.72 mL, 76.20 mmol) was added slowly. The reaction was stirred at room temperature for 20 h. The reaction was ended by the addition of water, and the product was extracted with DCM (3 x 100 mL). The organic portion was dried over $MgSO_4$ and the volatiles were removed in vacuo to yield **2.1** as a clear liquid (3.79 g, 46%). ^{1}H-NMR ($CDCl_3$, 298 K, 300 MHz) δ: 6.38-6.43 (d, 1H, olefinic H), δ: 6.16-6.10 (m, 1H, C*H*=CH_2), δ: 5.84-5.81 (d, 1H, olefinic H), δ: 4.12 (m, 2H, CH_2O), δ: 2.27-2.22 (m, 2H, CCH_2), δ: 1.96 (t, 1H, C*H*C), δ: 1.86-1.78 (m, 2H, CCH_2CH_2), δ: 1.67-1.56 (m, 2H, CH_2CH_2O). ^{13}C-NMR (DMSO-d_6, 298 K, 300 MHz) δ: 166.4, 149.0, 133.7, 130.8, 128.3, 64.1, 28.0, 25.5, 24.5. Mass spectrum *m/z* 195.2 (10, $M^{+\bullet}$), 140.0 (10), 123.0 (100), 95.0 (80), 82.0 (35), 55.1 (75).

Acrylic acid 4-(1*H*-[1,2,3]triazol-4-yl)-butyl ester, 2.2, and Acrylic acid 4-(1-hydroxymethyl-1*H*-[1,2,3]triazol-4-yl)-butyl ester, 2.3. To a solution of 5-hexyn-1-acrylate (4.73 g, 31.16 mmol) in 20 mL t-BuOH/H_2O (2/1), azidomethyl pivalate (AMP, 4.89 g, 31.16 mmol), $CuSO_4.5H_2O$ (0.39 g, 3.11 mmol), and sodium ascorbate (0.62 g,

1.56 mmol) were added. The solution was stirred at room temperature for 24 h. The product was extracted with ethyl acetate (EtOAc, 3 x 100 mL), and washed with 5% aqueous ammonium hydroxide solution and brine. The combined organic portion was dried over $MgSO_4$ and the volatiles were removed in vacuo. The pivaloyloxymethyl (POM)-protected acrylate (5 g) was treated with 0.1 M NaOH/MeOH (178 mL, 1.1 eq.). The solution was stirred at 0 ºC for 10 min, and then was neutralized with 1.0 M HCl to pH 6-7. The product was extracted with DCM, and dried over $MgSO_4$. The volatiles were removed in vacuo. The crude product was further purified by column chromatography, using hexane:EtOAc (1:1) as an eluent, to yield a mixture of products **2.2** and **2.3** as a clear liquid (1.82 g, 58% yield). ^{1}H-NMR (DMSO, 298 K, 300 MHz) δ: 14.60 (s, 1H, N*H*), δ: 7.60 (s, 1H, Ar), δ: 7.11 (s, 1H, O*H*), δ: 5.56 (m, 2H, CH_2-OH), δ: 6.29-5.94 (m, 3H, CH_2=C*H*), δ: 4.12 (t, 2H, CH_2O), δ: 2.67 (t, 2H, CH_2-Ar), δ: 1.65 (m, 4H, CH_2CH_2). ^{13}C-NMR ($CDCl_3$, 298 K, 300 MHz) δ: 166.1, 130.5, 128.4, 83.7, 68.7, 63.9, 27.5, 24.8, 17.9. Mass spectrum *m/z* 153.2 (3, $M^{+\bullet}$), 141.1 (100), 133.0 (10), 129.1 (5).

2.2.4 Polymer synthesis

The random copolymerization of **2.2** and **2.3** and terpolymerization of **2.2, 2.3** and PEGMEA were carried out in DMSO (~1 M) with AIBN (2 mol%) as the initiator in an air-free tube. Following three cycles of freeze-pump-thaw, the solution was stirred at 60 ºC for 30 min. The resulting polymers were precipitated in a mixture of hexane and EtOAc (1:1), and dried under vacuum at 45 ºC for 2 d.

2.2.5 Acid doped polymer preparation

A varying mole % of TFA ranging from 20 to 130% compared to moles of free triazole content was added to a solution of 30% PEGMEA terpolymer (contains 30 wt% of EtOAc) in MeOH (~50 mg/mL). The solution was stirred at room temperature for 10 min, and then dried under vacuum at 45 ºC overnight.

2.3 Results and discussion

2.3.1 Monomer synthesis

The synthesis of the new monomers (Schemes 2.1 and 2.2) was achieved in three steps. Acryloyl chloride was reacted with 5-hexyn-1-ol in dichloromethane to yield 5-hexyn-1-acrylate, **2.1**. The [3+2] cycloaddition of acrylate **2.1** with azidomethyl pivalate was carried out under common "click" conditions (Cu(II) sulfate and sodium ascorbate in water/alcohol mixtures) to afford the pivaloyloxymethyl (POM)- protected triazole.[4] Removal of POM was accomplished with 0.1 M NaOH/MeOH to yield a mixture of compounds **2.2** and **2.3**. The methanol substituted triazole is thought to be a result of the reaction between the cleaved triazoyl anion and formaldehyde (both formed during deprotection). Given the similarity in retention factor between the two products, **2.3** could not be separated by column chromatography. The presence of the free N*H* triazole was confirmed using ^{1}H NMR spectroscopy by the disappearance of signals at δ 1.11 and δ 6.26 ppm, corresponding to the protons of POM protecting group, a shift of the proton on the heterocycle ring from δ 7.99 ppm to δ 7.60 ppm, and the appearance of a new peak at δ 14.60 ppm corresponding to the triazole N*H*. Initially, the deprotection was performed on a small scale (0.7 g) yielding only 4% mole of byproduct **2.3**; however,

upon scale-up it became exceedingly difficult to produce monomer with less than 27% mole of **2.3**. Therefore, model polymers were made using a monomer mixture containing 27% mole of **2.3** for the PEGMEA incorporation study and with 30% mole of **2.3** for the acid doping study.

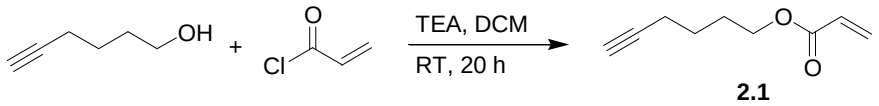

Scheme 2.1. Synthesis of 5-hexyn-1-acrylate.

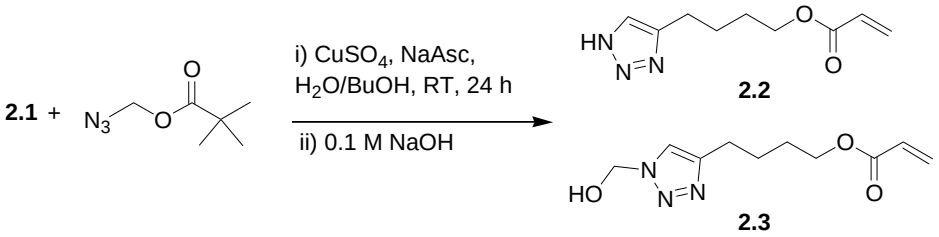

Scheme 2.2. Synthetic route to 1,2,3-triazole functional acrylate monomers.

2.3.2 Polymer synthesis

Random copolymer and terpolymers with compositions varying from 0 to 52% of PEGMEA were prepared (Scheme 2.3). All polymerizations were carried out for 30 min at 60 °C in DMSO at a total monomer concentration of 1.0 M, and were initiated with AIBN (2% mole). Given the complexity of the repeat units a general nomenclature will be used to describe the polymer structures. The polymers are designated as T5A-*l*-*m*PEG-*n*D, where *l* is the mole percent of **2.3** in the monomer mixture of **2.2** and **2.3**, *m* is mole percent of PEGMEA incorporation, and *n* is mole percent of TFA added compared to the mole fraction of free triazole in the backbone. It was found that after fully drying the

resulting polymers, dissolution in any solvent became difficult; therefore, the compositions of wet polymers were determined by ^{1}H NMR, neither ethyl acetate nor hexane chemical shifts interfered with the analysis. Molecular weight determination of T5A-27-30PEG was attempted by GPC; however, the polymer adsorbed to the column complicating a reliable comparison with the calibration data.

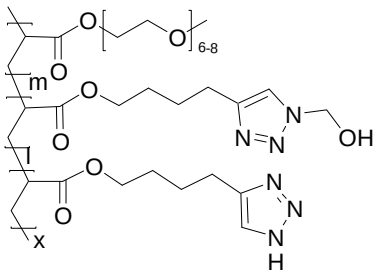

Scheme 2.3. Structure of prepared co- and ter- polymers.

2.3.3 Acid doped polymer preparation

Due to the aforementioned difficulty to dissolve fully dried polymers, "wet" polymers were used in the acid doping study. The weight percent of polymer in a stock solution was determined by both ^{1}H-NMR and gravimetric methods. The values obtained were within 5% and the ^{1}H-NMR data was used to calculate the required quantities of trifluoroacetic acid. A varying mole % of TFA ranging from 20 to 130% compared to moles of 1*H*-1,2,3-triazole content was added to a solution of 30% PEGMEA terpolymer (contains 30 wt% of EtOAc) in MeOH(~50 mg/mL). The solution was stirred at room temperature for 10 min, and then dried under vacuum at 45 ºC overnight.

2.3.4 Thermal analysis

Thermogravimetric analysis results can be seen in Figure 2.1, all polymers were thermally stable up to approximately 220 ºC, and thermal decomposition onset temperature increased with the degree of incorporation of PEGMEA. The decomposition of the copolymer proceeded in two steps, while that of the terpolymers proceeded in three steps. The second weight loss of the terpolymers was attributed to the loss of PEGMEA segments.

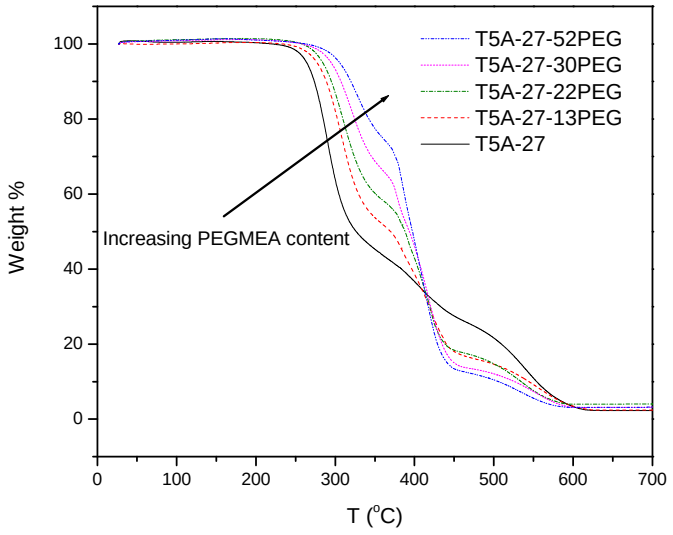

Figure 2.1. TGA traces of polymers with increasing amounts of PEG.

The DSC traces in Figure 2.2 showed that polymers T5A-27, T5A-27-13PEG, T5A-27-22PEG, and T5A-27-30PEG were fully amorphous and displayed a single glass transition temperatures (T_g), whereas polymer T5A-27-52PEG was semicrystalline and displayed a melting peak at 9 ºC with ΔH_m of 3.9 J/g. The T_g values are reported in Table 2.1. As expected, T_g decreases with addition of PEGMEA.

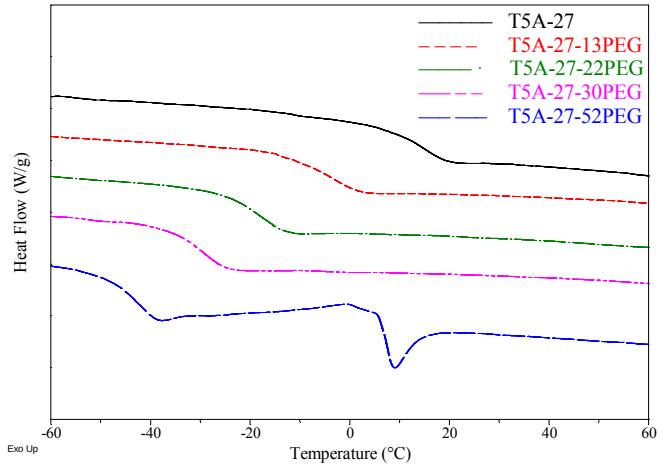

Figure 2.2. DSC traces of polymers with increasing amounts of PEG.

Table 2.1. T_g values for all polymers and acid doped polymers.

Material	T_g (ºC)
T5A-27	16
T5A-27-13PEG	-3
T5A-27-22PEG	-19
T5A-27-30PEG	-29
T5A-27-52PEG	-43
T5A-4-30PEG	-24
T5A-20-30PEG	-28
T5A-30-28PEG	-25
T5A-30-28PEG-20D	-26
T5A-30-28PEG-50D	-25
T5A-30-28PEG-80D	-25
T5A-30-28PEG-100D	-21
T5A-30-28PEG-130D	-27
B5A-35PEG[1, 2]	2

2.3.5 Proton conductivity as a function of polymer composition

The composition of the triazole containing polymers was varied in order to study the effects of charge carrier density, polymer matrix mobility and heterocycle nature on the proton conductivity of the resulting materials. The different compositions were

designed to isolate each effect from the other structural factors and general trends and interesting observations can be extracted through methodical examination of our results.

2.3.5.1 Charge carrier density

The effect of charge carrier density on proton conductivity was examined originally via two avenues, doping of triazole rings with a strong acid and substitution of triazole motifs by low molecular weight polyethylene glycol. However, an additional approach was derived from our synthetic strategy which generated varying amounts of N-methyl hydroxyl susbstituted triazole as a co-product.

2.3.5.1.1 Influence of N-methyl hydroxyl substituted triazole

The effect of N-methyl hydroxy substituted triazole on the proton conductivity (σ) is illustrated in a log(σ) vs. 1000/T(K) plot (Figure 2.3). The conductivity increases approximately an order of magnitude throughout the studied temperature range when the fraction of N-methyl hydroxyl substituents decreased from 27% mole to 4% mole. Values for T5A-4-30PEG are 0.62 μS/cm at 80 °C and 17.8 μS/cm at 200 °C, spanning 1.5 orders of magnitude. The conductivity should increase upon complete removal of the co-product **2.3**, however, given the time consuming nature of the multiple small scale syntheses required, this was not pursued any further. We expect that the observed trends outlined in this work will remain qualitatively the same if co-product **2.3** was completely eliminated. Insight into the effect of substituting the more basic benzimidazole by 1,2,3-triazole as the proton carrier can be obtained by comparing the conductivity of T5A-4-30PEG with that of B5A-35PEG, an analogous benzimidazole polyacrylate previously

reported by this group.[1, 2] The conductivity of T5A-4-30PEG is approximately 0.5 to 1.5 orders of magnitude higher than B5A-35PEG at 200 °C and 80 ºC respectively. The improved conductivity may be attributed to several factors, the lower T_g of T5A-4-30PEG (-24 °C vs. 2 °C for B5A-35PEG), the decreased basicity of the protonic charge carrier (pK_a of 1,2,3-triazole = 9.26, pK_a of benzimidazole = 12.17),[4, 5] and a lower number of conformational changes necessary for proton hopping in 1,2,3-triazole vs benzimidazole.[6] These factors are intimately coupled in that altering only one can have pronounced effects on the others; therefore, investigating each factor in a decoupled fashion would be a formidable task. However, to investigate general trends in a parallel manner to our reported benzimidazole acrylate materials, the effect of systematic increases in PEG content as a means to lower the polymer glass transition temperature and vary the charge carrier density are detailed below.

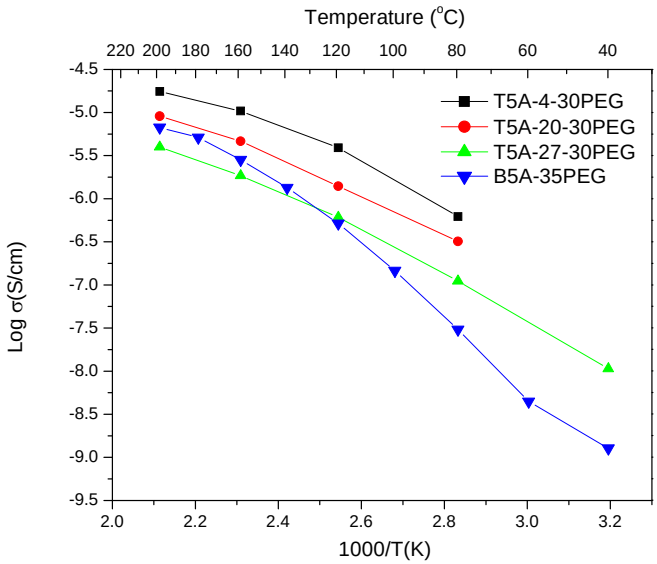

Figure 2.3. Conductivity of T5A-PEGMEA copolymers with increasing triazole content.

2.3.5.1.2 Influence of polyethylene glycol methyl ether acrylate side groups

A plot of log(σ) vs. 1000/T(K) is shown in Figure 2.4 for T5A-27 and the four PEGMEA terpolymers prepared. The T5A-27 conductivity trace spans 3 orders of magnitude from 80 to 200 °C, with a maximum conductivity of 0.87 μS/cm. The initial PEG incorporation of 13% mole provides a large initial decrease in the conductivity temperature dependence, and an associated conductivity increase over the entire temperature range with a jump of nearly 1.5 orders of magnitude at 80 °C and ~0.75 orders of magnitude at 200 °C. Further increases in the amount of PEG resulted in small incremental improvements up to 30% PEG where conductivity of 3.98 μS/cm and 0.11 μS/cm were observed at 200 °C and 80 °C respectively. A drop in conductivity upon reaching 52% PEG is most likely due to the lower charge carrier density resulting from the high PEG loading.

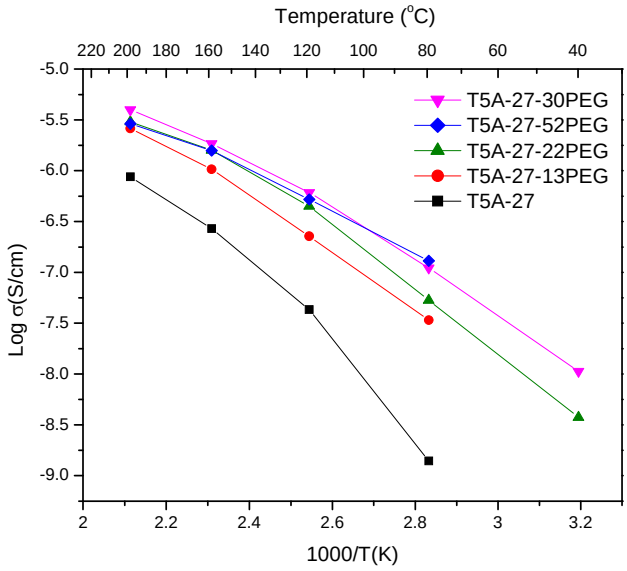

Figure 2.4. Conductivity of polymers with increasing PEG content.

The convex shape of the curves suggests non-Arrhenius behavior.[7] In general, the bulk conductivity depends on the mobility, the number of charge carriers, and the charge of the carriers. In polymer systems where the charge carrier and the density remain constant, conductivity is solely a function of the free volume conformational changes,[8] with the temperature dependence being described by the Vogel-Tamman-Fulcher (VTF) equation describing polymer motion.[9]

$$\sigma = \sigma_0 \exp[-B/(T-T_0)] \quad (1)$$

Since the conductivity is, in part, governed by the free volume conformational changes,[8] it is expected that log(σ) vs. $T-T_g$ curves would converge given a constant protonic charge carrier density. A plot of log(σ) vs. $T-T_g$ for T5A and T5A-PEGMEA terpolymers (see Figure 2.5) provides qualitative insight into the effect of lowering charge carrier concentration as a result of increased PEG loading. The curves for T5A-27-13PEG, -22PEG, and, -30PEG converge around one curve and T5A-27 and T5A-27-52PEG converge around a second curve with slightly lower values. Incorporation of PEG affects two competing factors that determine conductivity, T_g and charge carrier density, such that a decrease in T_g is accompanied by a decrease in charge carrier density. In studies where benzimidazole is the protonic charge carrier reported by our group,[17] and by Persson and Jannasch,[10] T_g reduction by incorporation of PEG results in increased conductivity below 160 °C on an absolute scale, however, in a normalized $T-T_g$ plot the reduction in charge carrier density is evident from a stepwise reduction in conductivity given a constant $T-T_g$ value.[10, 11] In this case, where the heterocycle is 1,2,3-triazole, introduction of PEG resulted in conductivity increases on both an absolute scale and a normalized $T-T_g$ scale. This implies that there may be a synergistic effect between PEG

and triazole strong enough to improve conductivity despite the decrease in the concentration of charge carriers. These observations suggest that the chemical composition of the polymer backbone may have an appreciable effect on proton transport. A similar effect has been observed for lithium ion conducting polymer systems where the conductivity increases as the dielectric constant of the polymer matrix increases.[12] While the nature of the observed effect is not well understood at this time, it may be that incorporating a high dielectric constant material (PEG) has a positive influence on conductivity.

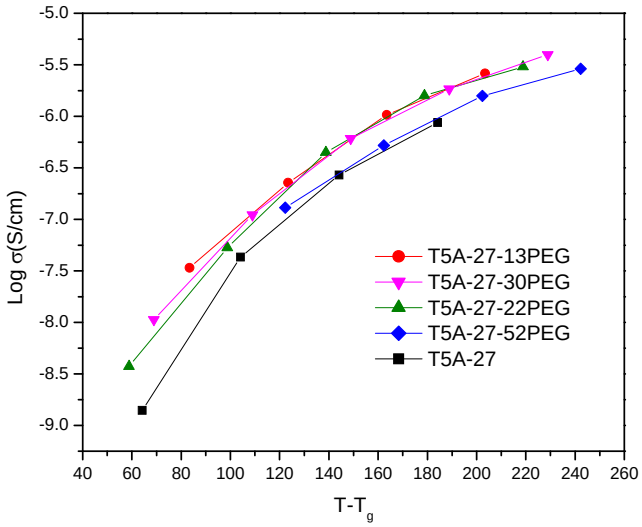

Figure 2.5. Normalized conductivity vs. T-T_g plot of polymers with increasing PEG content.

2.3.5.1.3 Trifluoroacetic acid doped materials

Doping polymer T5A-30-28PEG with TFA shows a significant increase in conductivity with up to 1.5 orders of magnitude improvement depending on doping level (Figure 2.6). The introduction of acid to di-nitrogen heterocyclic proton conducting

polymers is well known to result in conductivity improvements, however, the maximum effect in imidazole based systems is generally found at ~15 mol% acid.[13] In our case continued conductivity improvements were observed up to 100 mol% TFA, this may be explained by the nature of the heterocycle. The addition of a third nitrogen provides an additional proton acceptor site in the heterocycle, therefore even when the triazole is fully protonated, there are two proton donor sites and one proton acceptor allowing for a proton conduction pathway. Further addition of TFA (130 mol%) to the system resulted in reduced conductivity.

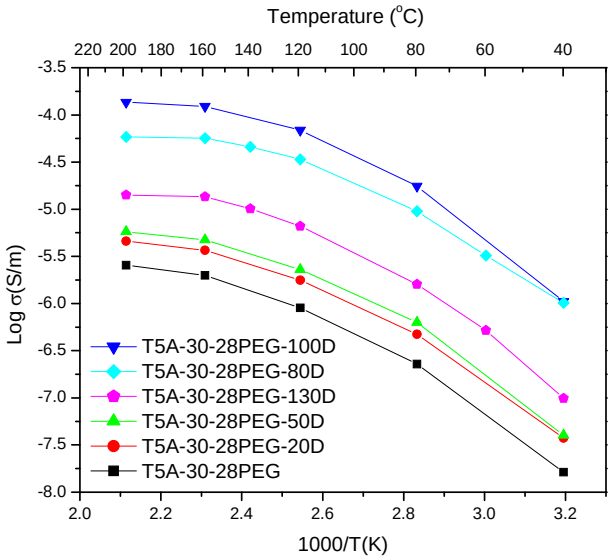

Figure 2.6. Conductivity of TFA doped terpolymers.

2.3.5.2 Nature of heterocycle and polymer matrix mobility

Although we were not able to isolate the effect of decreased heterocycle basicity on proton conduction, direct replacement of 1,2,3-triazole for benzimidazole onto an acrylate backbone lead to significant increases in chain mobility due to reduced T_g (Table 2.1). This may be attributed to the large difference in melting point of benzimidazole

(177 °C) and 1,2,3-triazole (25 °C). The indication is that utilization of 1,2,3-triazole as the protonic charge carrier will produce inherently more mobile polymeric systems, resulting in systems with reduced temperature dependence.

A systematic increase in the mole fraction of N*H*-triazole results in steady conductivity increases (Figure 2.3), however, it is striking that there is a minimal associated increase in T_g as the charge carrier density increases, this is in contrast to the trend observed in benzimidazole containing polymers.[10] An interesting extension would be to investigate the effect of tether length on conductivity in 1,2,3-triazole containing polymers, by reducing tether length the volume fraction of charge carriers can be increased. In the case of benzimidazole[7] and imidazole[14] tether length reduction results in increased T_g and the conductivity displays an increase in temperature dependence. Given the observed low T_g with tethered 1,2,3-triazole, it may be possible to increase the volume fraction of charge carriers without adversely affecting the temperature dependence of the conductivity.

2.4 Conclusion

Random copolymers and terpolymers of 1,2,3-triazole-containing acrylate and PEGMEA have been synthesized and characterized. A comparison of the conductivity of the 1,2,3-triazole based polyacrylate with 30% PEGMEA with the benzimidazole analog allowed us to probe the effect of using the more weakly basic 1,2,3-triazole as the proton carrier. The triazole containing polyacrylate showed higher proton conductivity and a less pronounced conductivity temperature dependence than the corresponding benzimidazole polyacrylate. This can be attributed in part to the smaller size and low melting point of the hererocycle itself, resulting in a lower T_g material when attached to a polymer

backbone. The conductivity increases as a function of absolute and a normalized temperature as PEGMEA incorporation increases until reaching a limit at 30 mole %. This finding indicates that T_g reduction with PEG in 1,2,3-triazole systems can counteract the associated reduction in charge carrier density. The lower conductivity observed for terpolymers with higher PEGMEA fractions suggests that at those compositions the decrease in charge carrier concentration becomes the limiting factor for proton transport over the backbone mobility. Doping the polymers with TFA resulted in further conductivity increases ranging from 0.5 to 1.5 orders of magnitude compared to the undoped membranes. Though these polyacrylates can only be regarded as model systems, the trends observed in this study should translate to better defined, chemically stable backbones.

2.5 References

1. Woudenberg, R. C.; Yavuzcetin, O.; Tuominen, M.; Coughlin, E. B. *Solid State Ionics* **2007,** 178, 1135-1141.

2. Woudenberg, R. C. Doctoral Thesis. University of Massachusetts, Amherst, MA, 2007.

3. Loren, J. C., Krasinski, A., Fokin, V.V., Sharpless, K.B. *Synlett* **2005,** 18, 2847-2850.

4. Sari, H.; Covington, A. K. *Journal of Chemical and Engineering Data* **2005,** 50, (4), 1425-1429.

5. Zhou, Z.; Li, S. W.; Zhang, Y. L.; Liu, M. L.; Li, W. *Journal of the American Chemical Society* **2005,** 127, (31), 10824-10825.

6. Zhou, Z.; Liu, R.; Wang, J. H.; Li, S. W.; Liu, M. L.; Bredas, J. L. *Journal of Physical Chemistry A* **2006,** 110, (7), 2322-2324.

7. Persson, J. C.; Jannasch, P. *Chemistry of Materials* **2003,** 15, (16), 3044-3045.

8. Wei, J.; Stone, C.; Steck, A. E., of Ballard Power Systems, Inc., June 6, 1995; U.S. Patent 5,422,411.

9. Ratner, M. A., In *Polymer Electrolyte Reviews*, Elsevier Applied Science: New York, 1987; pp 173-235.

10. Persson, J. C.; Jannasch, P. *Chemistry of Materials* **2006,** 18, (13), 3096-3102.

11. Woudenberg, R. C.; Yavuzcetin, O.; Tuominen, M.; Coughlin, E. B. *Solid State Ionics* **2007**, 178, 1135-1141.

12. Sun, X. G.; Kerr, J. B. *Macromolecules* **2006,** 39, (1), 362-372.

13. Schuster, M. F. H.; Meyer, W. H.; Schuster, M.; Kreuer, K. D. *Chemistry of Materials* **2004,** 16, (2), 329-337.

14. Herz, H. G.; Kreuer, K. D.; Maier, J.; Scharfenberger, G.; Schuster, M. F. H.; Meyer, W. H. *Electrochimica Acta* **2003,** 48, (14-16), 2165-2171.

CHAPTER 3

POLYACRYLATES CONTAINING 1*H*-1,2,3-TRIAZOLE MOIETIES: NUMBER OF TRIAZOLES PER REPEAT UNIT EFFECT

3.1 Introduction

1*H*-1,2,3-Triazole has recently drawn interest as an alternative heterocycle for use in PEMFCs due to its electrochemical stability and high proton conductivity. A study by Zhou and co-workers apparently demonstrated that a pronounced increase in conductivity was observed in vinyl-based polymers when the heterocyclic group was changed from an imidazole moiety to a triazole moiety.[1] Similar to the work on imidazole,[2] and benzimidazole,[3, 4] 1*H*-1,2,3-triazole has been tethered to several flexible polymeric backbones including polyacrylate,[5] polysiloxane,[6] and polyphosphazene.[7] Proton conductivities of these polymers depend strongly on mobility and charge carrier density.

In this chapter, we report the synthesis and characterization of polyacrylates containing a different number of 1*H*-1,2,3-triazoles per repeat unit. The various monomers used in this study were obtained as a direct consequence of the copper catalyzed alkyne-azide coupling, so-called "Click Chemistry",[8-10] using pivaloyloxymethyl (POM) substituted azide. [11, 12] These polymers were designed to investigate the effect of charge carrier density on proton conductivity by introducing more than one triazole per repeat unit. Conductivities of the polymers determined using impedance spectroscopy are compared and reported.

3.2 Experimental

3.2.1 Materials

1,3-Propanediol, 1,1,1-tris(hydroxymethyl)ethane, pentaerythritol, 3-butyn-1-ol, sodium hydride (NaH), sodium hydroxide (NaOH), propargyl bromide, acryloyl chloride, triethylamine (TEA), copper(II) sulfate ($CuSO_4.5H_2O$), sodium ascorbate, *t*-butanol (*t*-BuOH), dimethyl sulfoxide (DMSO), and trifluoroacetic acid (TFA) were purchased either from Sigma-Aldrich or VWR and used as received. Regenerated cellulose dialysis tubing with a molecular weight cutoff of 3,500 Daltons was purchased from Fisher Scientific. 2,2′-Azobis(2-methylpropionitrile) (AIBN) was purchased from Sigma-Aldrich, and recrystallized from methanol before use. 3-(Prop-2-yn-1-yloxy)propan-1-ol, **3.2a**,[13] 3-(prop-2-ynyloxy)-2,2-bis[(prop-2-ynyloxy)methyl]propan-1-ol, **3.2c**,[14] and azidomethyl pivalate (AMP),[11] were prepared as reported in the literature.

3.2.2 Characterization

^{1}H-NMR (300 MHz) and ^{13}C-NMR (75 MHz) spectra were obtained on a Bruker DPX-300 NMR Spectrometer with the samples dissolved in either chloroform-*d* ($CDCl_3$) or methanol-d_4 (CD_3OD). Molecular weight and polydispersity index (PDI) were measured by gel permeation chromatography (GPC) in DMF at 50 ºC with a flow rate of 0.75 mL/min on systems equipped with two-column sets (from Polymer Laboratories), and refractive index detectors (HP 1047A). Poly(methyl methacrylate) (PMMA) standards were used for molecular weight calibration. Thermogravimetric analysis (TGA) was carried out using a TA Instruments TGA 2950 thermogravimetric analyzer with a heating rate of 10 ºC/min from room temperature to 500 ºC under nitrogen. Glass

transition temperatures were obtained by differential scanning calorimetry (DSC) using a TA instruments Dupont DSC 2910. Samples were analyzed with a heating rate of 10 ºC/min from -100 ºC to 150 ºC under a flow of nitrogen (50 mL/min). To prepare the polymer for impedance measurement it was cast from a methanol solution in a small cylinder formed by punching a 0.3175 cm diameter hole through a 0.0125 cm thick piece of Kapton®. The sample was then inserted between two 1.25 cm diameter gold-coated blocking electrodes and dried at 30 ºC under vacuum for 8 hours to evaporate the methanol. The cell geometry of the complete assembly closely approximates a parallel-plate capacitor in which the polymer is the dielectric medium. To ensure an anhydrous and inert environment, the measurement was conducted under vacuum. At temperatures between 40 and 200 ºC, the impedance response was sampled logarithmically from 0.1 Hz to 300 kHz with a constant excitation voltage of 0.1 Vrms using a Solartron 1287 potentiostat and 1252A frequency response analyzer. By geometrically fitting[15] the impedance response that corresponds to proton conduction in the DC limit, we determined the approximate proton resistance. From the resistance the conductivity was calculated by accounting for the well-defined cell geometry.

3.2.3 Monomer and polymer synthesis

Synthesis of 3-(prop-2-yn-1-yloxy)propyl acrylate, 3.3a. To a solution of compound **3.2a** (0.80 g, 7.0 mmol, 1 equiv.) and triethylamine (1.3 mL, 9.1 mmol, 1.2 equiv.) in anhydrous THF (20 mL), acryloyl chloride (0.68 mL, 8.4 mmol, 1.2 equiv.) was added slowly with stirring at 0 ºC. A white precipitate of triethylammonium hydrochloride formed, and the reaction was stirred for 16 h at room temperature. The precipitate was removed by filtration. The mixture was diluted with 50 mL of water. The

product was extracted with ethyl acetate (3 x 50 mL), dried over $MgSO_4$, filtered, and concentrated. The crude product was further purified by column chromatography, using hexane:ethyl acetate (1:4) as an eluent, to give 0.82 g of the product. Yield: 70%. ^{1}H-NMR (300 MHz, $CDCl_3$) δ: 1.97 (m, 2H), 2.42 (s, 1H), 3.62 (t, 2H), 4.15 (s, 2H), 4.26 (t, 2H), 5.80–6.38 (m, 3H). ^{13}C-NMR (75 MHz, $CDCl_3$) δ: 28.85, 58.19, 61.58, 66.43, 74.38, 79.87, 128.46, 130.70, 166.18. EI-HRMS (m/z): calculated 169.1898 [M+1], found 169.0876.

Synthesis of 2-methyl-3-(prop-2-yn-1-yloxy)-2-[(prop-2-yn-1-yloxy)methyl]propyl acrylate, 3.3b. Compound **3.3b** was prepared as described for **3.3a**. Yield: 44%. ^{1}H-NMR (300 MHz, $CDCl_3$) δ: 1.00 (s, 3H), 2.40 (s, 2H), 3.42 (s, 4H), 4.12 (m, 6H), 5.80–6.43 (m, 3H). ^{13}C-NMR (75 MHz, $CDCl_3$) δ: 17.24, 39.77, 58.64, 66.61, 72.19, 74.24, 79.82, 128.50, 130.58, 166.03. EI-HRMS (m/z): calculated 251.2903 [M+1], found 251.1288.

Synthesis of 3-(prop-2-yn-1-yloxy)-2,2-bis[(prop-2-yn-1-yloxy)methyl]propyl acrylate, 3.3c. Compound **3.3c** was prepared as described for **3.3a**. Yield: 51%. ^{1}H-NMR (300 MHz, $CDCl_3$) δ: 2.39 (s, 3H), 3.55 (s, 6H), 4.11 (s, 6H), 4.21 (s, 2H), 5.80–6.42 (m, 3H). ^{13}C-NMR (75 MHz, $CDCl_3$) δ: 44.10, 58.69, 63.43, 68.60, 74.30, 79.76, 128.50, 130.58, 165.87. EI-HRMS (m/z): calculated 305.3377 [M+1], found 305.1380.

Synthesis of 3-[(1-{[(2,2-dimethylpropanoyl)oxy]methyl}-1*H*-1,2,3-triazol-4-yl)methoxy]propyl acrylate, 3.4a. To a solution of compound **3.3a** (0.82 g, 4.88 mmol, 1 equiv.) in 20 mL *t*-BuOH/H_2O (2/1), azidomethyl pivalate (AMP, 0.92 g, 5.86 mmol, 1.2 equiv.), $CuSO_4.5H_2O$ (0.06 g, 0.24 mmol, 0.05 equiv.), and sodium ascorbate (0.29 g, 1.46 mmol, 0.3 equiv.) were added. The solution was stirred at

room temperature for 21 h. The product was extracted with ethyl acetate (3 x 50 mL) and washed with ammonium hydroxide aqueous solution and brine. The organic portion was dried over $MgSO_4$ and the volatiles were removed in vacuo. The crude product was further purified by column chromatography, using hexane:ethyl acetate (1:4) as an eluent, to give 0.8 g of product. Yield: 50%. ^{1}H-NMR (300 MHz, $CDCl_3$) δ: 1.18 (s, 9H), 1.96 (m, 2H), 3.62 (t, 2H), 4.24 (t, 2H), 4.63 (s, 2H), 5.84–6.36 (m, 3H), 6.22 (s, 2H), 7.79 (s, 1H). ^{13}C-NMR (75 MHz, $CDCl_3$) δ: 26.80, 28.91, 38.77, 61.53, 64.23, 67.10, 69.66, 123.91, 128.40, 130.74, 145.73, 166.14, 177.74. FAB-HRMS (m/z): calculated 326.1638 [M+1], found 326.1738.

Synthesis of 3-[1-(2,2-dimethyl-propionyloxymethyl)-1*H*-[1,2,3]triazol-4-yloxy]-2-[1-(2,2-dimethyl-propionyloxymethyl)-1*H*-[1,2,3]triazol-4-yloxymethyl]-2-methyl-propyl acrylate, 3.4b. Compound **3.4b** was prepared as described for **3.4a**. Yield: 83%. ^{1}H-NMR (300 MHz, $CDCl_3$) δ: 0.94 (s, 3H), 1.18 (s, 18H), 3.39 (s, 4H), 4.05 (s, 2H), 4.59 (s, 4H), 5.80–6.40 (m, 3H), 6.23 (s, 4H), 7.78 (s, 2H). ^{13}C-NMR (75 MHz, $CDCl_3$) δ: 17.27, 26.81, 38.78, 40.01, 64.73, 66.61, 69.71, 72.58, 123.89, 128.36, 130.74, 145.83, 165.98, 177.73. FAB-HRMS (m/z): calculated 565.2908 [M+1], found 565.2922.

Synthesis of 3-[1-(2,2-dimethyl-propionyloxymethyl)-1*H*-[1,2,3]triazol-4-ylmethoxy]-2,2-bis-[1-(2,2-dimethyl-propionyloxymethyl)-1*H*-[1,2,3]triazol-4-ylmethoxymethyl]-propyl acrylate, 3.4c. Compound **3.4c** was prepared as described for **3.4a**. Yield: 61%. ^{1}H-NMR (300 MHz, $CDCl_3$) δ: 1.16 (s, 27H), 3.46 (s, 6H), 4.11 (s, 2H), 4.55 (s, 6H), 5.80–6.42 (m, 3H), 6.22 (s, 6H), 7.78 (s, 3H). ^{13}C-NMR (75 MHz, $CDCl_3$) δ: 26.82, 38.79, 44.46, 63.26, 64.73, 68.87, 69.78, 123.98, 128.31, 130.75, 145.63, 165.76, 177.69. FAB-HRMS (m/z): calculated 776.3865 [M+1], found 776.3991.

Synthesis of POM-protected polyacrylate 3.5a. The homopolymerization in THF (~1 M) with AIBN (2 mol%) was carried out in an air-free tube. After three cycles of freeze-pump-thaw, the solution was stirred at 60 ºC for 23 h. The solution was precipitated in hexane to yield POM-protected polymer in a quantitative yield. ^{1}H-NMR (300 MHz, CD_3OD) δ: 1.16 (s, 9H), 1.50–2.50 (m, 3H), 1.87 (s, 2H), 3.57 (s, 2H), 4.12 (s, 2H), 4.56 (s, 2H), 6.32 (s, 2H), 8.13 (s, 1H).

Synthesis of POM-protected polyacrylate 3.5b. The polymer was prepared as described for POM-protected polyacrylate **3.5a**. ^{1}H-NMR (300 MHz, CD_3OD) δ: 0.88 (s, 3H), 1.15 (s, 18H), 1.50–2.50 (m, 3H), 3.35 (s, 4H), 3.95 (s, 2H), 4.54 (s, 4H), 6.32 (s, 4H), 8.11 (s, 2H).

Synthesis of POM-protected polyacrylate 3.5c. The polymer was prepared as described for POM-protected polyacrylate **3.5a**. ^{1}H-NMR (300 MHz, CD_3OD) δ: 1.15 (s, 27H), 1.50–2.50 (m, 3H), 3.45 (s, 6H), 4.04 (s, 2H), 4.51 (s, 6H), 6.32 (s, 6H), 8.10 (s, 3H).

Synthesis of polyacrylate 3.5a. Polyacrylate containing POM-protected triazole (0.29 g, 0.91 mmol, 1 equiv.) was treated with 0.1 M NaOH/MeOH (10 mL, 1.0 mmol, 1.1 equiv.) at room temperature under N_2 for 1 h. The solution was neutralized with 1 M HCl aq. solution to pH 8. The solution was concentrated in vacuo followed by dialysis against water and then methanol to yield polyacrylate **3.5a**. ^{1}H-NMR (300 MHz, CD_3OD) δ: 1.50–2.50 (m, 3H), 1.86 (s, 2H), 3.53 (s, 2H), 4.11 (s, 2H), 4.60 (s, 2H), 7.75 (s, 1H). ^{13}C-NMR (75 MHz, CD_3OD) δ: 28.62, 34.85, 41.54, 61.84, 63.09, 66.55, 128.55, 142.38, 174.70.

Synthesis of polyacrylate 3.5b. The polymer was prepared as described for polyacrylate **3.5a**. ^{1}H-NMR (300 MHz, CD_3OD) δ: 0.83 (s, 3H), 1.50–2.50 (m, 3H), 3.35 (s, 4H), 3.91 (s, 2H), 4.51 (s, 4H), 7.72 (s, 2H). ^{13}C-NMR (75 MHz, CD_3OD) δ: 16.72, 25.88, 30.86, 39.70, 63.56, 66.95, 72.29, 128.41, 142.42, 174.29.

Synthesis of polyacrylate 3.5c. The polymer was prepared as described for polyacrylate **3.5a**. ^{1}H-NMR (300 MHz, CD_3OD) δ: 1.50–2.50 (m, 3H), 3.42 (s, 6H), 4.04 (s, 2H), 4.51 (s, 6H), 7.70 (s, 3H). ^{13}C-NMR (75 MHz, CD_3OD) δ: 25.84, 30.82, 44.17, 64.02, 65.91, 68.54, 128.30, 142.31, 174.27.

Synthesis of but-3-yn-1-yl acrylate, 3.7. Compound **3.7** was prepared as described for **3.3a**. Yield: 75%. ^{1}H-NMR (300 MHz, $CDCl_3$) δ: 2.02 (s, 1H), 2.57 (m, 2H), 4.27 (m, 2H), 5.80–6.43 (m, 3H). ^{13}C-NMR (75 MHz, $CDCl_3$) δ: 18.97, 62.21, 69.94, 79.97, 128.09, 131.26, 165.91. EI-HRMS (m/z): calculated 125.1372 [M+1], found 125.0599.

Synthesis of 2-(1-{[(2,2-dimethylpropanoyl)oxy]methyl}-1*H*-1,2,3-triazol-4-yl)ethyl acrylate, 3.8. Compound **3.8** was prepared as described for **3.4a**. Yield: 68%. ^{1}H-NMR (300 MHz, $CDCl_3$) δ: 1.18 (s, 9H), 3.13 (m, 2H), 4.44 (m, 2H), 5.81-6.42 (m, 3H), 6.21 (s, 2H), 7.63 (s, 1H). ^{13}C-NMR (75 MHz, $CDCl_3$) δ: 25.29, 26.72, 38.71, 62.97, 69.58, 123.04, 128.12, 131.02, 144.59, 165.87, 177.71. FAB-HRMS (m/z): calculated 282.1376 [M+1], found 282.1482.

Synthesis of POM-protected polyacrylate 3.9. The polymer was prepared as described for POM-protected polyacrylate **3.5a**. ^{1}H-NMR (300 MHz, CD_3OD) δ: 1.15 (s, 9H), 1.50–2.50 (m, 3H), 3.05 (s, 2H), 4.31 (s, 2H), 6.31 (s, 2H), 8.04 (s, 1H).

Synthesis of polyacrylate 3.9. The polymer was prepared as described for polyacrylate **3.5a**. ^{1}H-NMR (300 MHz, CD_3OD) δ: 1.50–2.50 (m, 3H), 3.00 (s, 2H), 4.25 (s, 2H), 7.64 (s, 1H). ^{13}C-NMR (75 MHz, CD_3OD) δ: 24.12, 34.43, 41.24, 63.18, 128.27, 141.68, 174.58.

3.2.4 Acid doped polymer preparation

A varying mole % of TFA, 25, 50, 75 and 100%, compared to moles of 1*H*-1,2,3-triazole content was added to a solution of the four polyacrylates in MeOH (~50 mg/mL). The solutions were stirred at room temperature for 10 min, and then cast onto the electrodes and dried as described in the characterization section.

3.3 Results and discussion

3.3.1 Monomer and polymer synthesis

The synthetic route to polyacrylates containing a different number of 1*H*-1,2,3-triazoles per repeat unit, all having the same spacer length from the polymer backbone, is shown in Scheme 3.1. The starting alcohols (**3.1a-c**) were first deprotonated with either NaH or NaOH, and then allowed to react with propargyl bromide. The resulting products (**3.2a-c**) were then allowed to react with acryloyl chloride in the presence of triethylamine to give the acrylate monomers **3.3a-c.** The overall yields ranged from 44 to 70%. The [3+2] cycloaddition of the acrylates with AMP was carried out under common click conditions (Cu(II) sulfate and sodium ascorbate in *t*-BuOH/water mixtures) to afford monomers containing pivaloyloxymethyl (POM)-protected triazoles (**3.4a-c**). AMP was selected due to the ease of cleavage of the POM protecting group, mild base, with the result being a 1*H*-1,2,3-triazole having the requisite labile proton for proton conduction.

Monomer **3.8** was synthesized using a similar procedure to that described above starting from 3-butyn-1-ol, **3.6** (Scheme 3.2).

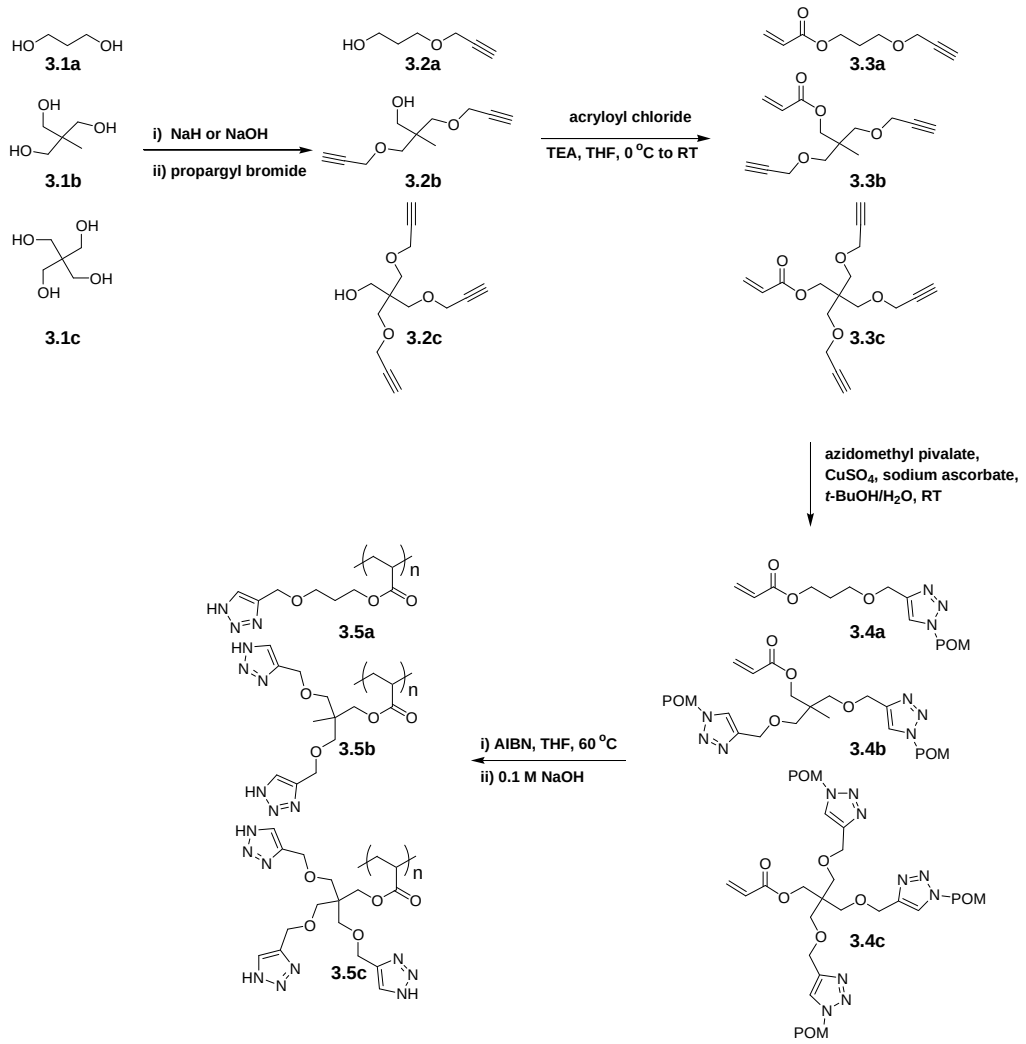

Scheme 3.1. Synthetic route to polyacrylates containing 1*H*-1,2,3-triazole moieties.

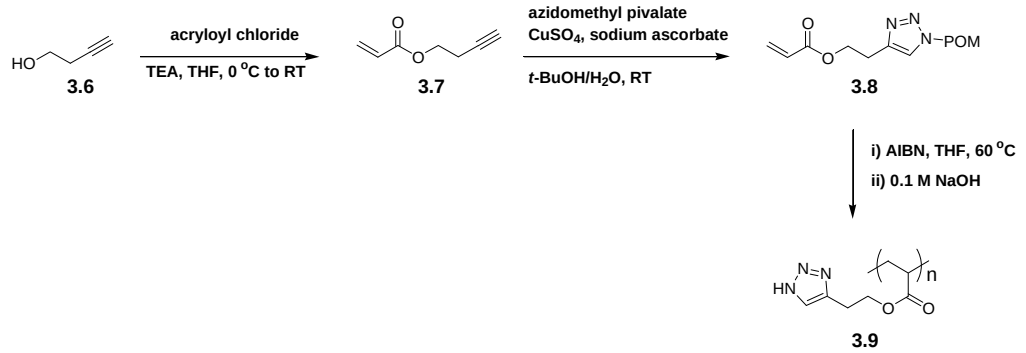

Scheme 3.2. Synthetic route to polyacrylate 3.9.

Polyacrylates containing POM-protected triazoles were obtained from polymerization of **3.4a-c** or **3.8** initiated with AIBN at 60 ºC for 23 h. Molecular weights of POM-protected polymers obtained from GPC are in the range of 7-9 kg/mol (Table 3.1). The removal of the POM protecting group with NaOH/MeOH followed by dialysis against water and methanol, respectively, yielded four different polyacrylates (**3.5a-c** and **3.9**). The ^{1}H-NMR spectra in Figure 3.1 show a shift of the peak of the proton on the triazole ring from δ 8.13 to δ 7.75 ppm, and the disappearance of the methylene and methyl resonance at δ 6.32 and δ 1.16 ppm indicates that the POM protecting group has been successfully removed. As determined by ^{1}H-NMR, more than 99% of the POM group has been removed for all polymers.

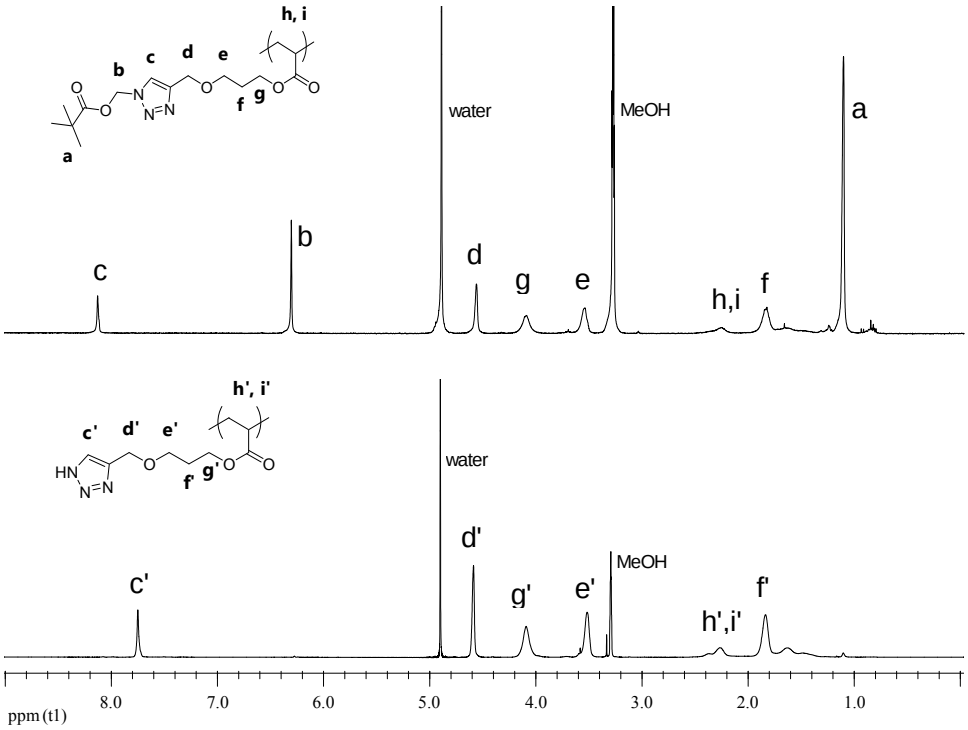

Figure 3.1. ^{1}H-NMR spectra of POM-protected polyacrylate 3.5a (top) and polyacrylate 3.5a (bottom) in CD_3OD.

3.3.2 Thermal analysis

The onset of decomposition, reported as the temperature corresponding to 5% weight loss as determined by TGA, and glass transition temperatures (T_g), determined by DSC, for the polymers are reported in Table 3.1. These polyacrylates are thermally stable up to approximately 200 ºC. All polymers are amorphous, and the T_g value increased from 12 to 52 ºC when the triazole content was increased from 32 to 47 wt.%. The weight % of triazole contained in each polymer was calculated by dividing the equivalent weight of triazole unit(s) (68 g/mol) by the equivalent weight of the polymer repeat unit. The incremental increase in T_g is presumably a result from a more highly hydrogen bonded network. Similar increases in T_g as a function of increasing heterocycle content have been reported for benzimidazole based polymers.[4]

Polyacrylate **3.5c** doped with different amount of TFA show similar T_g values (44-45 ºC), and these values are comparable to that of the undoped polymer (52 ºC). As reported earlier in Chapter 2 and by our group, the change in T_g was not significant when polyacrylates and polysiloxanes containing 1*H*-1,2,3-triazole were doped with varying amount of TFA.[5, 6]

Table 3.1. Physical and thermal properties of the polymers studied.

Polymer	Wt.% triazole	M_n (g/mol)[a]	PDI[a]	Decomp.onset (ºC)[b]	T_g (ºC)[c]
polyacrylate **3.5a**	32	7,800	1.69	214	12
polyacrylate **3.5b**	40	7,500	1.24	222	44
polyacrylate **3.5c**	47	9,400	1.25	263	52
polyacrylate **3.9**	40	7,900	1.62	230	46

[a] Determined by GPC on the POM-protected polymers using DMF as an eluent and calibrated against PMMA standards
[b] 5% weight loss as determined by TGA with a heating rate of 10 ºC/min from RT to 500 ºC under N_2.
[c] Obtained from DSC on the second heating cycle.

3.3.3 Proton conductivity

3.3.3.1 Homopolymers

In general, bulk conductivity depends on a number of factors including segmental mobility and charge carrier density.[16] As shown in Figure 3.2, proton conductivity of polyacrylate **3.5a** was higher than that of polyacrylates **3.5b** and **3.5c** throughout the temperature range studied with a maximum conductivity of 17.5 μS/cm. This can be attributed to the lower T_g of **3.5a** relative to the other samples. At lower temperatures, where conductivity is more influenced by mobility, a larger difference in conductivity was observed. The similarity of the conductivity curves for polyacrylates **3.5b** and **3.5c** suggest that there is an interplay of segmental mobility and charge carrier density. The decrease in segmental mobility, as evidenced by the higher T_g of **3.5c** versus **3.5b**, is apparently being offset by the increase in the number of protogenic groups per repeat unit. The influence of the spacer length between the protogenic group and the polymer backbone can be clearly seen when comparing the conductivities of polyacrylate **3.9** which are approximately 0.5 and 2 orders of magnitude lower than that of polyacrylate **3.5a** at 200 ºC and 80 ºC, respectively. A decrease in conductivity is observed when the spacer length is reduced. The similar dependence of conductivity on spacer length has also been observed for oligomers and polymers containing nitrogen-based heterocycles.[2, 16, 17]

Conductivity in polyelectrolytes as a function of temperature does not follow Arrhenius behavior, but can be described by the Vogel-Tamman-Fulcher (VTF) equation.[18]

$$\sigma = \sigma_0 \exp[-B/(T-T_0)] \qquad (1)$$

Since the conductivity (σ) is, in part, governed by the free volume conformational changes,[19] it is expected that log (σ) vs. T-T_g curves would converge given a constant protogenic charge carrier density. The normalized conductivity vs. T-T_g plot is shown in Figure 3.3. The similarity in shape of the curves suggests that all of these polymers have the same proton transport mechanism.[3] The effect of charge carrier reduction in the system was clearly observed when the wt.% of triazole was decreased from 47 to 32, while the spacer length was fixed.

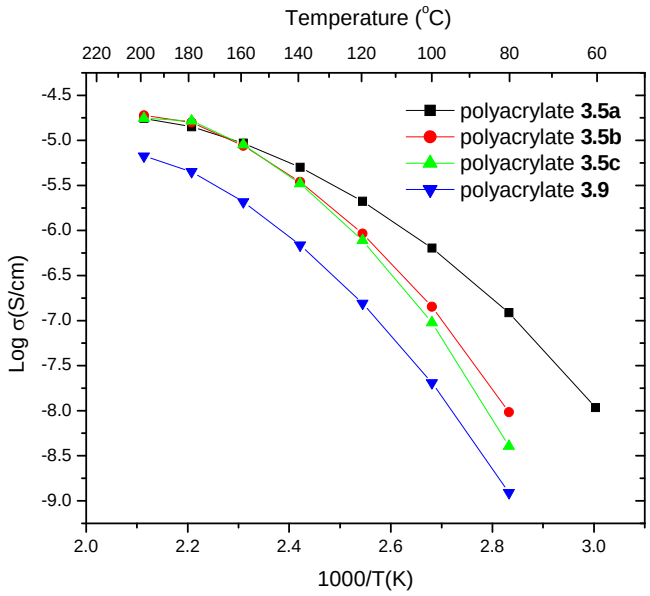

Figure 3.2. Conductivity plot of polyacrylates containing different triazole contents.

One would expect that the conductivity curves of **3.5b** and **3.9** would converge given almost identical triazole content (40 wt.%) and T_g (44 vs. 46 ºC) in a normalized plot; however, that was not the case. The conductivity of polyacrylate **3.9** was lower than that of polyacrylate **3.5b**, and was even lower than that of polyacrylate **3.5a** (32 wt.% with one triazole per repeat unit). These observations suggest that besides segmental

mobility and charge carrier density, there is at least one more factor that influences proton conductivity. Similar to the previous work in our group on terpolymers of 1*H*-1,2,3-triazole containing polyacrylate and poly(ethylene glycol)methyl ether acrylate,[5] the chemical composition of the polymer, i.e. the presence of oxygen atoms, may have an effect on proton transport. In addition, the branching structure of polyacrylate **3.5b** could possibly provide a more closely packed heterocycle network, leading to a more continuous hydrogen pathway for proton transport.

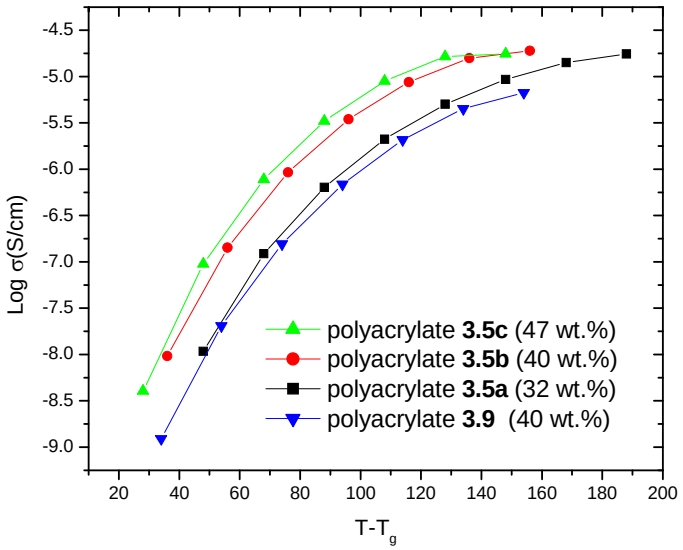

Figure 3.3. Conductivity vs. T-T$_g$ plot of the polyacrylates.

3.3.3.2 Trifluoroacetic acid doped materials

The conductivity plot of TFA doped polyacrylate **3.5a** is shown in Figure 3.4. The same trend was observed for the other three polymers studied. Doping the polyacrylates containing 1,2,3-triazole with TFA increased the conductivity of the membranes up to approximately 1.5 to 2 orders of magnitude when 50 mol% of TFA was added (Figure

3.5). On the other hand, the optimized TFA doping levels of polyacrylates containing poly(ethylene glycol)methyl ether, polyphosphazene and polysiloxanes with pendant triazole reported earlier by our group were 100%, 100%, and 75%, respectively.[5-7] It should be noted that the degree of doping was from the feed ratio of TFA to triazole; therefore, the difference in the maximum doping level could arise from the loss of TFA during the conductivity measurement which was conducted at high temperatures under vacuum. A more accurate doping study with a determination of TFA amount should be performed. Despite the fluctuation, the maximum doping level (50-100%) is still greater compared to the imidazole based system with the maximum doping of ~15 mol% acid. This observation is likely due to the addition of the third nitrogen that could provide an additional proton acceptor site.

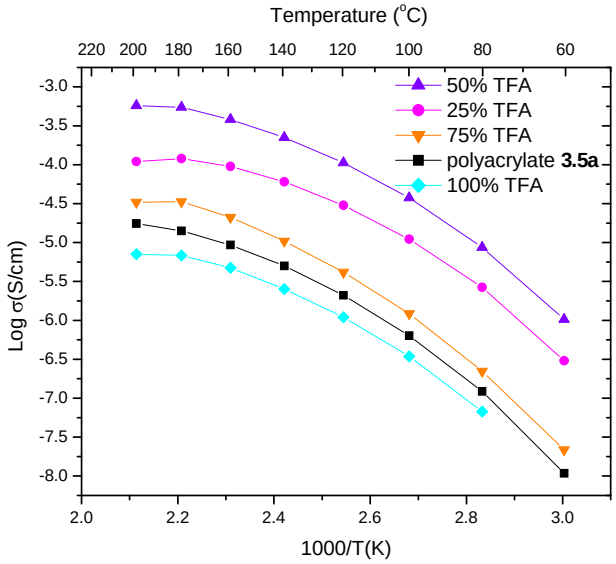

Figure 3.4. Conductivity of TFA doped polyacrylate 3.5a.

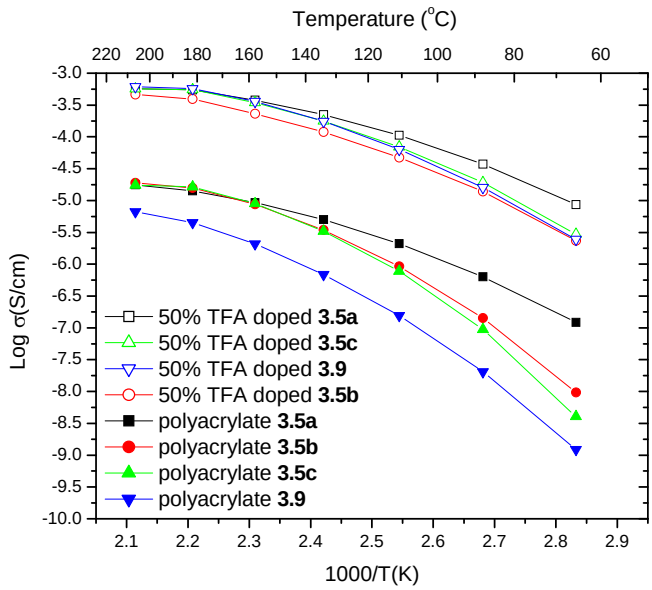

Figure 3.5. Proton conductivity plot of undoped and 50% TFA doped polyacrylates.

3.4 Conclusion

A series of polyacrylates containing a different number of 1*H*-1,2,3-triazole pendants have been successfully synthesized and characterized. The polymers are completely amorphous and thermally stable up to approximately 200 ºC. The proton conductivity is predominately governed by two competing factors: segmental mobility and charge carrier density of the protogenic side-groups. Introduction of more than one triazole per repeat unit did not result in an increase in conductivity as it was offset by the accompanying increase in T_g. Furthermore, a correlation between side-chain spacer length and proton conductivity was shown. Doping the polymers with TFA resulted in further conductivity increases with a maximum of 2 orders of magnitude compared to the undoped membranes.

3.5 References

1. Zhou, Z.; Li, S. W.; Zhang, Y. L.; Liu, M. L.; Li, W. *Journal of the American Chemical Society* **2005,** 127, (31), 10824-10825.

2. Scharfenberger, G.; Meyer, W. H.; Wegner, G.; Schuster, M.; Kreuer, K. D.; Maier, J. *Fuel Cells* **2006,** 6, (3-4), 237-250.

3. Persson, J. C.; Jannasch, P. *Chemistry of Materials* **2006,** 18, (13), 3096-3102.

4. Persson, J. C.; Jannasch, P. *Solid State Ionics* **2006,** 177, (7-8), 653-658.

5. Martwiset, S.; Woudenberg, R. C.; Granados-Focil, S.; Yavuzcetin, O.; Tuominen, M. T.; Coughlin, E. B. *Solid State Ionics* **2007,** 178, (23-24), 1398-1403.

6. Granados-Focil, S.; Woudenberg, R. C.; Yavuzcetin, O.; Tuominen, M. T.; Coughlin, E. B. *Macromolecules* **2007,** 40, (24), 8708-8713.

7. Higami, M.; Woudenberg, R. C.; Granados-Focil, S.; Yavuzcetin, O.; Tuominen, M. T.; Coughlin, E. B. *PMSE Preprints* **2007,** 97, 551-552.

8. Rostovtsev, V. V.; Green, L. G.; Fokin, V. V.; Sharpless, K. B. *Angewandte Chemie, International Edition in English* **2002,** 41, (14), 2596-2599.

9. Victoria D. Bock; Henk Hiemstra; Maarseveen, J. H. v. European Journal of Organic Chemistry 2006, 1, 51-68.

10. Kolb, H. C.; Finn, M. G.; Sharpless, K. B. *Angewandte Chemie, International Edition in English* **2001,** 40, (11), 2004-2021.

11. Loren, J. C.; Krasinski, A.; Fokin, V. V.; Sharpless, K. B. *Synlett* **2005**, (18), 2847-2850.

12. Thibault, R. J.; Takizawa, K.; Lowenheilm, P.; Helms, B.; Mynar, J. L.; Frechet, J. M. J.; Hawker, C. J. *Journal of the American Chemical Society* **2006,** 128, (37), 12084-12085.

13. Kang, S. K.; Kim, K. J.; Hong, Y. T. *Angew. Chem. Int. Ed.* **2002,** 41, (9), 1584-1586.

14. Calvo-Flores, F. G.; Isac-Garcia, J.; Hernandez-Mateo, F.; Perez-Balderas, F.; Calvo-Asin, J. A.; Sanchez-Vaquero, E.; Santoyo-Gonzalez, F. *Organic Letters* **2000,** 2, (16), 2499-2502.

15. Macdonald, J. R., Impedance Spectroscopy. In Wiley: New York, 2005; pp 16-20.

16. Persson, J. C.; Jannasch, P. *Chemistry of Materials* **2003,** 15, (16), 3044-3045.

17. Schuster, M.; Meyer, W. H.; Wegner, G.; Herz, H. G.; Ise, M.; Schuster, M.; Kreuer, K. D.; Maier, J. *Solid State Ionics* **2001,** 145, (1-4), 85-92.

18. Ratner, M. A., In *Polymer Electrolyte Reviews*, Elsevier Applied Science: New York, 1987; pp 173-235.

19. Schuster, M. F. H.; Meyer, W. H.; Schuster, M.; Kreuer, K. D. *Chemistry of Materials* **2004,** 16, (2), 329-337.

CHAPTER 4

POLYNORBORNENES CONTAINING 1*H*-1,2,3-TRIAZOLE AND POLYHEDRAL OLIGOMERIC SILSESQUIOXANE

4.1 Introduction

1*H*-1,2,3-triazole has been tethered to several flexible polymeric backbones including polyacrylates,[1, 2] polysiloxanes[3] and polyphosphazenes.[4] Proton conductivities of these polymers depend strongly on segmental mobility and charge carrier density. A maximum conductivity of $10^{-3.5}$ S/cm at 200 °C under anhydrous condition was obtained from polysiloxanes containing 1*H*-1,2,3-triazole. Although the polysiloxanes show high proton conductivities, these low T_g polymers lack long term stability for use as membranes in fuel cells. A hybrid organic-inorganic composite membrane would be one approach to improve the proton exchange membrane properties, as it can presumably combine thermal and oxidative/reductive stabilities of an inorganic material with the flexibility, strength and processibility of organic materials.[5-7] Polyhedral oligomeric silsesquioxanes (POSS) are one class of materials that have shown the ability to be copolymerized with common monomers to form hybrid materials.[8-13] POSS is a cubic caged nanoparticle containing a Si_8O_{12} core with organic periphery, including aliphatic, aromatic and aryl substituents.[6] Polyvinyl imidazole/POSS nanocomposites have been shown to exhibit an improvement in proton conductivity when compared with the pure polyvinyl imidazole.[14] The conductivity reaches 10 x 10^{-4} S/cm at 200 °C when the membrane was doped with phosphoric acid.

In this work, to obtain a membrane with good thermal and mechanical properties, 1*H*-1,2,3-triazole was tethered to a relative high T_g backbone, polynorbornene. Structure-

property relationships of polynorbornenes with pendant triazole moieties were investigated. To study the possibility of increasing oxidative stability and mechanical strength of the norbornenyl polymers, copolymers with varying degrees of norbornene containing POSS were synthesized and characterized.

4.2 Experimental

4.2.1 Materials

5-Norbornene-2-methanol, *cis*-5-norbornene-*exo*-2,3-dicarboxylic anhydride, 5-norbornene-2-carboxylic acid, sodium hydride (NaH), propargyl bromide, *N,N'*-dicyclohexylcarbodiimide (DCC), 4-(dimethylamino)pyridine (DMAP), 3-butyn-1-ol, copper(II) sulfate ($CuSO_4.5H_2O$), sodium ascorbate and *t*-butanol (*t*-BuOH) were purchased either from Sigma-Aldrich or VWR and used as received. NorbornenylethylIsobutyl POSS® (NB-POSS) was purchased from Hybrid Plastics and used as received. cis-exo-2,3-Bis(hydroxymethyl) bicyclo[2.2.1]hept-5-ene, **4.4**,[15] azidomethyl pivalate (AMP)[16] and the third generation Grubbs catalyst,[17] were prepared as reported in the literature.

4.2.2 Synthesis

5-Prop-2-ynyloxymethyl-bicyclo[2.2.1]hept-2-ene, 4.2. To a solution of 5-norbornene-2-methanol, **4.1**, (0.98 g, 8.05 mmol, 1 equiv.) in DMF (50 mL), NaH (0.58 g, 24.15 mmol, 3 equiv.) was added. The solution was stirred at room temperature under N_2 for 5 min. Propargyl bromide (2.40 g, 16.1 mmol, 2 equiv.) was added slowly with stirring at 0 ºC. The reaction was stirred at room temperature for 19 h. The mixture was diluted with 100 mL of water. The product was extracted with hexane (3 x 50 mL), dried

over $MgSO_4$, filtered, and concentrated. The crude product was further purified by column chromatography, using hexane:diethyl ether (95:5) as an eluent, to give a mixture of endo and exo product. Yield: 60%. ^{1}H-NMR ($CDCl_3$, 298 K, 300 MHz) δ: 0.49-0.54, 1.41-1.44 and 1.78-1.87 (m, 4H), 1.11-1.32 (m, 4H), 1.57-2.37 (m, 2H), 2.39-2.42 (m, 2H), 2.76-2.92 (m, 4H), 3.12-3.58 (m, 4H), 4.10 (d, 2H), 4.16 (d, 2H), 5.95-6.14 (m, 4H). ^{13}C-NMR ($CDCl_3$, 298 K, 300 MHz) δ: 29.16, 29.73, 38.59, 38.73, 41.53, 42.21, 43.70, 43.92, 45.04, 49.39, 58.09, 58.18, 73.90, 74.00, 74.14, 74.79, 80.04, 80.13, 132.42, 136.53, 136.70, 137.22. EI-HRMS (m/z): calculated 162.2283 [M+1], found 162.1039.

2,2-Dimethyl-propionic acid 4-(bicyclo[2.2.1]hept-5-en-2-ylmethoxymethyl)-[1,2,3]triazol-1-ylmethyl ester, 4.3. To a solution of compound **4.2** (0.78 g, 4.81 mmol, 1 equiv.) in 10 mL *t*-BuOH/H_2O (2/1), azidomethyl pivalate (AMP, 0.91 g, 5.77 mmol, 1.2 equiv.), $CuSO_4.5H_2O$ (0.06 g, 0.24 mmol, 0.05 equiv.), and sodium ascorbate (0.29 g, 1.46 mmol, 0.3 equiv.) were added. The solution was stirred at room temperature for 18 h. The product was extracted with ethyl acetate (3 x 50 mL) and washed with ammonium hydroxide aqueous solution and brine. The organic portion was dried over $MgSO_4$ and the volatiles were removed in vacuo. The crude product was further purified by column chromatography, using hexane:ethyl acetate (1:1) as an eluent, to give 1.02 g of product. Yield: 66%. ^{1}H-NMR ($CDCl_3$, 298 K, 300 MHz) δ: 0.49-0.54 and 1.41-2.42 (m, 10H), 1.19 (s, 18H), 2.76-2.92 (m, 4H), 3.11-3.60 (m, 4H), 4.59 and 4.65 (s, 4H), 5.85-6.15 (m, 4H), 6.22 (s, 4H), 7.78 and 7.80 (s, 2H). ^{13}C-NMR ($CDCl_3$, 298 K, 300 MHz) δ: 26.81, 27.15, 29.12, 29.60, 29.69, 38.68, 38.79, 41.49, 42.16, 43.65, 43.90, 44.98, 49.38, 64.16, 64.24, 69.66, 74.47, 75.41, 123.82, 123.86, 132.30, 136.49, 136.68, 137.24, 146.10, 146.20, 177.78. FAB-HRMS (m/z): calculated 320.3988 [M+1], found 320.1971.

5,6-Bis-prop-2-ynyloxymethyl-bicyclo[2.2.1]hept-2-ene, 4.5. To a solution of compound **4.4** (2.0 g, 12.99 mmol, 1 equiv.) in DMSO (20 mL), NaOH (2.07 g, 51.95 mmol, 4 equiv.) in 10 mL of water was added. The solution was stirred at room temperature under N_2 for 30 min. Propargyl bromide (7.7 g, 51.95 mmol, 4 equiv.) was added slowly. The reaction was stirred at 40 ºC for 21 h. The mixture was diluted with 100 mL of water. The product was extracted with diethyl ether (3 x 50 mL), dried over $MgSO_4$, filtered, and concentrated. The crude product was further purified by column chromatography, using hexane:ethyl acetate (2:3) as an eluent, to give the product. Yield: 15%. ^{1}H-NMR ($CDCl_3$, 298 K, 300 MHz) δ: 1.29-1.50 (m, 2H), 1.80 (m, 2H), 2.43 (s, 2H), 2.77 (m, 2H), 3.38-3.72 (m, 4H), 4.15 (s, 4H), 6.15 (t, 2H). ^{13}C-NMR ($CDCl_3$, 298 K, 300 MHz) δ: 40.48, 42.76, 44.82, 58.22, 71.49, 74.26, 79.96, 137.35. FAB-HRMS (m/z): calculated 231.3022 [M+1], found 231.1356.

2,2-Dimethyl-propionic acid 4-{5-[1-(2,2-dimethyl-propionyloxymethyl)-1*H*-[1,2,3]triazol-4-ylmethoxymethyl]-bicyclo[2.2.1]hept-5-en-2-ylmethoxymethyl}-[1,2,3]triazol-1-ylmethyl ester, 4.6. To a solution of compound **4.5** (0.50 g, 2.17 mmol, 1 equiv.) in 10 mL *t*-BuOH/H_2O (2/1), azidomethyl pivalate (AMP, 1.02 g, 6.52 mmol, 3 equiv.), $CuSO_4.5H_2O$ (0.054 g, 0.22 mmol, 0.1 equiv.), and sodium ascorbate (0.26 g, 1.30 mmol, 0.6 equiv.) were added. The solution was stirred at room temperature for 41 h. The product was extracted with ethyl acetate (3 x 50 mL) and washed with ammonium hydroxide aqueous solution and brine. The organic portion was dried over $MgSO_4$ and the volatiles were removed in vacuo. The crude product was further purified by column chromatography, using hexane:ethyl acetate (2:3) as an eluent, to give 0.19 g of product. Yield: 16%. ^{1}H-NMR ($CDCl_3$, 298 K, 300 MHz) δ: 1.19 (s, 18H), 1.39 (m, 2H), 1.77 (m,

2H), 2.72 (m, 2H), 3.37-3.69 (m, 4H), 4.61 (s, 4H), 6.15 (t, 2H), 6.25 (s, 4H), 7.85 (s, 2H). ^{13}C-NMR ($CDCl_3$, 298 K, 300 MHz) δ: 26.83, 38.80, 40.53, 42.74, 44.80, 64.24, 69.77, 72.01, 124.09, 137.31, 145.83, 177.78. FAB-HRMS (m/z): calculated 545.6433 [M+1], found 545.3071.

Synthesis of bicyclo[2.2.1]hept-5-ene-2-carboxylic acid but-3-ynyl ester, 4.8. To a solution of 5-norbornene-2-carboxylic acid (2.0 g, 14 mmol, 1 equiv.) in dichloromethane (35 mL), *N,N′*-dicyclohexylcarbodiimide (3.6 g, 17 mmol, 1.2 equiv.), 4-(dimethylamino)pyridine (0.18 g, 1.5 mmol, 0.1 equiv.) and 3-butyn-1-ol (1.3 mL, 17 mmol, 1.2 equiv.) were added. The solution was stirred at room temperature under N_2 for 19 h. The mixture was diluted with 100 mL of water. The product was extracted with ethyl acetate (3 x 50 mL), dried over $MgSO_4$, filtered, and concentrated. The crude product was further purified by column chromatography, using hexane:ethyl acetate (4:1) as an eluent, to give the mixture of endo and exo products. Yield: 87%. ^{1}H-NMR ($CDCl_3$, 298 K, 300 MHz) δ: 1.23-1.41 (m, 4H), 1.88 (m, 4H), 1.98 (s, 2H), 2.45 (m, 4H), 2.88-3.20 (m, 6H), 4.04-4.19 (m, 4H), 5.93-6.16 (m, 4H). ^{13}C-NMR ($CDCl_3$, 298 K, 300 MHz) δ: 19.00, 29.16, 30.30, 41.64, 42.53, 43.06, 43.20, 45.73, 46.32, 46.67, 49.60, 61.87, 62.00, 69.77, 69.86, 80.14, 80.25, 132.35, 135.70, 137.78, 138.08, 174.43, 175.93.

Synthesis of bicyclo[2.2.1]hept-5-ene-2-carboxylic acid 2-[1-(2,2-dimethyl-propionyloxymethyl)-1*H*-[1,2,3]triazol-4-yl]-ethyl ester, 4.9. Compound **4.9** was prepared as described for **4.3,**[18] using compound **4.8** (1.3 g, 7.1 mmol, 1 equiv.), azidomethyl pivalate (AMP, 1.3 g, 8.5 mmol, 1.2 equiv.), $CuSO_4.5H_2O$ (0.09 g, 0.36 mmol, 0.05 equiv.), and sodium ascorbate (0.42 g, 2.1 mmol, 0.3 equiv.) in *t*-BuOH/H_2O (2/1) mixture (10 mL). Yield: 69%. ^{1}H-NMR ($CDCl_3$, 298 K, 300 MHz) δ: 1.15 (s, 18H),

1.20-1.39 (m, 4H), 1.83-2.19 (m, 4H), 2.87-3.05 (m, 10H), 4.27 (m, 4H), 5.78-6.15 (m, 4H), 6.19 (s, 4H), 7.62 (s, 2H). ^{13}C-NMR ($CDCl_3$, 298 K, 300 MHz) δ: 25.45, 26.80, 29.14, 30.30, 38.75, 41.58, 42.48, 43.04, 43.23, 45.66, 46.30, 46.53, 49.58, 62.70, 62.91, 69.90, 122.97, 132.21, 135.65, 137.81, 138.04, 144.83, 144.91, 174.48, 175.99, 177.78. FAB-HRMS (m/z): calculated 348.4089 [M+1], found 348.1923.

Polymerization. A typical ring-opening metathesis polymerization was carried out as follows. A solution of norbornenyl monomer(s) in dichloromethane (0.2 M) was first purged with N_2 for 5 min. A solution of the third generation Grubbs catalyst in dichloromethane (0.005 M) was then introduced. For all polymerizations, the target molecular weight was 50,000 g/mol, with the exception of polynorbornene with an ester linkage (10,000 g/mol). The solution was stirred at room temperature for 5-10 min and was terminated by the addition of excess ethyl vinyl ether. The solution was concentrated and precipitated in cold diethyl ether.

Deprotection of POM. A typical deprotection of POM was carried out as follows. Polynorbornene containing POM-protected triazole (1 molar equiv.) was treated with 0.1 M NaOH/MeOH (1.1 molar equiv.) at room temperature under N_2 for 2 h. The solution was neutralized with 1 M HCl to a pH 7. The polymer was precipitated into water. The polymer was collected and washed with water before drying at 30 °C under vacuum overnight.

4.2.3 Characterization

^{1}H-NMR (300 MHz) and ^{13}C-NMR (75 MHz) spectra were obtained on a Bruker DPX-300 NMR Spectrometer with the samples dissolved in either chloroform-*d* ($CDCl_3$) or dimethyl sulfoxide-d_6 (DMSO- d_6). Molecular weight and polydispersity index (PDI)

were measured by gel permeation chromatography (GPC) in THF at 40 ºC with a flow rate of 1 mL/min on systems equipped with two-column sets (from Polymer Laboratories), and refractive index detectors (K-2301). Polystyrene (PS) standards were used for molecular weight calibration. Fourier transform infrared (FTIR) spectra were measured on a Perkin-Elmer Spectrum One FT-IR spectrometer equipped with a universal ATR sampling accessory. Thermogravimetric analysis (TGA) was carried out using a TA Instruments TGA 2950 thermogravimetric analyzer with a heating rate of 10 ºC/min from room temperature to 500 ºC under nitrogen. Glass transition temperatures were obtained by differential scanning calorimetry (DSC) using a TA Instruments DSC Q200 V23.5. Samples were analyzed with a heating rate of 10 ºC/min from 0 ºC to 170 ºC under a flow of helium (25 mL/min). WAXD was performed using Ni-filtered Cu Kα radiation (λ=1.54 Å) from a Rigaku rotating anode (operated at 60 kV, 45 mA). The X-ray was collimated by a set of three pinholes. Dynamic mechanical analysis (DMA) was performed on a TA Instruments DMA 2980. Samples were analyzed in tension at 1.0 Hz over a temperature range of 25-150 °C at a ramp of 10 °C /min. Samples were prepared from press-molding at 80 °C for 10 min. Sample dimensions were 6 mm long, 2 mm wide, and 0.3 mm thick. Film preparation and impedance measurement were carried out as reported earlier.[18]

4.3 Results and discussions

4.3.1 Synthesis

4.3.1.1 Monomer synthesis

The synthesis of the norbornenyl monomers is shown in Scheme 4.1. The starting alcohols (**4.1** and **4.4**) were first deprotonated with NaH, and then allowed to react with propargyl bromide. Compound **4.7** was allowed to react with 5-norbornene-2-carboxylic acid via DCC coupling. The [3+2] cycloaddition of compounds **4.2**, **4.5** and **4.8** with AMP was carried out in the presence of copper (II) sulfate and sodium ascorbate in *t*-BuOH/water mixtures to afford monomers containing pivaloyloxymethyl (POM)-protected triazoles (**4.3**, **4.6** and **4.9**).

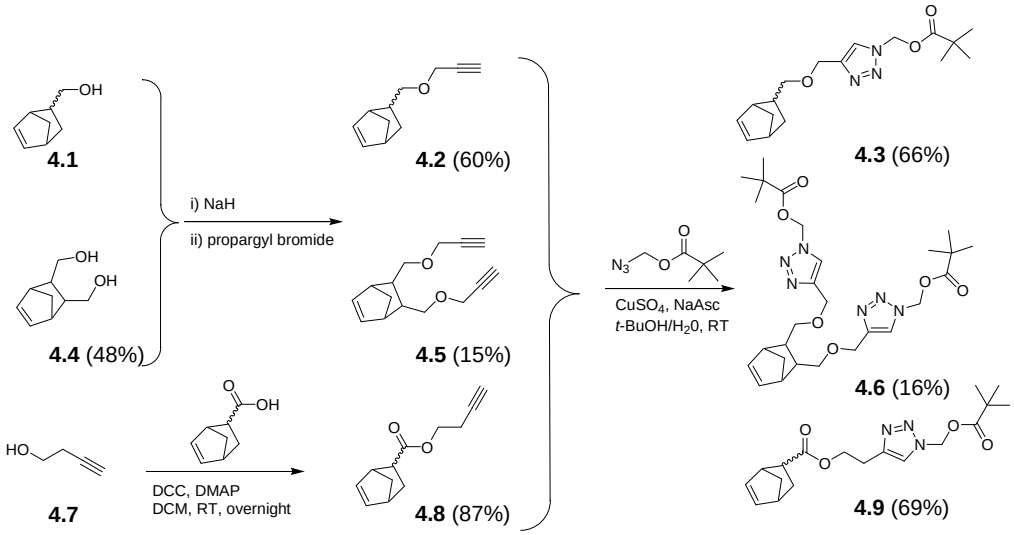

Scheme 4.1. Synthetic route to POM-protected norbornene monomers.

4.3.1.2 Polymer synthesis

The norbornene-based homopolymers containing POM-protected triazole(s) were obtained from ring-opening metathesis polymerization (ROMP) of **4.3** or **4.6** or **4.9** initiated with the third generation Grubbs catalyst in dichloromethane. The copolymers with composition varying from 2-9 mol% of NB-POSS were prepared using a similar procedure to that described above, Scheme 4.2. The percentages of POSS incorporation

in each polymer were determined by ^{1}H-NMR, and are in agreement with the feed ratio (Figure 4.1). Molecular weights of POM-protected polymers obtained from GPC are in the range of 41-56 kg/mol for the polymers with an ether linkage(s), and is 12 kg/mol for the polymer with an ester linkage, all polymers have narrow PDIs (Table 4.1). Removal of the POM protecting group was accomplished with 0.1 M NaOH/MeOH. The presence of the free NH triazole was confirmed using ^{1}H-NMR by a shift of the resonance for the proton on the heterocycle ring from δ 8.14 to δ 7.77, and the disappearance of resonances corresponding to the POM group at δ 6.32 and δ 1.14 ppm. More than 98% of protecting groups were successfully removed for all polymers. Polynorbornenes with one triazole and two triazoles per repeat unit are designated as PNB and PNB2, respectively. Polynorbornenyl copolymers are designated as PNB-x%POSS, where x is mole percent of POSS incorporation. A copolymer of PNB2 with 10 mol% of POSS was also synthesized, and is referred to as PNB2-10%POSS. The chemical structures of these polymers are shown in Figure 4.2.

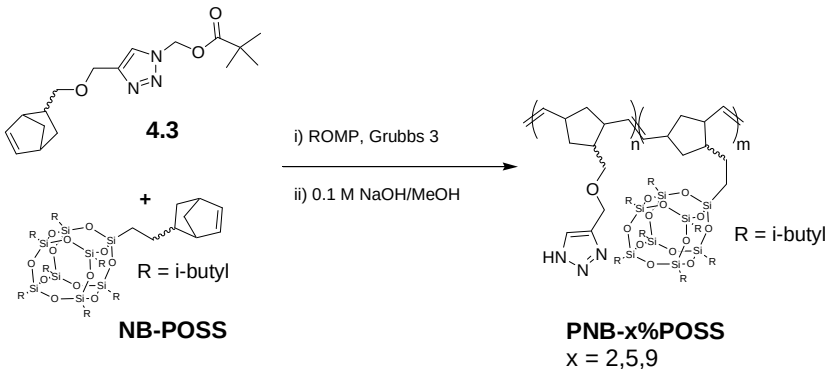

Scheme 4.2. Copolymerizations of norbornenes containing triazole and POSS.

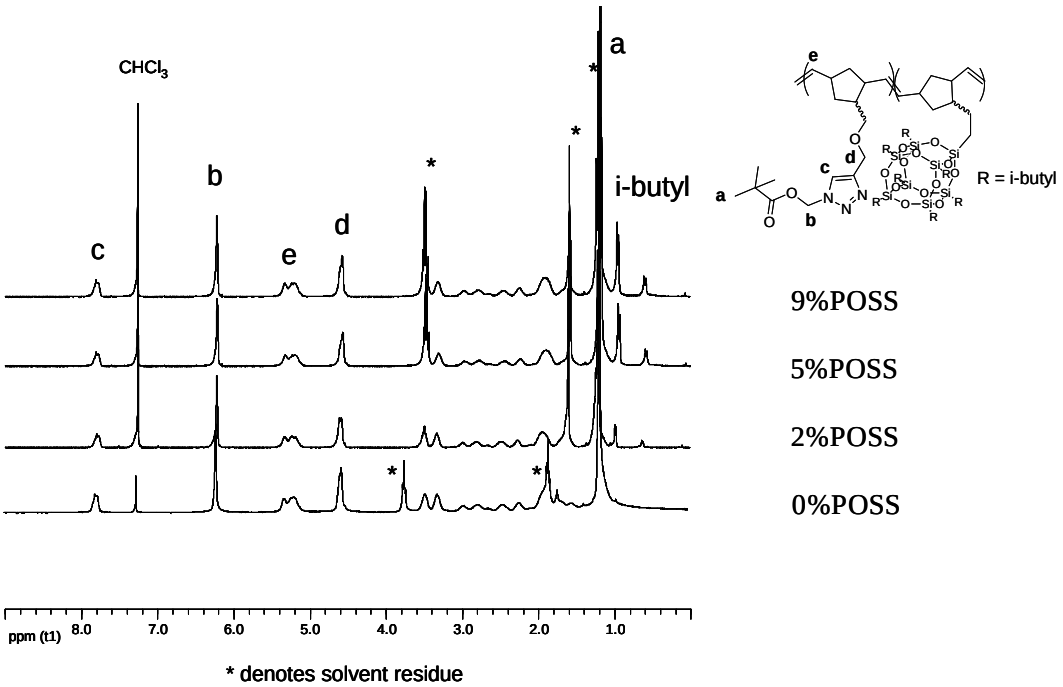

Figure 4.1. ^{1}H-NMR spectra of POM-protected polynorbornenes.

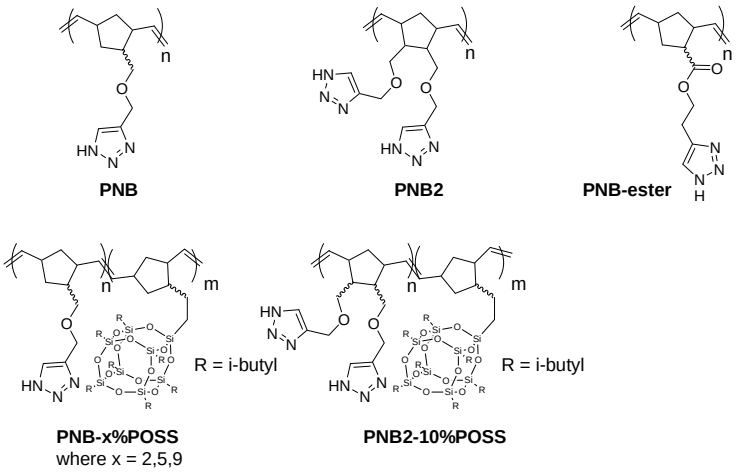

Figure 4.2. Chemical structures of polynorbornenes.

Table 4.1. Physical and thermal properties of polynorbornenes studied.

Polymer	Wt.% triazole	M_n[a]	PDI[a]	$T_{5\%}$ (ºC)[b]	T_g (ºC)[c]
PNB	33	50,500	1.20	335	68
PNB-2%POSS	30	55,200	1.17	349	64
PNB-5%POSS	27	41,000	1.20	354	72
PNB-9%POSS	22	56,500	1.14	348	71
PNB2	43	49,700	1.08	293	64
PNB2-10%POSS	32	43,800	1.13	291	60
PNB-ester	29	12,400	1.10	233	72

[a] Determined by GPC on the triazole-protected polymers using THF as an eluent and calibrated against PS standards.
[b] 5% weight loss as determined by TGA with a heating rate of 10 ºC/min from RT to 500 ºC under N_2.
[c] Obtained from DSC on the second heating cycle.

Figure 4.3 shows infrared spectra of the norbornenyl homopolymer, copolymers and NB-POSS monomer. As the degree of POSS incorporation increases, the intensities of the bands corresponding to NB-POSS increase. The absence of the bending and stretching bands of Si-OH at 890 cm^{-1} and 3250 cm^{-1} confirms that there was no hydrolysis at the POSS cage.[19]

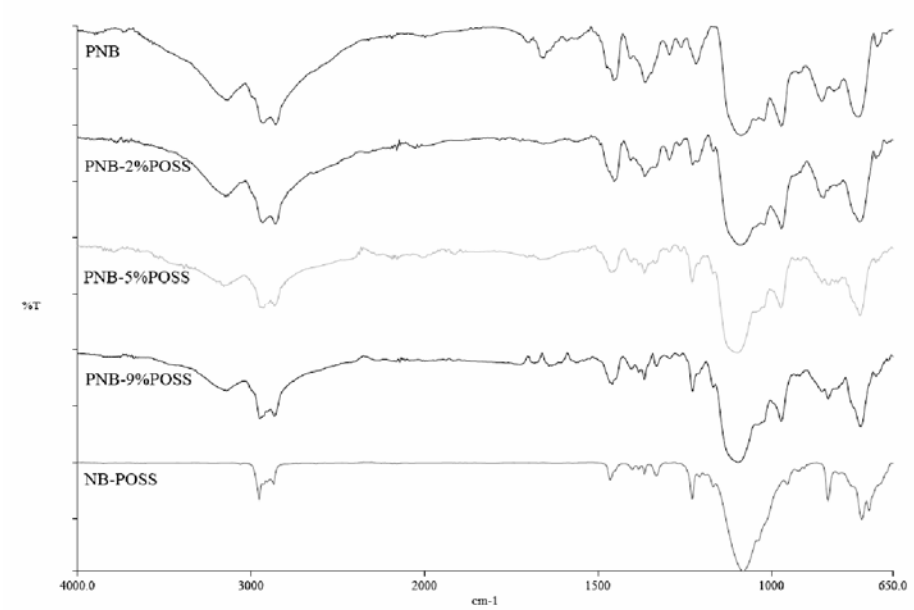

Figure 4.3. IR spectra of the polymers studied and NB-POSS.

4.3.2 Thermal analysis

The 5% decomposition temperatures and glass transition temperatures (T_g) of the polymers are listed in Table 4.1. All polymers with an ether linkage(s) are stable up to approximately 300 °C, while the one with an ester linkage is stable up to only 230 °C. Although it has been reported that addition of POSS increases decomposition temperatures of several polymers,[6, 20] only a moderate increase in decomposition temperature (up to 19 °C) was observed in this study.

All polymers are amorphous and display a single T_g. Similar to previous work by our group on copolymers of dicyclopentadiene and mono-or tris(norbornenyl)-substituted polyhedral oligomeric silsesquioxanes,[13] POSS incorporation has little effect on T_g. In addition, Xu and coworkers have reported that at low POSS loading, less than 3-4 mol%, POSS acts as an inert diluent, thus decreasing the T_g.[21] A slight drop in T_g was observed when 2 mol% POSS was incorporated.

4.3.3 Proton conductivity

4.3.3.1 Structure-property relationship

In general, proton conductivity strongly depends on two competing factors: segmental mobility and charge carrier density.[22] Our group has previously shown that introduction of more than one triazole per repeat unit in a polyacrylate system did not result in an increase in conductivity as it was offset by the accompanying increase in T_g.[2] The same explanation can still be used for polynorbornene containing triazole system. As shown in Figure 4.4 (left), PNB2, having two triazoles per repeat unit, shows ~1.5 orders of magnitude higher conductivity when compared to PNB, which has only one triazole. The normalized conductivity versus T-T_g plot in Figure 4.4 (right) clearly shows the

decrease in conductivity with decreasing triazole content. As the two polymers have similar T_g's (68 vs. 64 °C), an increase in wt.% triazole, calculated by dividing the equivalent weight of triazole unit(s) by the equivalent weight of the polymer repeat unit, from 33% to 43% can account for the observed increase in proton conductivity.

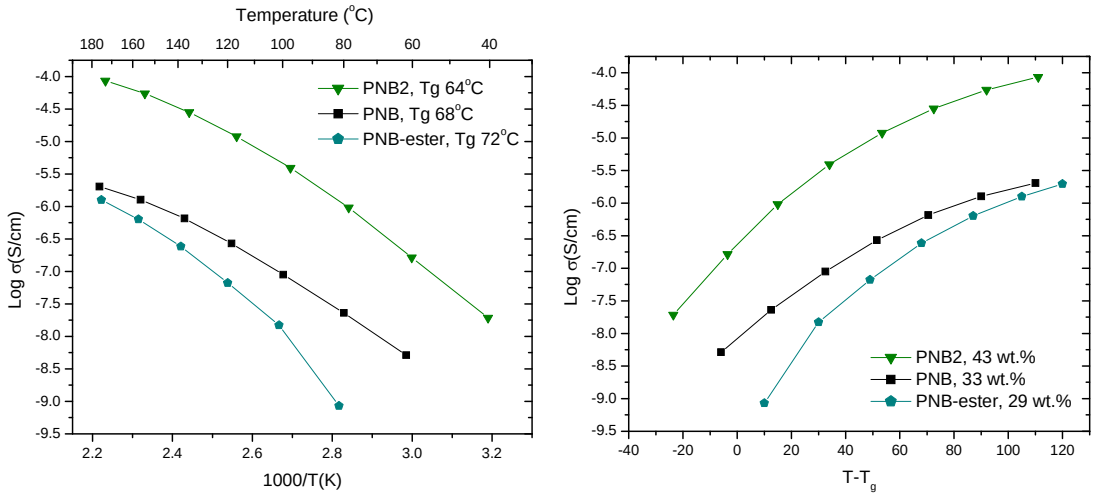

Figure 4.4. Proton conductivity (left) and normalized (right) plots of PNB, PNB2 and PNB-ester.

Polynorbornenes containing triazole with different linkages are also compared. Although the molecular weight of PNB-ester is almost 5 times lower than that of PNB, we do not expect this difference to affect proton conductivity since it has been reported that the effect of molecular weight on proton conductivity of poly(5-vinyltetrazole) is limited.[23] The polymer with the ether linkage shows a higher proton conductivity. This is not surprising as PNB has a lower T_g and a higher wt.% of triazole compared to PNB-ester.

4.3.3.2 POSS incorporation

Proton conductivities of PNB and the PNB-x%POSS series are shown in Figure 4.5 (left). A small increase in conductivity was observed when 2% of NB-POSS was introduced, while introduction of 5 and 9% of NB-POSS did not result in an increase in conductivity. The normalized conductivity vs. T-T_g plot in Figure 4.5 (right) shows that conductivity decreases with decreasing wt.% of triazole, with the exception of PNB-2%POSS. A drop in T_g is thought to account for the improvement in conductivity when 2% of POSS was incorporated.

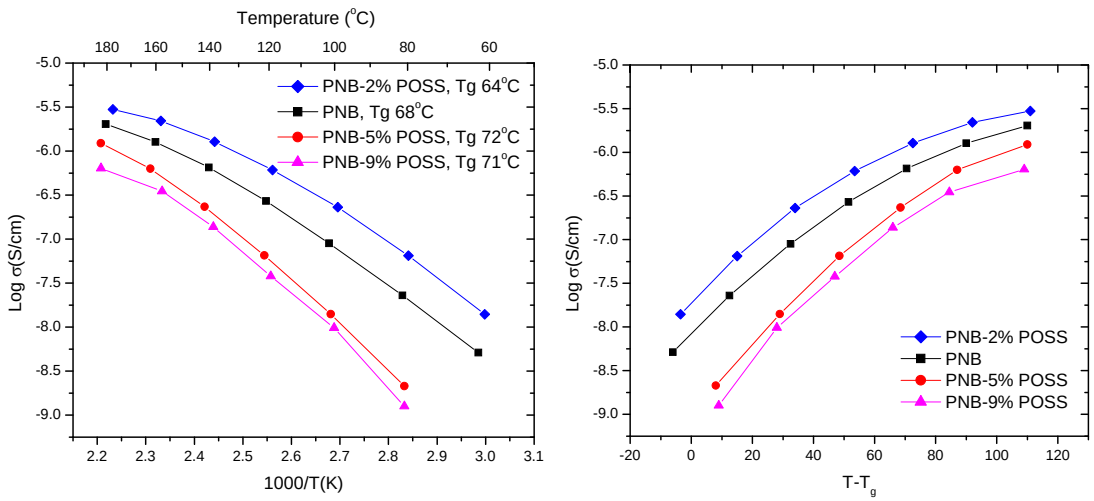

Figure 4.5. Proton conductivity (left) and normalized (right) plots of PNB and PNB-x%POSS.

To further investigate the effect of POSS incorporation on proton conductivity, POSS was introduced to a polymer that has a higher triazole content, PNB2. Proton conductivities of PNB2 and PNB2-10%POSS were compared. Although their T_g's are comparable, a nearly 2 order of magnitude drop in conductivity was observed in both general (left) and normalized (right) plots, Figures 4.6, when 10 mol% POSS was introduced. A decrease in conductivity can be attributed to the decrease in triazole

content from 43 to 32 wt.%. Another pair of polymers of interest to compare are PNB and PNB2-10%POSS as they have similar T_g values (68 vs. 60 °C) and triazole content (33 vs. 32 wt.%). Proton conductivity of PNB2-10%POSS is approximately 0.25 order of magnitude lower in both plots (Figure 4.6).

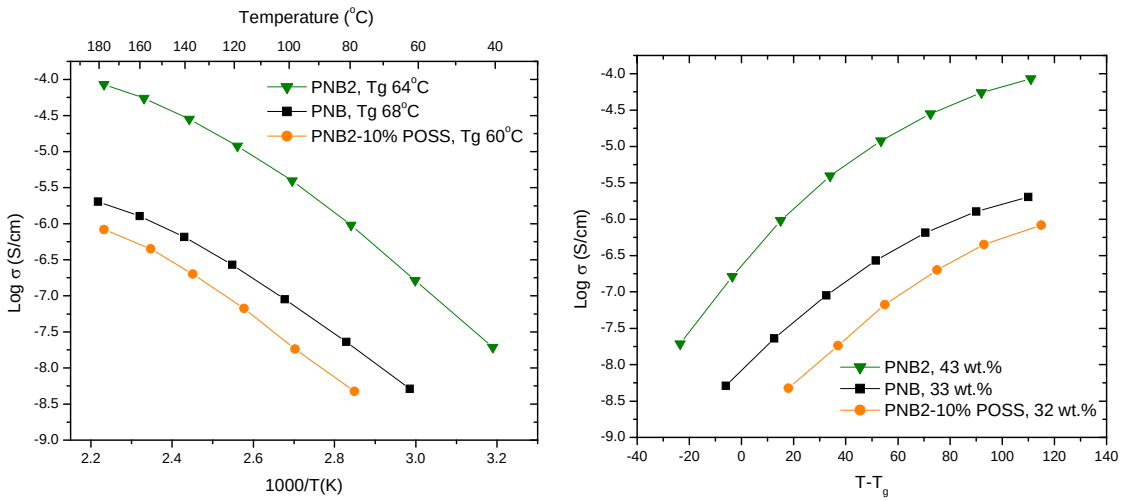

Figure 4.6. Proton conductivity (left) and normalized (right) plots of PNB, PNB2 and PNB2-10%POSS.

Putting all of these findings together, at low POSS loadings, incorporation of POSS affects two competing factors that determine conductivity, T_g and charge carrier density, such that a decrease in T_g is accompanied by a decrease in charge carrier density. An increase in conductivity with 2% POSS incorporation shows that segmental mobility is more influential in this system. In contrast to the work on polyvinyl imidazole/POSS nanocomposites,[14] a high POSS loading does not provide an increase in proton conductivity of polynorbornenes with a pendant triazole. This observation could be due to the low dielectric constant of POSS, as a non-polar environment is reported to be less favorable for proton conduction.[1] The bulkiness of POSS, which may disrupt a hydrogen

bonding pathway for proton transport, could also account for the decrease in proton conductivity at high POSS loadings.

4.3.4 Morphology

Samples for WAXD were cast from concentrated solutions of polymer in THF and then thermally annealed at 80 °C under vacuum for 24 h. A photographic plate kept at a distance of 139 mm was used to collect WAXD patterns. The WAXD patterns of PNB, PNB2 and PNB2 doped with 100 mol% TFA are shown in Figure 4.7. The 2θ (°) and d-spacing (Å) values are listed in Table 4.2. It has been previously reported that polynorbornene shows two amorphous halo peaks at 2θ of 10 and 18 °.[24] The former peak corresponds to the interchain spacing, and the latter peak corresponds to the spacing between the neighboring CH_2 groups. Our three samples show similar WAXD patterns and no crystallinity was observed. A shift in the 2θ values in the low angle peak could be due to the steric repulsion between triazole-containing side chains.

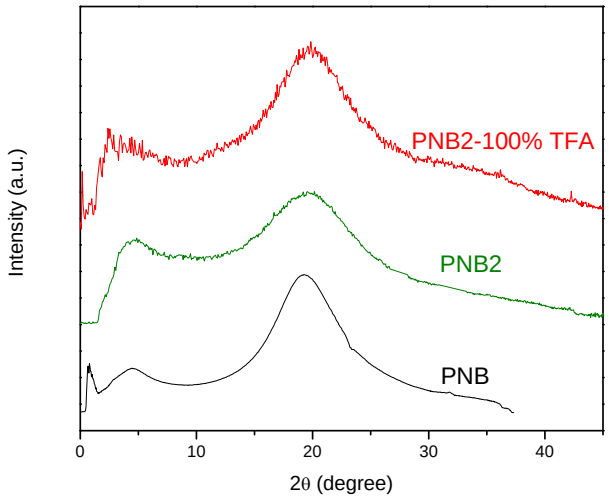

Figure 4.7. WAXD patterns of PNB, PNB2 and 100% TFA-doped PNB2.

Table 4.2. Two theta values and Bragg d-spacings of WAXD patterns

Polymer	1st: 2θ (°)/d-spacing (Å)	2nd: 2θ (°)/d-spacing (Å)
PNB	19.3/4.6	4.6/19.1
PNB2	19.6/4.5	4.8/18.4
PNB2-100%TFA	19.9/4.5	4.7/18.8

4.3.5 Mechanical properties

Since PNB and PNB-2%POSS show the highest conductivities among the polymers studied, the mechanical properties of these polymers were studied by DMA. The samples for DMA were prepared by press molding at 80 °C for 10 min. There was almost no difference in T_g values obtained from DSC of the powdery polymers and the pressed polymers. However, the T_g values obtained from the peak maximum of the tan δ curves in DMA were 25-40 °C higher than those from DSC. When a heating rate for DMA was changed from 3 to 10 °C /min, the T_g values did not changed significantly (Figure 4.8). In agreement with the DSC data, there was a drop in T_g from 108 to 91 °C, at a heating rate of 10 °C /min, when 2% of POSS was introduced (Table 4.2).

As shown in Figure 4.9, the storage moduli of PNB and PNB-2%POSS are comparable within experimental errors. These storage moduli are also compared to that of Nafion,[25, 26] and listed in Table 4.3. Our polynorbornenes show a higher mechanical strength compared to Nafion at low temperatures (below ~60 °C) and comparable value at high temperatures.

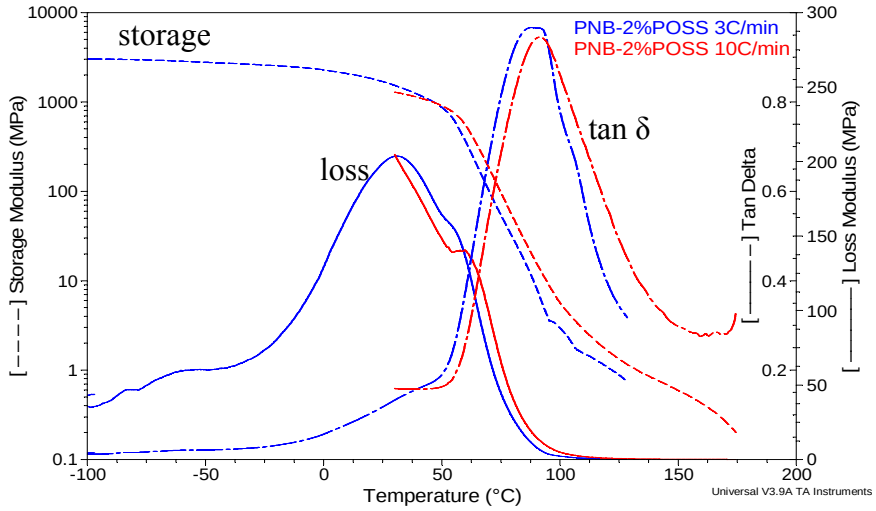

Figure 4.8. Storage modulus, loss modulus and tan δ of PNB-2%POSS at different heating rates obtained with an oscillation frequency of 1 Hz.

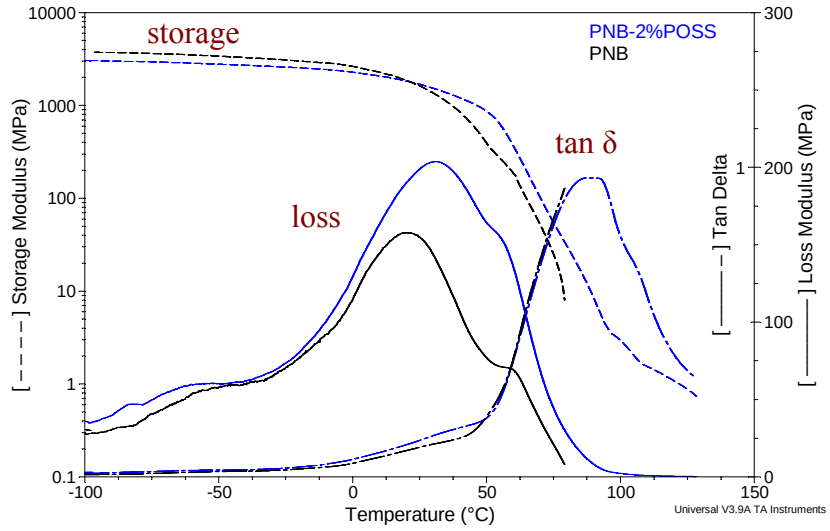

Figure 4.9. Storage modulus, loss modulus and tan δ of PNB and PNB-2%POSS. Data were obtained with an oscillation frequency of 1 Hz and a heating rate of 3 °C/min.

Table 4.3. T_g and storage modulus as a function of temperature.

	$T_{g\ (DSC)}$[a] °C	$T_{g\ (DMA)}$ °C	G' (MPa) 3 °C/min			
			30 °C	60 °C	90 °C	130 °C
PNB	68	108[b]	1,360	186	~7	NA
PNB-2%POSS	64	91[b] (89[c])	1,540	357	8.1	0.7
Nafion® 117[25]	NR	NR	600	NR	NR	50
Nafion[26](4 °C/min)	NR	NR	~200	~110	~15	~1.5

[a] DSC on the 2nd heating cycle of the press-molded samples (heating rate = 10°C/min).
[b] Determined from the maximum of tan δ at a heating rate of 10 °C/min.
[c] Determined from the maximum of tan δ at a heating rate of 3 °C/min.
NA = Not available. NR = Not reported.

4.4 Conclusion

Homopolymers and copolymers of norbornene containing 1*H*-1,2,3-triazole and norbornene containing POSS have been successfully synthesized and characterized. A maximum conductivity of 85.6 μS/cm was obtained at 180 °C under anhydrous condition from polynorbornene containing two triazole groups per repeat unit. A small POSS loading provided a slight increase in proton conductivity, which could be due to a drop in glass transition temperature. These polynorborne-based materials also show good thermal properties, and their mechanical properties at low temperatures are comparable to that of Nafion. However, it should be reminded that the operating temperatures of Nafion are below 100 °C, while those of our polynorbornenes with triazole pendant are higher and reaching 180 °C. To achieve a mechanically stable membrane based on polynorbornenes, the uses of crosslinking and nanopourous filling should be explored.

4.5 References

1. Martwiset, S.; Woudenberg, R. C.; Granados-Focil, S.; Yavuzcetin, O.; Tuominen, M. T.; Coughlin, E. B. *Solid State Ionics* 2007, 178, (23-24), 1398-1403.

2. Martwiset, S.; Yavuzcetin, O.; Thorn, M.; Versek, C.; Tuominene, M.; Coughlin, E. B. *Journal of Polymer Science Part a-Polymer Chemistry* 2008, Accepted.

3. Granados-Focil, S.; Woudenberg, R. C.; Yavuzcetin, O.; Tuominen, M. T.; Coughlin, E. B. *Macromolecules* 2007, 40, (24), 8708-8713.

4. Higami, M.; Granados-Focil, S.; Thorn, M.; Versek, C.; Tuominen, M.; Coughlin, E. B. 2008, Manuscript in preparation.

5. Joshi, M.; Butola, B. S. *Journal of Macromolecular Science-Polymer Reviews* 2004, C44, (4), 389-410.

6. Li, G. Z.; Wang, L. C.; Ni, H. L.; Pittman, C. U. *Journal of Inorganic and Organometallic Polymers* 2001, 11, (3), 123-154.

7. Phillips, S. H.; Haddad, T. S.; Tomczak, S. J. *Current Opinion in Solid State & Materials Science* 2004, 8, (1), 21-29.

8. Seurer, B.; Coughlin, E. B. *Macromolecular Chemistry and Physics* 2008, 209, (19), 2040-2048.

9. Seurer, B.; Coughlin, E. B. *Macromolecular Chemistry and Physics* 2008, 209, (12), 1198-1209.

10. Zheng, L.; Kasi, R. M.; Farris, R. J.; Coughlin, E. B. *Journal of Polymer Science Part a-Polymer Chemistry* 2002, 40, (7), 885-891.

11. Jeon, H. G.; Mather, P. T.; Haddad, T. S. *Polymer International* 2000, 49, (5), 453-457.

12. Kopesky, E. T.; Haddad, T. S.; Cohen, R. E.; McKinley, G. H. *Macromolecules* 2004, 37, (24), 8992-9004.

13. Constable, G. S.; Lesser, A. J.; Coughlin, E. B. *Macromolecules* 2004, 37, (4), 1276-1282.

14. Pu, H.-t.; Qin, S.; Yang, Z.-l.; Wan, D.-c.; Yuan, J.-j. *Gongneng Cailiao FIELD Full Journal Title:Gongneng Cailiao* 2007, 38, (9), 1499-1502,1506.

15. Zhang, M. J.; Flynn, D. L.; Hanson, P. R. *Journal of Organic Chemistry* 2007, 72, (9), 3194-3198.

16. Loren, J. C.; Krasinski, A.; Fokin, V. V.; Sharpless, K. B. *Synlett* 2005, (18), 2847-2850.

17. Love, J. A.; Morgan, J. P.; Trnka, T. M.; Grubbs, R. H. *Angewandte Chemie-International Edition* 2002, 41, (21), 4035-4037.

18. Martwiset, S.; Yavuzcetin, O.; Thorn, M.; Versek, C.; Tuominen, M.; Coughlin, E. B. *Journal of Polymer Science Part A: Polymer Chemistry* 2009, 47, (1), 188-196.

19. Tabacchi, G.; Gianotti, E.; Fois, E.; Martra, G.; Marchese, L.; Coluccia, S.; Gamba, A. *Journal of Physical Chemistry C* 2007, 111, (13), 4946-4955.

20. Zheng, L.; Farris, R. J.; Coughlin, E. B. *Journal of Polymer Science Part a-Polymer Chemistry* 2001, 39, (17), 2920-2928.

21. Xu, H. Y.; Kuo, S. W.; Lee, J. S.; Chang, F. C. *Macromolecules* 2002, 35, (23), 8788-8793.

22. Persson, J. C.; Jannasch, P. *Chemistry of Materials* 2003, 15, (16), 3044-3045.

23. Pu, H.; Wu, J.; Wan, D.; Chang, Z. *Journal of Membrane Science* 2008, 322, (2), 392-399.

24. Shin, B. G.; Cho, T. Y.; Yoon, D. Y.; Liu, B. Y. *Macromolecular Research* 2007, 15, (2), 185-190.

25. Hartmann-Thompson, C.; Merrington, A.; Carver, P. I.; Keeley, D. L.; Rousseau, J. L.; Hucul, D.; Bruza, K. J.; Thomas, L. S.; Keinath, S. E.; Nowak, R. M.; Katona, D. M.; Santurri, P. R. *Journal of Applied Polymer Science* 2008, 110, (2), 958-974.

26. Noto, V.; Lavina, S.; Negro, E.; Vittadello, M.; Conti, F.; Piga, M.; Pace, G. *Journal of Power Sources* 2009, 187, (1), 57-66.

CHAPTER 5

SUMMARY AND FUTURE OUTLOOK

This chapter consists of two sections. The first section summarizes the results from Chapter 2 through Chapter 4. In the second section, possible project extensions are discussed.

5.1 Dissertation summary

The overall project goal was to determine the factors governing proton transport in heterocyclic proton conducting systems including mobility, protogenic group identity, and charge carrier density. In Chapter 2, random copolymer and terpolymers of 1,2,3-triazole-containing acrylates and poly(ethylene glycol)methyl ether acrylate (PEGMEA) were synthesized and characterized. Introduction of PEG graft chains increased conductivity on both an absolute and normalized scale T-T_g up to 30% mole PEGMEA. This finding indicated that the increase in mobility could counteract the decrease in charge carrier density. However, a drop in conductivity was observed with further PEGMEA incorporations, suggesting that at those compositions, the decrease in charge carrier concentration became the dominating factor for proton transport over the increase in mobility. In comparison to polyacrylate with 30% mole PEGMEA with the corresponding benzimidazole analog reported earlier by our group,[1] the triazole analog showed a higher proton conductivity, and a less pronounced conductivity temperature dependence. These observations could be explained by the smaller size, and the low melting point of triazole compared to benzimidazole. Further increases in conductivity were achieved through the addition of trifluoroacetic acid (TFA). A maximum increase of

1.5 orders of magnitude in conductivity was observed when the polymer was doped with 100% mole of TFA.

While Chapter 2 focused on the effects of mobility and protogenic group, Chapter 3 discussed the effect of charge carrier density on proton conduction. The charge carrier density has only been tuned by varying the spacer length of the polymers. In this work, we investigated the charge carrier density effect by introducing multiple protogenic groups per repeat unit. Polyacrylates containing a different number of 1*H*-1,2,3-triazole groups per repeat unit were synthesized. The result showed that introduction of more than one triazole per repeat unit did not result in an increase in conductivity as there was an accompanying increase in T_g. A maximum conductivity of 17.5 μS/cm was obtained at 200 °C under anhydrous condition.

Besides providing a high conductivity, a good polyelectrolyte membrane should be thermally and mechanically stable. In Chapter 4, the effect of charge carrier density on conductivity was also studied in a higher T_g polymeric backbone system. Polynorbornenes containing one and two triazole group(s) per repeat unit were synthesized. Polynorbornene with two triazole groups showed 1.5 orders of magnitude higher conductivity relative to the polymer with only one triazole group. Since the two polymers share similar T_g values, the increase in triazole content could account for the observed increase in proton conductivity. To further improve the thermal and mechanical properties of the membrane, polyhedral oligomeric silsesquioxanes (POSS) was incorporated into the norborne-based polymers. These polymers were stable up to ~300 °C, and a moderate improvement in thermal stability was observed when POSS was introduced. A small increase in conductivity was observed with 2% mole of POSS

incorporation. A drop in conductivity was observed at higher POSS loadings. The increase in conductivity at 2% POSS loading could be attributed to a drop in T_g. At high POSS loadings, the low dielectric constant, and the bulkiness of POSS were thought to provide an unfavorable environment, and to disrupt a hydrogen bonding pathway, respectively, for proton transport. The mechanical properties of polynorbornenes with triazole moieties at low temperatures are comparable to that of Nafion.

In summary, we have demonstrated that proton conductivity depends on protogenic group, mobility, and charge carrier density. The smaller heterocycle with a lower melting point, triazole, showed a higher conductivity compared to benzimidazole. The maximum conductivity was obtained when mobility and charge carrier density are in balance. Doping the triazole-based polymers with a strong acid increased the conductivity up to 1.5 orders of magnitude. The maximum conductivity in this dissertation was obtained in polynorbornene containing two triazole groups per repeat unit. When the polymer was doped with 100% mole TFA, the conductivity reached 1.3 mS/cm at 200 °C under anhydrous condition. To compare with other heterocycle-tethered polymers reported in the literature, the proton conductivity of our polynorbornene is only half an order of magnitude lower than that of polysiloxane containing triazole, which showed the highest conductivity (Figure 5.1).[2] Furthermore, it should be stressed that our norbornene-based polymer shows a much higher storage modulus (~1000 MPa) relative to polysiloxane at room temperature. As shown in Figure 5.1, proton conductivity increases with increasing temperature in the heterocyclic systems, while the conductivity of Nafion decreases over the same temperature range.[3] Since the two systems show a maximum conductivity at the opposite ends of the temperature sweep, combining them in

such a way that protons conduct through vehicular mechanism at low temperatures and though Grotthuss mechanism at high temperatures would possibly provide a membrane with a high conductivity throughout the entire operating temperature range.

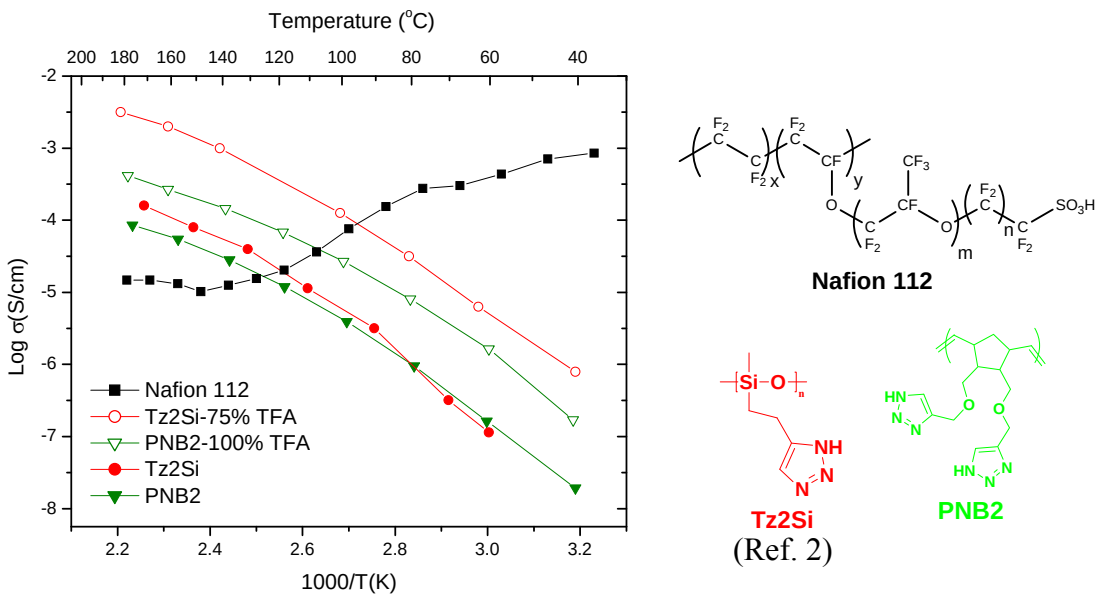

Figure 5.1. Conductivity of polymers containing triazoles compared to Nafion 112.

5.2 Future outlook

5.2.1 Extensions of the current work

Triazole-tethered polynorbornenes have been shown to provide a high proton conductivity and good thermal and mechanical stability. Hydrogenation of these polymers would prevent them from crosslinking, thus increasing chemical stability. Although a small increase in conductivity was observed when POSS was introduced, the idea of incorporating of inorganic compounds into the membrane in order to improve the thermal and mechanical stability should still be explored further. The incorporation of

inorganic compounds should not disrupt a hydrogen bonding pathway for proton transport. Small inorganic compounds with high dielectric constant are recommended.

5.3.2 A new heterocycle for uses in PEMFCs

As mentioned earlier, nitrogen-based heterocycles are shown to provide comparable proton conductivities to that of hydrated polymers.[4] Various heterocycles were investigated as potential protogenic groups for use in fuel cell membranes. Heterocyclic compounds, shown in Figure 5.2, were either dissolved in DMSO, or blended with the commercially available poly(ethylene glycol)methyl ether (PEGME, M_n ~550) or the in-house-synthesized poly(poly(ethylene glycol)methyl ether acrylate) (P(PEGMEA)). The proton conductivity plot in Figure 5.3 shows that 6-chloropurine has a higher conductivity compared to 1,2,3-triazole and imidazole in both DMSO and PEGME matrices. The electrochemical stability of the compounds with high conductivities were also studied using cyclic voltammograms (Figure 5.4). It turned out that chloropurine is not as electrochemically stable relative to purine, triazole and imidazole.

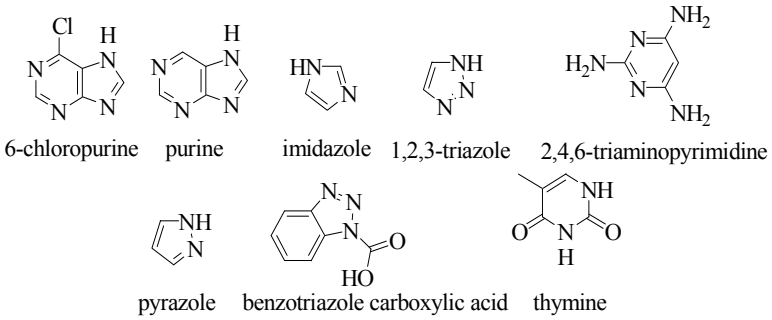

Figure 5.2. Chemical structures of heterocyclic compounds used in the screening tests.

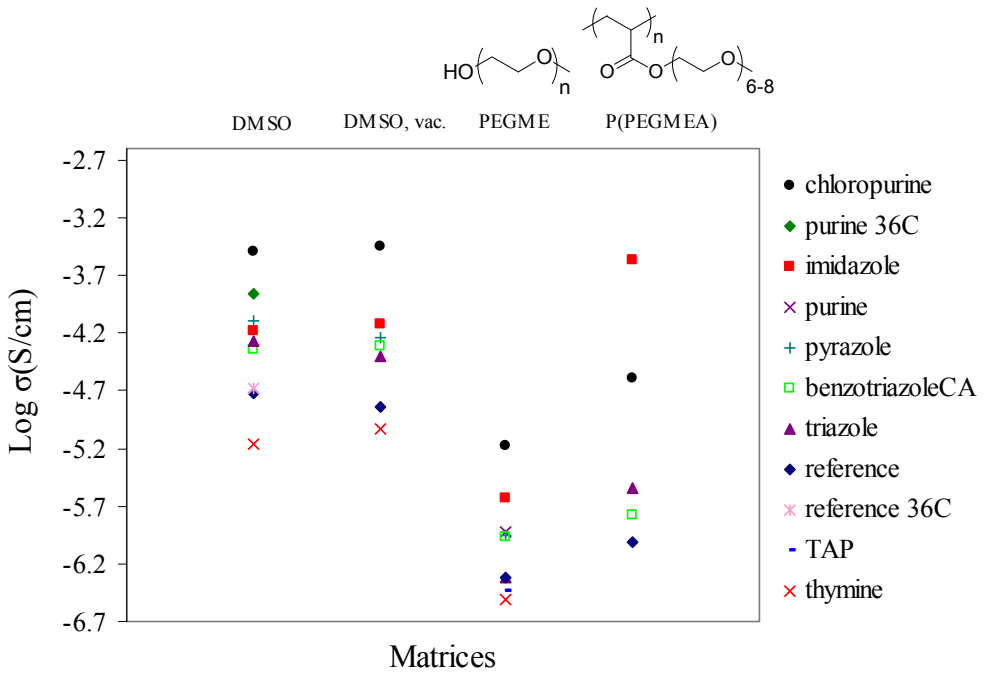

Figure 5.3. The conductivities of heterocyclic compounds in different matrices.

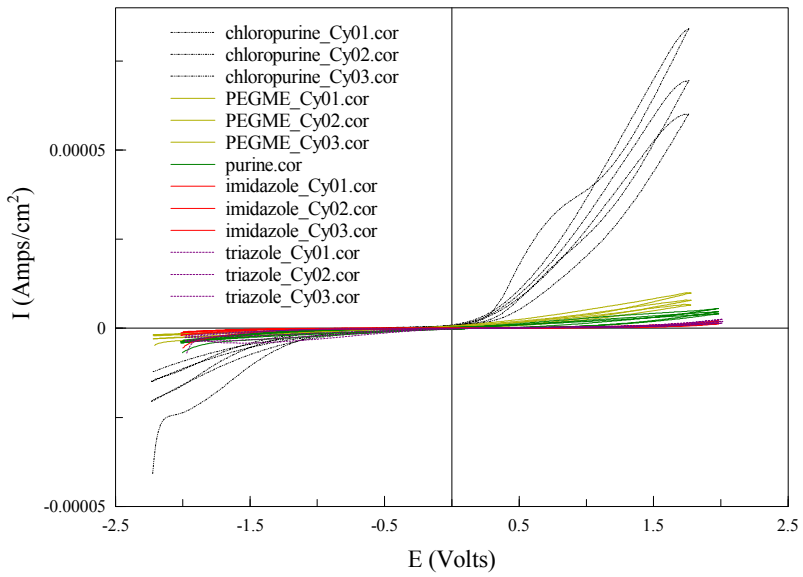

Figure 5.4. Typical cyclic voltammograms of 6-chloropurine, purine, imidazole, 1,2,3-triazole; C = 0.67 M in PEGME, and PEGME at 25 ºC.

Zhou and coworkers hypothesized that the high conductivity of polyvinyl triazole was due to a lower melting point, and the tautomerization or intermolecular proton transfer from N2 to N3 of 1*H*-1,2,3-triazole.[5] Similar to 1,2,3-triazole, purine exhibits aromaticity and tautomerism.[6] The acidity of purine ($pK_a1 = 2.4$, $pK_a2 = 8.9$) is comparable to that of 1,2,3-triazole ($pK_a1 = 1.17$, $pK_a2 = 9.26$). Since purine is shown to have a high proton conductivity, good electrochemical stability, and similar chemical properties relative to triazole, purine is considered to be a very promising new protogenic group for uses in PEMFCs.

5.3 References

1. Woudenberg, R. C.; Yavuzcetin, O.; Tuominen, M.; Coughlin, E. B. *Solid State Ionics* **2007,** 178, 1135-1141.

2. Granados-Focil, S.; Woudenberg, R. C.; Yavuzcetin, O.; Tuominen, M. T.; Coughlin, E. B. *Macromolecules* **2007,** 40, (24), 8708-8713.

3. Woudenberg, R. C. Doctoral Thesis. University of Massachusetts, Amherst, MA, 2007.

4. Kreuer, K. D.; Fuchs, A.; Ise, M.; Spaeth, M.; Maier, J. *Electrochimica Acta* **1998,** 43, (10-11), 1281-1288.

5. Zhou, Z.; Li, S. W.; Zhang, Y. L.; Liu, M. L.; Li, W. *Journal of the American Chemical Society* **2005,** 127, (31), 10824-10825.

6. Brown, E. G., *Ring Nitrogen and Key Biomolecules*. 1998; p 250 pp.

CHAPTER 6

SYNTHESIS OF POLY(2-(DIMETHYLAMINO)ETHYL METHACRYLATE) FOR SENSOR APPLICATIONS

6.1 Introduction

A study on the molecular weight driven competitive adsorption of poly(ethylene oxide) (PEO) on silica by Fu and co-workers. showed that the coadsorption comprises of three steps: the transport-limited adsorption, the exchange of short and long chains, and the equilibration of the long chains.[1] They also demonstrated that when the short chains with molecular weight of 30 kg/mol were displaced by longer chains, the displacement was fast and nearly complete. For the short chains with the molecular weight of 120 kg/mol, the displacement by longer chains was slower and less complete. Similarly, the work by Dijt *et al*. showed that the displacement of 7 kg/mol PEO chains by 400 kg/mol PEO chains were completed within minutes. Besides PEO, the displacement of polystyrene (PS) by poly(methyl methacrylate) (PMMA) was reported to take several hours.[2, 3] The long displacement time was thought to be due to the relatively rigid chains of PS and PMMA which resulted in a limited surface mobility. The adsorption of cationic polyelectrolyte poly(2-(dimethylamino)ethyl methacrylate), PDMAEMA, onto silica was also studied, and it was shown that the adsorption was driven by electrostatic interactions.[4] A study on the effect of molecular weight on the coadsorption of PDMAEMA would provide insight on the influences of surface mobility and electrostatic attractions on adhesion.

Previous work by Kozlova and Santore demonstrated how a negatively charged planar silica surface carrying 11 nm-diameter patches of PDMAEMA (molecular weight

of 31,300 g/mol and a polydispersity of 1.1), could be tuned to manipulate the adhesion of 0.5 μm negatively charged silica spheres (Figure 6.1).[5, 6] The particle adhesion was found to be influenced by the average spacing of the patches. An interesting extension of this work would be to study the effect of patchy size by varying the molecular weight of PDMAEMA, and the effect of charge density by comparing the homopolymer and copolymer with the same molecular weight on the adhesion.

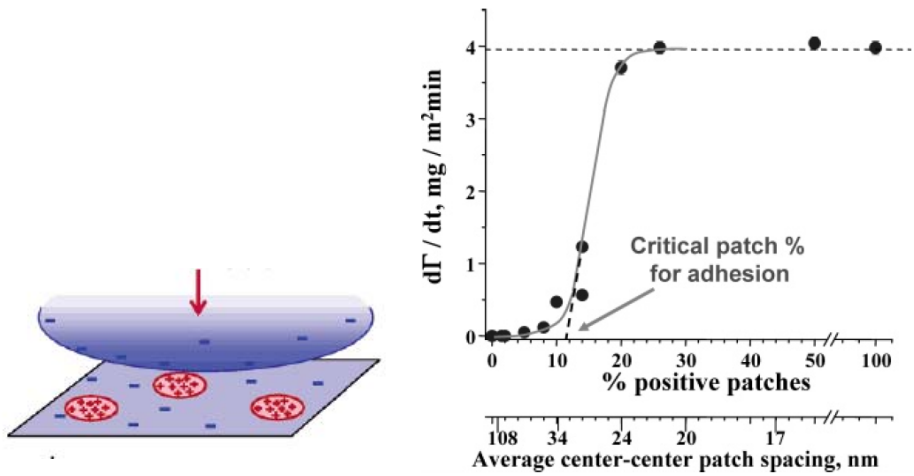

Figure 6.1. A cartoon representing the interaction of nanopatchy surface with colloidal-scale objects (left), and adhesion rates of 460 nm silica particles as a function of patch density (from reference 5).

In collaboration with Prof. Maria Santore (Polymer Science and Engineering Department) and Prof. Jeffrey Davis (Chemical Engineering Department) at the University of Massachusetts Amherst, the joint project goal is to develop a robust renewable surface that can be used to distinguish particles from size 50 nm to 5 μm based on their dynamic adhesion signatures. The project has been divided into three areas: synthesis of functionalized polymers (the Coughlin group), adhesion study (the Santore group), and system modeling (the Davis group).

Due to recent anthrax incidents, there is a demand for field sensors that could identify bacteria and viruses. Existing technologies, such as chip-based PCR and DNA fingerprinting, are not practical for field applications as the procedures require skilled operators, sample preparation, and controlled analysis conditions. In addition, the chips cannot tolerate harsh temperature and chemical conditions.

While a high precision chip analysis system relies on biomolecular recognition of target molecules which reside within organisms, our approach, a screening field sensor, should classify molecules based on surface properties, size, and shape. Because this approach requires no need to access the inside of the particle, it will be more convenient and less expensive. Moreover, field-based sensor should be renewable and be able to classify threat agents. Potential targets include viruses, spores, and bacteria. Variations driving selectivity include the overall size, the average charge density, the average surface hydrophobicity, and the hardness or softness of the particle.

In the synthetic portion of this team project, well-controlled PDMAEMAs with different molecular weights were synthesized via atom transfer radical polymerization (ATRP). Fluorescently-labeled PDMAEMAs were also synthesized, and would be used to distinguish different molecular weight components in a study of competitive adsorption of PDMAEMA chains. PDMAEMA is a weak polyelectrolyte, and its protonation is pH-dependent. At pH 6.1, PDMAEMA is reported to be 70% protonated.[5] Fluorescent, including rhodamine-, anthracene-, and fluorescein-based, compounds were used as ATRP initiators to ensure the presence of one dye molecule on every polymer chain. It has been reported that rhodamine and fluorescein are pH-sensitive.[7] While rhodamine generates stronger signals at low pHs, fluorescein shows the opposite. These

dye-labeled PDMAEMAs could be used in several pH conditions, to which they are tuned to provide varying degrees of protonation.

6.2 Experimental

6.2.1 Materials

Copper (I) bromide (CuBr) (Aldrich; 99.999%), (1,1,4,7,10,10-hexamethyltriethylenetetramine (HMTETA) (Aldrich; 97%), *p*-toluenesulfonyl chloride (*p*-TsCl) (Aldrich; 99%), lissamine rhodamine B sulfonyl chloride (Acros; 99+%), and 9-anthracenemethanol (Aldrich; 97%) were used as received. Regenerated cellulose dialysis tubing with a molecular weight cutoff of 6,000-8,000 Daltons was purchased from Fisher Scientific. 2-(Dimethylamino)ethyl methacrylate (DMAEMA) (Aldrich; 98%) was passed through a short neutral alumina column prior to use.

6.2.2 Synthesis

6.2.2.1 Synthesis of poly(2-(dimethylamino)ethyl methacrylate) (PDMAEMA)

Polymerization. In a modification of a literature preparation,[8] a typical ATRP was carried out as follows. CuBr was placed into a dried ATRP tube. The tube was then flushed with dry N_2 for 15 min. The deoxygenated solvents mixture (isopropanol/water (9/1 v/v), deoxygenated DMAEMA and HMTETA were added to the tube and then stirred until the system became homogenous. Three cycles of freeze-pump-thaw were conducted followed by the addition of *p*-TsCl. Three more cycles of freeze-pump-thaw were performed. The solution was then stirred at room temperature. The molar ratio of CuBr/HMTETA/*p*-TsCl was 1/1/1, and the volume ratio of DMAEMA to solvents

mixture was 1/1. Copper was removed by passing through a short alumina column. The polymer solution was concentrated and precipitated in hexane.

6.2.2.2 Synthesis of rhodamine-terminated PDMAEMA

Polymerization. The polymerizations of rhodamine-terminated PDMAEMAs were carried out as described above using lissamine rhodamine B sulfonyl chloride as initiator. The reaction mixture was stirred at 45 ºC. An aliquot of the polymerization medium was withdrawn for conversion analysis by ^{1}H NMR. Copper was removed by passing through a short alumina column. The polymer solution was concentrated and precipitated in hexane. The polymer was redissolved in water and dialyzed against water for 1 week followed by the purification with preparative GPC.

6.2.2.3 Synthesis of anthracene-terminated PDMAEMA

Synthesis of 9-anthracenemethyl-2-bromoisobutyrate (AMBIB), 6.1. In a modification of a literature preparation,[9] triethylamine (TEA, 2.78 mL, 20.0 mmol, 2 equiv.) was added to a solution of 9-anthracenemethanol (2.08 g, 10.0 mmol, 1 equiv.) in 50 mL of anhydrous tetrahydrofuran. The resulting solution was cooled in an ice bath, and 2-bromoisobutyryl bromide (1.85 mL, 15.0 mmol, 1.5 equiv) was added slowly with stirring. A white precipitate of triethylammonium hydrobromide formed, and the reaction was stirred for 19 h at room temperature. The precipitate was removed by filtration. The mixture was diluted with 50 mL of water. The product was extracted with dichloromethane (3 x 50 mL), dried over $MgSO_4$, filtered, and concentrated. The crude product was further purified by column chromatography, using hexane:ethyl acetate (9:1)

as an eluent, to give 2.78 g of the product (77% yield). ^{1}H-NMR ($CDCl_3$, 298 K, 300 MHz) δ: 8.53 (s, 1H, Ar), 8.36-8.34 (m, 2H, Ar), 8.06-8.03 (m, 2H, Ar), 7.60-7.50 (m, 4H, Ar), 6.23 (s, 2H, CH_2), 1.88 (s, 6H, $(CH_3)_2$). ^{13}C-NMR ($CDCl_3$, 298 K, 300 MHz) δ: 171.94 (COO), 131.36(Ar), 131.15(Ar), 129.45(Ar), 129.13(Ar), 126.75(Ar), 125.53(Ar), 125.16(Ar), 123.92(Ar), 60.74(CH_2), 55.97(CBr), 30.73(CH_3). UV-Vis (chloroform): λ_{max} (nm)/ε ($Lmol^{-1}cm^{-1}$) = 334/3578, 350/6447, 368/9297, 388/8485.

Polymerization. The polymerizations of anthracene-terminated PDMAEMAs were carried out as described above using AMBIB as initiator and acetone as solvent. The reaction mixture was stirred at 60 ºC for 24 h. Copper was removed by passing through a short alumina column. The polymer solution was concentrated and precipitated in hexane.

6.2.2.4 Synthesis of fluorescein-terminated PDMAEMA

Synthesis of bifuctional fluorescein-based initiator, 6.2. In a modification of a literature preparation,[10] fluorescein (1.6 g, 4.81 mmol, 1 equiv.) was dissolved in anhydrous THF (20 mL) followed by the addition of TEA (2.1 mL, 14.4 mmol, 3 equiv.). The resulting solution was cooled in an ice bath, and 2-bromoisobutyryl bromide (1.5 mL, 12.0 mmol, 2.5 equiv.) was added slowly with stirring. A white precipitate of triethylammonium hydrobromide was formed, and the reaction was stirred for 24 h at room temperature. The precipitate was removed by filtration, and the volatiles were removed in vacuo. The crude product was further purified by column chromatography, using chloroform as an eluent, to give the product (33% yield). ^{1}H-NMR ($CDCl_3$, 298 K, 400 MHz): δ (ppm) 2.07 (2, 12H, CH_3), 6.87-8.07 (m, 10H, Ar-H). ^{13}C-NMR ($CDCl_3$,

298 K, 400 MHz): δ (ppm) 30.53, 55.01, 81.46, 110.03, 116.86, 117.30, 123.98, 125.33, 125.96, 129.11, 130.15, 135.39, 151.56, 152.12, 152.98, 169.14, 169.73. IR: 1756 (C=O), 1610, 1420, 1240, 1151, 1099, 993, 884, 758 cm^{-1}.

Polymerization. The polymerizations of fluorescein-terminated PDMAEMAs were carried out as described above using fluorescein-based initiator, **6.2**. The reaction mixture was stirred at room temperature. Copper was removed by passing through a short alumina column. The polymer solution was concentrated and precipitated in hexane.

6.2.3 Characterization

^{1}H-NMR (300 MHz) was obtained on a Bruker DPX-300 NMR Spectrometer with the samples dissolved in chloroform-*d*. Molecular weight and polydispersity index (PDI) were measured by gel permeation chromatography (GPC) in DMF at 50 ºC with a flow rate of 0.75 mL/min on systems equipped with two-column sets (from Polymer Laboratories) and refractive index detector (HP 1047A). Poly(methyl methacrylate) standards were used for molecular weight calibration. UV–vis spectra were obtained using a Perkin-Elmer Lambda 2 series spectrophotometer with PECSS software. FTIR spectra were measured on a Perkin-Elmer Spectrum One FT-IR spectrometer equipped with a universal attenuated total reflectance (ATR) sampling accessory.

6.3 Results and discussion

6.3.1 Synthesis

Poly(2-(dimethylamino)ethyl methacrylate)s (PDMAEMAs) with different end groups, including toluene sulfonyl, rhodamine, anthracene and fluorescein groups, have been successfully synthesized.

6.3.1.1 Synthesis of toluene sulfonyl-PDMAEMA

Controlled polymerization of DMAEMAs have been carried out via ATRP using *p*-toluenesulfonyl chloride as initiator, Scheme 6.1. The ratio of initiator/CuBr/HMTETA was 1/1/1. Similar to previous reports on the polymerization of DMAEMA,[8, 11] a mixture of isopropanol and water was used as solvent to provide a fast polymerization rate at ambient temperature. The transesterification reaction between isopropanol and DMAEMA is insignificant due to steric effects,[12] and this was confirmed by ^{1}H-NMR, Figure 6.2 (top). The molecular weights and PDIs of obtained PDMAEMAs are summarized in Table 6.1. A higher molecular weight observed compared the theoretical molecular weight is due to the loss of the initiator through hydrolysis reaction.

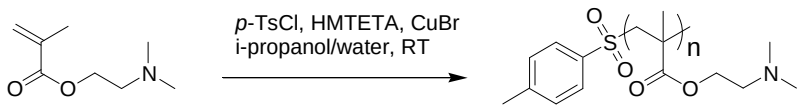

Scheme 6.1. ATRP of DMAEMA.

Table 6.1. Physical properties of the obtained PDMAEMAs.

Polymer	M_n (GPC)	PDI
T1	16,300	1.10
T2	69,100	1.12
T3	100,300	1.14
T4	204,900	1.39

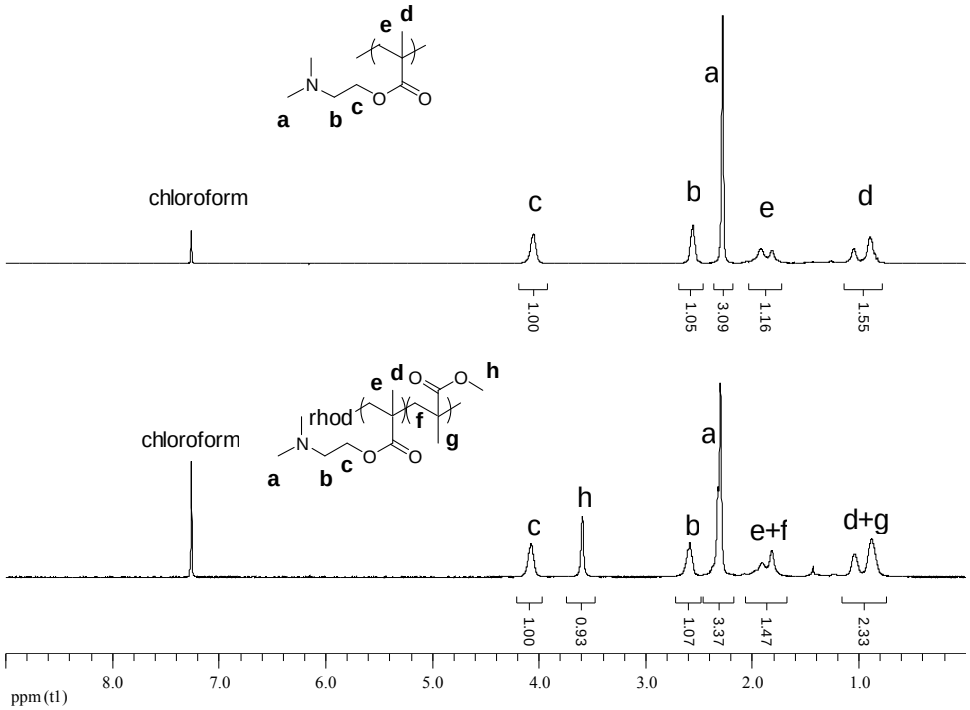

Figure 6.2. ^{1}H-NMR spectra of homopolymer T2 (top) and copolymer Rco1 (bottom).

6.3.1.2 Synthesis of rhodamine-terminated PDMAEMA

Lissamine rhodamine B sulfonyl chloride was used as initiator in the polymerizations to provide a 100% dye attachment onto polymer chains. The ratio of initiator/CuBr/HMTETA was 1/1/1, and the reaction temperature was 45 ºC. The transesterification reaction of DMAEMA and methanol was observed when methanol was used as solvent.[12] PMMA formations were calculated from ^{1}H-NMR spectra, Figure 6.1 (bottom), and they were in the range of 27 to 56 mol%. The transesterification was avoided by using isopropanol/water mixture as solvent to provide the homopolymers with different molecular weights. The summary of rhodamine-terminated PDMAEMAs synthesis is shown in Table 6.2. These homopolymers and copolymers with comparable

molecular weights will be used to study the effect of charge density on adhesion where the patchy size is held constant.

Table 6.2. Summary of rhodamine-terminated polymers.

Polymer	M_n (GPC)	PDI	Mol% PMMA (NMR)
R1	24,500	1.13	0
R2	41,800	1.11	0
R3	60,400	1.15	0
R4	89,900	1.17	0
Rco1	25,200	1.06	38
Rco2	42,000	1.05	27
Rco3	106,700	1.16	56

As rhodamine dye has an absorption maximum at 560 nm, UV detector near that wavelength was used to monitor the presence of the dye. GPC traces (UV detector at 550 nm) in Figure 6.3 show an incorporation of the dye to the polymer chains. While dye residues were observed in the crude polymers, they were completely removed after further purification by preparative GPC. The UV-vis spectra of the free dye and the purified rhodamine-labeled polymer in Figure 6.4 have identical shape and comparable extinction coefficients (~88,000 $M^{-1}cm^{-1}$ at 568 nm in MeOH).

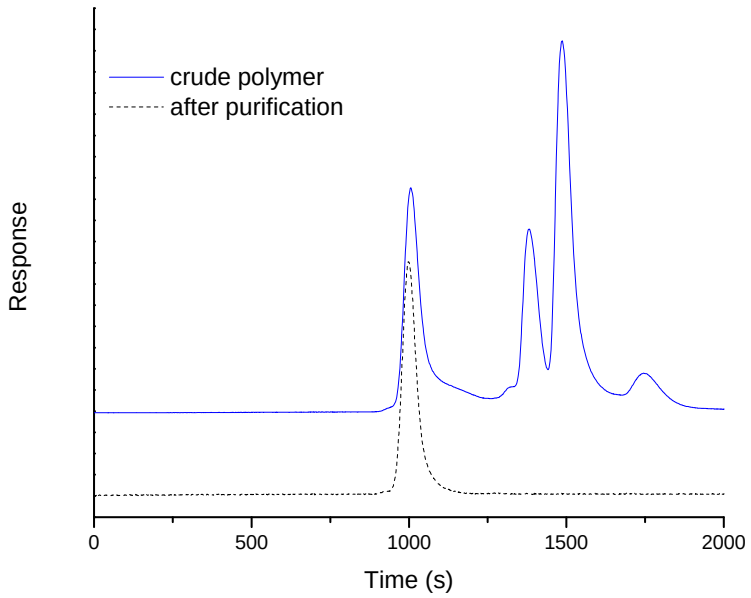

Figure 6.3. GPC (UV detector at 550 nm) traces of rhodamine-terminated PDMAEMA Rco2 before (solid line) and after purification by preparative GPC (dashed line).

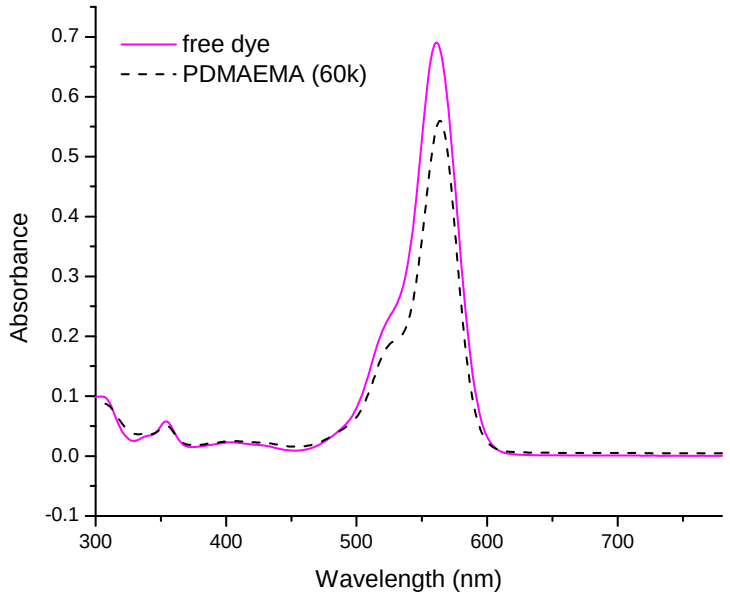

Figure 6.4. UV-Vis spectra of lissamine rhodamine B sulfonyl chloride (solid line) and rhodamine-terminated PDMAEMA R3 after preparative GPC (dashed line).

6.3.1.3 Synthesis of anthracene-terminated PDMAEMA

The anthracene-based compound, AMBIB, was synthesized as reported earlier by reacting 9-anthracenemethanol with 2-bromoisobutyryl bromide (Scheme 6.2).[9] AMBIB was then used as initiator in the ATRP of DMAEMA. PDMAEMAs with low PDIs were obtained, Table 6.3. Several conditions were evaluated in order to obtain such a low PDI. The 1/1/1 ratio of AMBIB/CuCl/HMTETA gave the lowest PDI and the highest initiator efficiency ($M_{n,cal}$ / $M_{n,GPC}$). A halide exchange of Cl for Br slows down propagation, and thus decreases the polydispersity. ^{1}H-NMR spectra in Figure 6.5 show the incorporation of the anthracene group into polymer chains. By assuming that each polymer chain contains only one anthracene group, the number-average molecular weight could be calculated from ^{1}H-NMR spectrum. The molecular weights obtained from GPC and NMR of polymer A3 are in good agreement. Therefore, only the molecular weights obtained from GPC are reported for the other polymers. The GPC traces in Figure 6.6 also confirm the presence of the anthracene end-group on the polymer and the absence of residual initiator. The UV-vis spectra of AMBIB and polymer A2 (Figure 6.7) are identical in both shape and peak positions, indicating that an anthracene group is present in the polymer.

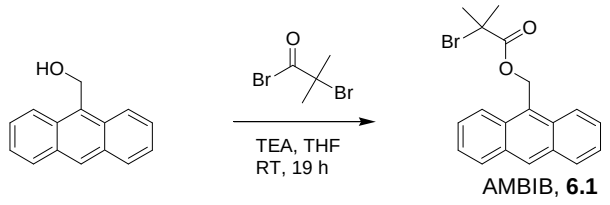

Scheme 6.2. Synthetic route to anthracene-based ATRP initiator.

Table 6.3. Molecular weights of anthracene end-capped PDMAEMA.

Polymer	$M_{n,cal}$[a]	$M_{n,GPC}$ (PDI)	$M_{n,NMR}$[b]	$M_{n,UV}$[b]	IE[c]
A1[d]	21600	19100 (1.37)	-	-	1.13
A2[d]	12800	13400 (1.31)	-	16800	0.96
A3[e]	14400	14200 (1.19)	14300	-	1.01
A4[f]	14800	15400 (1.30)	-	-	0.96
A5[h]	13900	16600 (1.30)	-	-	0.84
A6[e]	25700	23300 (1.23)	-	-	1.10
A7[e]	41700	32500 (1.23)	-	-	1.28

[a] $M_{n,cal}$ = (monomer mass (g) / mol of initiator) x (% conversion)
[b] $M_{n,NMR}$ and $M_{n,UV}$ are calculated by assuming that only one anthracene group is incorporated into each polymer chain.
[c] Initiator efficiency = $M_{n,cal}$ / $M_{n,GPC}$
[d] AMBIB/CuBr/HMTETA (1/1/1), acetone, 60 ºC, 24 h
[e] AMBIB/CuCl/HMTETA (1/1/1), acetone, 60 ºC, 24 h
[f] AMBIB/CuBr/HMTETA (1/1/1), toluene, 60 ºC, 24 h
[h] AMBIB/CuBr/HMTETA (1/1/1), acetone, RT, 46 h

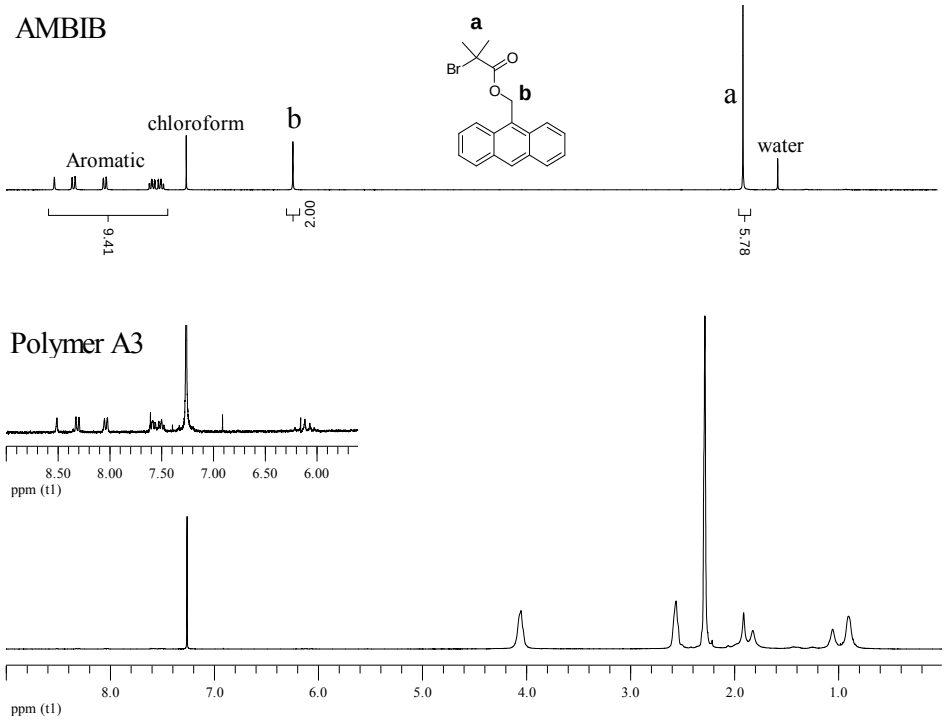

Figure 6.5. ^{1}H-NMR spectra of AMBIB and anthracene end-capped PDMAEMA A3 in $CDCl_3$.

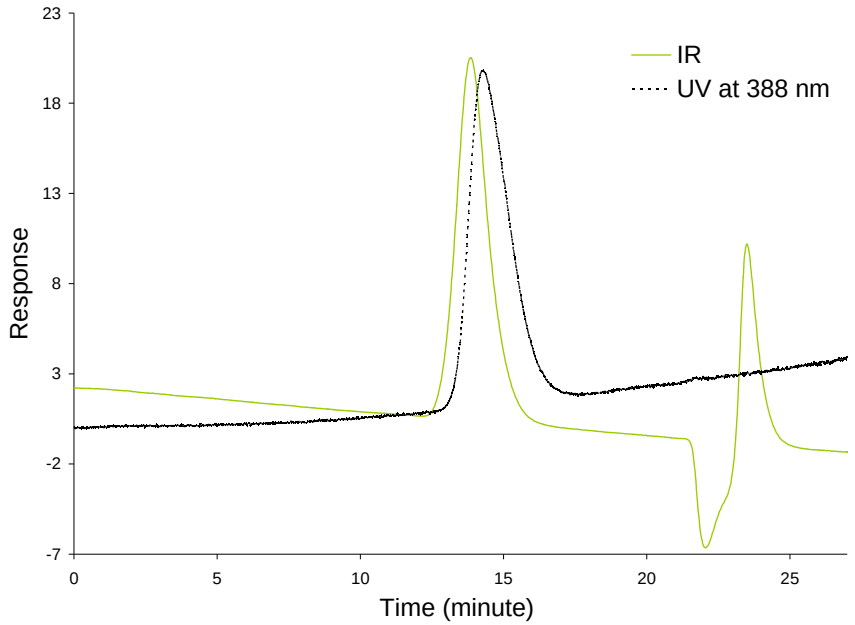

Figure 6.6. GPC traces (IR and UV detectors) of polymer A2.

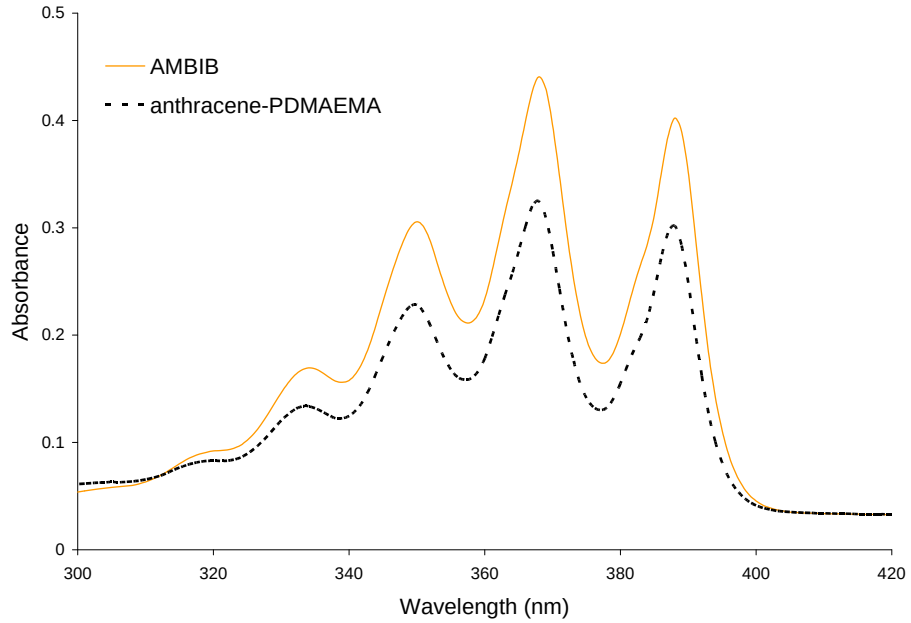

Figure 6.7. UV-Vis spectra of AMBIB and anthracene end-capped PDMAEMA A2 in chloroform: AMBIB (0.017 mg/mL = 0.074 mmol/L, solid line), polymer A2 (0.60 mg/mL, dashed line).

6.3.1.4 Synthesis of fluorescein-terminated PDMAEMA

A bifunctional fluorescein-based initiator for ATRP was obtained from a reaction of fluorescein and 2-bromoisobutyryl bromide in excess (Scheme 6.3). The presence of the two isobutyryl bromide groups was confirmed by the ratio of the integration of the CH_3 resonance at 2.07 ppm to that of Ar-H peaks at 6.87-8.07 ppm (12H to 10H) in ^{1}H-NMR spectrum (Figure 6.8 (top)), and the presence of 17 different carbons in ^{13}C-NMR spectrum (Figure 6.8 (bottom)). IR spectrum in Figure 6.9 shows an appearance of a C=O stretch at 1756 cm^{-1} and a disappearance of OH stretch at 3000 cm^{-1}. Different molecular weight fluorescein end-capped PDMAEMAs with low PDI were obtained, and are listed in Table 6.4. The incorporation of fluorescein group into the polymer chain was confirmed by ^{1}H-NMR.

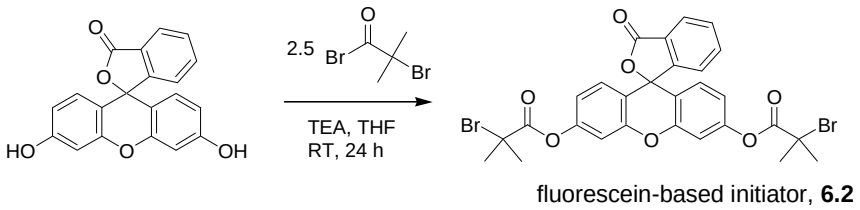

Scheme 6.3. Synthetic route to fluorescein-based ATRP initiator.

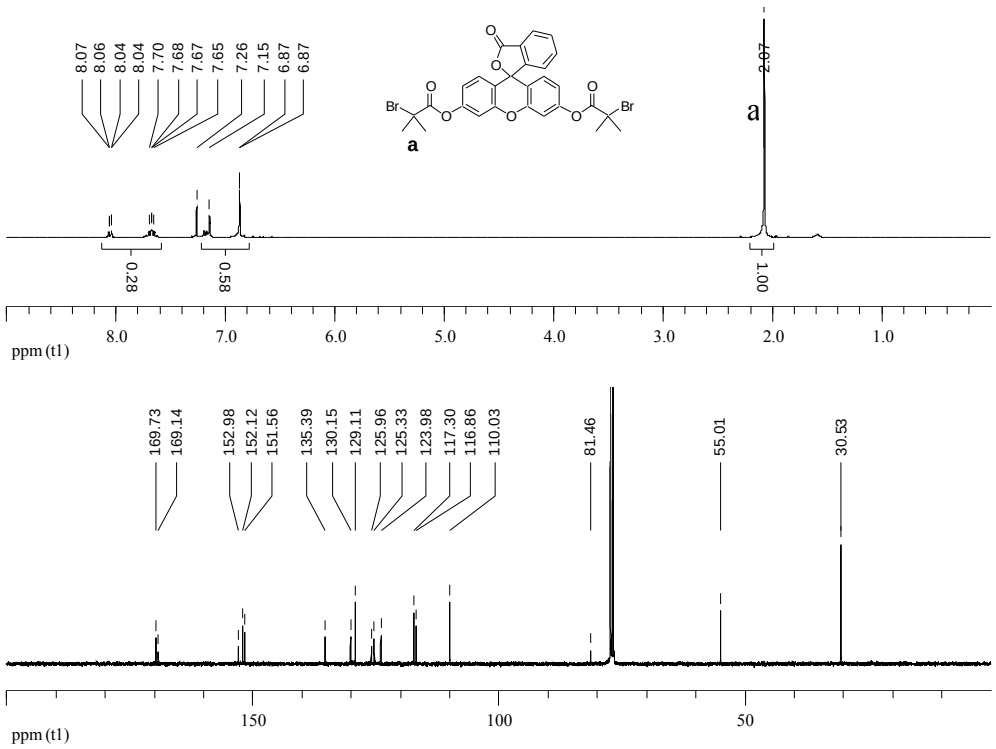

Figure 6.8. ^{1}H-NMR (top) and ^{13}C-NMR (bottom) spectra of fluorescein-based initiator.

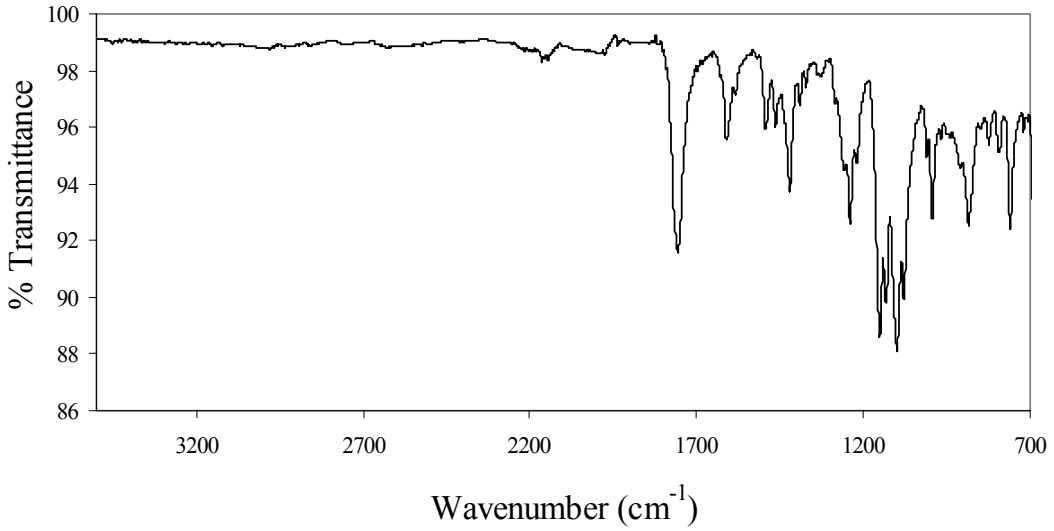

Figure 6.9. IR spectrum of fluorescein-based initiator.

Table 6.4. Molecular weights of fluorescein end-capped PDMAEMA.

Polymer	Solvent	Ligand	Rxn. time	% Conv.	$M_{n,cal}$[a]	$M_{n,GPC}$ (PDI)
F1	i-propanol	PMDETA	9 h	82	24,600	25,300 (1.21)
F2	i-propanol	HMTETA	9 h	86	25,800	26,900 (1.21)
F3	acetone	HMTETA	18.5 h	62	30,900	23,200 (1.16)
F4	acetone	HMTETA	18.5 h	64	9,600	6,800 (1.27)
F5	i-propanol	HMTETA	16 h	87	52,200	37,100 (1.19)

[a] $M_{n,cal}$ = (monomer mass (g) / mol of initiator) x (% conversion)

6.3.2 Ongoing collaborative work

6.3.2.1 The Santore group: adhesion study

6.3.2.1.1 Overview

The following work is being carried out by Surachate Kalasin, a graduate student in the Physics Department at the University of Massachusetts Amherst. PDMAEMA is deposited onto an acid-treated microscope slide via controlled flow deposition. Monodisperse silica particles with the size of 1 μm, purchased from GelTech, are used as model particles. The adhesion studies are employed in a steady shear flow chamber. The effect of flow rate on adhesion signatures, such as rolling, skipping, and arrest, are also studied. Near-Brewster reflectometry is used to track the total surface mass, and total internal reflectance fluorescence (TIRF) is used to measure the deposition of the fluorescent species. Particle motion are monitored with an optical microscopy.[5]

6.3.2.1.2 Preliminary results

PDMAEMAs (T1, T2, and T3) and PDMAEMA-co-PMMAs (Rco1, Rco2, and Rco3), with different molecular weights, are deposited onto acid-treated microscope slides via controlled flow deposition at a wall shear of 5 s^{-1}. The depositions are

monitored by Near-Brewster reflectometry, and are plotted in Figure 6.10. Similar to the noncompetitive adsorption kinetics of PEO reported earlier,[1] the polymer deposition rate depends on molecular weight, and it is inversely proportional to molecular weight. In the case of PEO, the adsorption kinetics has been described by the Leveque equation.

$$\frac{d\Gamma}{dt} = 0.538\left(\frac{\gamma}{L}\right)^{1/3} D^{2/3} C_b \qquad (1)$$

where γ is the wall shear rate, L is the lateral distance from the cell entrance to the point of observation, D is the diffusion coefficient of the adsorbing species, and C_b is the bulk solution concentration.

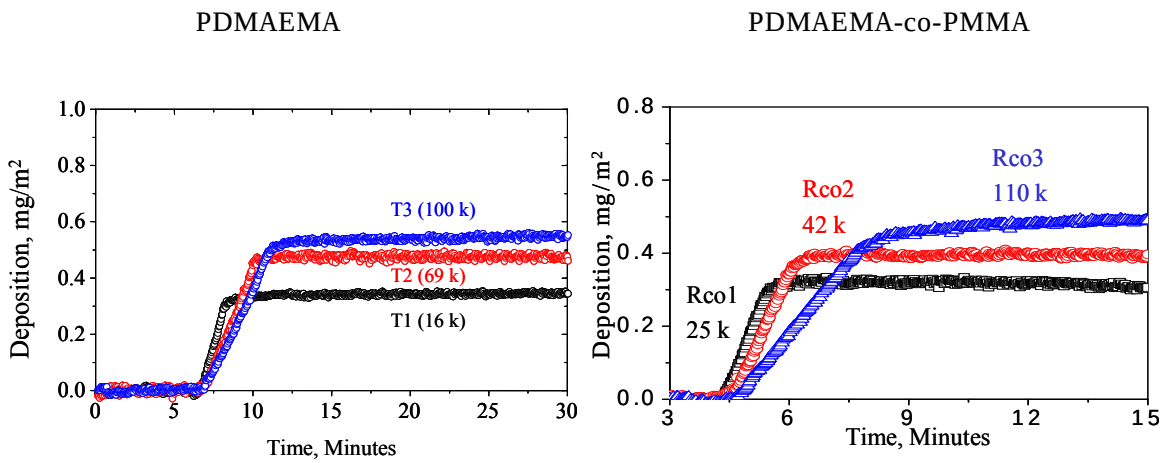

Figure 6.10. Plots of the deposition of the homopolymers (left) and the copolymers (right) onto acid-treated glass slides as a function of time.

Different percentages of positive patches are used as surfaces in the studies of the adhesion of 1 μm silica particles. The acid-treated glass slide was used as a reference, and no particle arresting on the surface was observed. On the other hand, when the polymer-deposited surfaces were used, the arresting was observed. The adhesion rates as a function of patch density of the homopolymers and the copolymers are shown in Figure 6.11. By varying the molecular weight, the adhesion threshold can be changed in both

systems, and it is observed that a number of patches for adhesion decreases with increasing molecular weight. In addition, the adhesion thresholds of the homopolymers are lower than those of the copolymers, suggesting the effect of charge density when the patchy size is fixed.

Although the trends look promising, it should be mentioned that the shear rate in the adhesion studies of silica particles onto the surfaces of PDMAEMA and PDMAEMA-co-PMMA were different (39 $s^{-1}$and 22 s^{-1}, respectively). A more systematic study, i.e. keeping all experimental parameters the same, on the effect of charge density on adhesion by comparing the homopolymers and copolymers, is in progress.

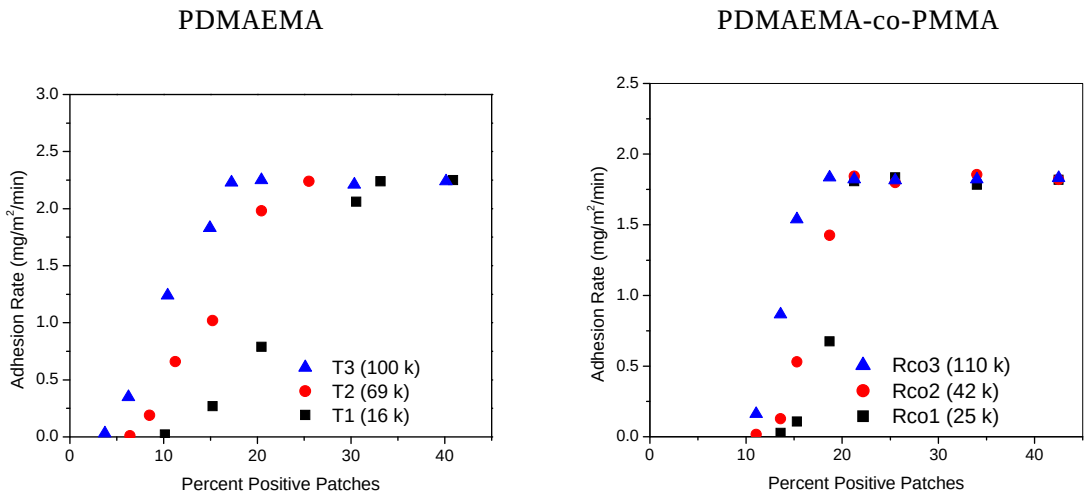

Figure 6.11. Adhesion rates of silica particles as a function of patch density of the homopolymers (shear rate 39 s^{-1}, left) and the copolymers (shear rate 22 s^{-1}, right).

6.3.2.2 The Davis group: system modeling

A fundamental, theoretical model of particle deposition, skipping, and rolling will be developed to account for the total hydrodynamic, electrostatic, and physicochemical

forces on the particles as they interact with patchy surfaces, in support of experiments in the Santore lab.

6.4 Summary and future outlook

Homopolymers of DMAEMA and copolymers of DMAEMA and MMA with narrow PDIs have been successfully synthesized via ATRP. Preliminary results on the adhesion study of 1-μm silica particles onto surfaces containing patches of these polycations reveal that particle adhesion depends on patchy size and cationic charge density. An interesting extension of this work would be to further increase the charge density by introducing multiple cations per repeat unit. Examples of these molecules are polyacrylates containing one, two, and three triazole group(s) reported in Chapter 3. The effects of surface morphology and chain extension on particle adhesion should also be explored. Block copolymers and triblock copolymers of cationic monomers can be synthesized by sequential ATRP using mono- and di-functionalized intiators, respectively. Chain extenders, such as poly(ethylene glycol), can be introduced to provide elasticity through a combination of ATRP and anionic polymerization. Besides positively charged patches, similar studies on hydrophobic patches would provide understanding on the effect of hydrophobic interactions on the adhesion.

6.5 References

1 Fu, Z. L.; Santore, M. M. *Langmuir* **1998**, 14, (15), 4300-4307.

2. Johnson, H. E.; Granick, S. *Science* **1992,** 255, (5047), 966-968.

3. Schneider, H. M.; Granick, S. *Macromolecules* **1992,** 25, (19), 5054-5059.

4. Shin, Y.; Roberts, J. E.; Santore, M. M. *Macromolecules* **2002,** 35, (10), 4090-4095.

5. Kozlova, N.; Santore, M. M. *Langmuir* **2006,** 22, (3), 1135-1142.

6. Santore, M. M.; Kozlova, N. *Langmuir* **2007,** 23, (9), 4782-4791.

7. Adamczyk, M.; Grote, J. *Bioorganic & Medicinal Chemistry Letters* **2003,** 13, (14), 2327-2330.

8. Chatterjee, U.; Jewrajka, S. K.; Mandal, B. M. *Polymer* **2005,** 46, (24), 10699-10708.

9. Zhang, H. Q.; Klumperman, B.; van der Linde, R. *Macromolecules* **2002,** 35, (6), 2261-2267.

10. Lu, X.; Zhang, L.; Meng, L.; Liu, Y. *Polymer Bulletin* **2007,** 59, (2), 195-206.

11. Lee, S. B.; Russell, A. J.; Matyjaszewski, K. *Biomacromolecules* **2003,** 4, (5), 1386-1393.

12. Bories-Azeau, X.; Armes, S. P. *Macromolecules* **2002,** 35, (27), 10241-10243.

BIBLIOGRAPHY

Adamczyk, M.; Grote, J. *Bioorganic & Medicinal Chemistry Letters* **2003**, 13, (14), 2327-2330.

Agmon, N. *Chemical Physics Letters* **1995**, 244, (5-6), 456-462.

Allcock, H. R.; Hofmann, M. A.; Ambler, C. M.; Lvov, S. N.; Zhou, X. Y. Y.; Chalkova, E.; Weston, J. *Journal of Membrane Science* **2002**, 201, (1-2), 47-54.

Bories-Azeau, X.; Armes, S. P. *Macromolecules* **2002**, 35, (27), 10241-10243.

Borup, R.; Meyers, J.; Pivovar, B.; Kim, Y. S.; Mukundan, R.; Garland, N.; Myers, D.; Wilson, M.; Garzon, F.; Wood, D.; Zelenay, P.; More, K.; Stroh, K.; Zawodzinski, T.; Boncella, J.; McGrath, J. E.; Inaba, M.; Miyatake, K.; Hori, M.; Ota, K.; Ogumi, Z.; Miyata, S.; Nishikata, A.; Siroma, Z.; Uchimoto, Y.; Yasuda, K.; Kimijima, K. I.; Iwashita, N. *Chemical Reviews* **2007**, 107, (10), 3904-3951.

Bouchet, R.; Miller, S.; Duclot, M.; Souquet, J. L. *Solid State Ionics* **2001**, 145, (1-4), 69-78.

Bourlinos, A. B.; Raman, K.; Herrera, R.; Zhang, Q.; Archer, L. A.; Giannelis, E. P. *Journal of the American Chemical Society* **2004**, 126, (47), 15358-15359.

Brown, E. G., *Ring Nitrogen and Key Biomolecules.* 1998; p 250 pp.

Calvo-Flores, F. G.; Isac-Garcia, J.; Hernandez-Mateo, F.; Perez-Balderas, F.; Calvo-Asin, J. A.; Sanchez-Vaquero, E.; Santoyo-Gonzalez, F. *Organic Letters* **2000**, 2, (16), 2499-2502.

Chatterjee, U.; Jewrajka, S. K.; Mandal, B. M. *Polymer* **2005**, 46, (24), 10699-10708.

Chuy, C.; Ding, J. F.; Swanson, E.; Holdcroft, S.; Horsfall, J.; Lovell, K. V. *Journal of the Electrochemical Society* **2003**, 150, (5), E271-E279.

Constable, G. S.; Lesser, A. J.; Coughlin, E. B. *Macromolecules* **2004**, 37, (4), 1276-1282.

Daniel, M. F.; Desbat, B.; Cruege, F.; Trinquet, O.; Lassegues, J. C. *Solid State Ionics* **1988**, 28, 637-641.

Ding, J. F.; Chuy, C.; Holdcroft, S. *Chemistry of Materials* **2001**, 13, (7), 2231-2233.

Donoso, P.; Gorecki, W.; Berthier, C.; Defendini, F.; Poinsignon, C.; Armand, M. B. *Solid State Ionics* **1988**, 28, 969-974.

Fujimura, M.; Hashimoto, T.; Kawai, H. *Macromolecules* **1981**, 14, (5), 1309-1315.

Fu, Z. L.; Santore, M. M. *Langmuir* **1998**, 14, (15), 4300-4307.

Gao, Y.; Robertson, G. P.; Guiver, M. D.; Jian, X. G. *Journal of Polymer Science Part A-Polymer Chemistry* **2003**, 41, (4), 497-507.

Gierke, T. D.; Hsu, W. Y. *ACS Symposium Series* **1982**, 180, 283-307.

Gierke, T. D.; Munn, G. E.; Wilson, F. C. *ACS Symposium Series* **1982**, 180, 195-216.

Gierke, T. D.; Munn, G. E.; Wilson, F. C. *Journal of Polymer Science, Part B: Polymer Physics* **1981**, 19, (11), 1687-1704.

Goward, G. R.; Schuster, M. F. H.; Sebastiani, D.; Schnell, I.; Spiess, H. W. *Journal of Physical Chemistry B* **2002**, 106, (36), 9322-9334.

Granados-Focil, S.; Woudenberg, R. C.; Yavuzcetin, O.; Tuominen, M. T.; Coughlin, E. B. *Macromolecules* **2007**, 40, (24), 8708-8713.

Grondin, J.; Rodriquez, D.; Lassegues, J. C. *Solid State Ionics* **1995**, 77, 70-75.

Guo, Q. H.; Pintauro, P. N.; Tang, H.; O'Connor, S. *Journal of Membrane Science* **1999**, 154, (2), 175-181.

Hartmann-Thompson, C.; Merrington, A.; Carver, P. I.; Keeley, D. L.; Rousseau, J. L.; Hucul, D.; Bruza, K. J.; Thomas, L. S.; Keinath, S. E.; Nowak, R. M.; Katona, D. M.; Santurri, P. R. *Journal of Applied Polymer Science* **2008**, 110, (2), 958-974.

Herz, H. G.; Kreuer, K. D.; Maier, J.; Scharfenberger, G.; Schuster, M. F. H.; Meyer, W. H. *Electrochimica Acta* **2003**, 48, (14-16), 2165-2171.

Herz, H. G.; Kreuer, K. D.; Maier, J.; Scharfenberger, G.; Schuster, M. F. H.; Meyer, W. H. *Electrochimica Acta* **2003**, 48, (14-16), 2165-2171.

Hickner, M. A.; Ghassemi, H.; Kim, Y. S.; Einsla, B. R.; McGrath, J. E. *Chemical Reviews* **2004**, 104, (10), 4587-4611.

Higami, M. Private communication.

Higami, M.; Woudenberg, R. C.; Granados-Focil, S.; Yavuzcetin, O.; Tuominen, M. T.; Coughlin, E. B. *PMSE Preprints* **2007**, 97, 551-552.

Himo, F.; Lovell, T.; Hilgraf, R.; Rostovtsev, V. V.; Noodleman, L.; Sharpless, K. B.; Fokin, V. V. *Journal of the American Chemical Society* **2005**, 127, (1), 210-216.

Hodgdon, R. B. *Journal of Polymer Science, Part A: Polymer Chemistry* **1968**, 6, (1PA1), 711-717.

Hsu, W. Y.; Gierke, T. D. *Journal of Membrane Science* **1983**, 13, (3), 307-326.

Hsu, W. Y.; Gierke, T. D. *Macromolecules* **1982**, 15, (1), 101-105.

Janik, M. J.; Davis, R. J.; Neurock, M. *Journal of Physical Chemistry B* **2004**, 108, (33), 12292-12300.

Jeon, H. G.; Mather, P. T.; Haddad, T. S. *Polymer International* **2000**, 49, (5), 453-457.

Johnson, H. E.; Granick, S. *Science* **1992**, 255, (5047), 966-968.

Joshi, M.; Butola, B. S. *Journal of Macromolecular Science-Polymer Reviews* **2004**, C44, (4), 389-410.

Kang, S. K.; Kim, K. J.; Hong, Y. T. *Angew. Chem. Int. Ed.* **2002**, 41, (9), 1584-1586.

Kerres, J. A. *Journal of Membrane Science* **2001**, 185, (1), 3-27.

Kobayashi, T.; Rikukawa, M.; Sanui, K.; Ogata, N. *Solid State Ionics* **1998**, 106, (3-4), 219-225.

Kolb, H. C.; Finn, M. G.; Sharpless, K. B. *Angewandte Chemie, International Edition in English* **2001**, 40, (11), 2004-2021.

Kopesky, E. T.; Haddad, T. S.; Cohen, R. E.; McKinley, G. H. *Macromolecules* **2004**, 37, (24), 8992-9004.

Kopitzke, R. W.; Linkous, C. A.; Nelson, G. L. *Journal of Polymer Science Part A-Polymer Chemistry* **1998**, 36, (7), 1197-1199.

Kozlova, N.; Santore, M. M. *Langmuir* **2006**, 22, (3), 1135-1142.

Kreuer, K. D. *Chemistry of Materials* **1996**, 8, (3), 610-641.

Kreuer, K. D., Technology and Applications. John Wiley & Sons Ltd: Chichester, U.K., **2003**; Vol. 3.

Kreuer, K. D. *Solid State Ionics* **1997**, 94, (1-4), 55-62.

Kreuer, K. D.; Fuchs, A.; Ise, M.; Spaeth, M.; Maier, *J. Electrochimica Acta* **1998**, 43, (10-11), 1281-1288.

Kreuer, K. D.; Paddison, S. J.; Spohr, E.; Schuster, M. *Chemical Reviews* **2004**, 104, (10), 4637-4678.

Kruczek, B.; Matsuura, T. *Journal of Membrane Science* **1998**, 146, (2), 263-275.

Lecolley, F.; Waterson, C.; Carmichael, A. J.; Mantovani, G.; Harrisson, S.; Chappell, H.; Limer, A.; Williams, P.; Ohno, K.; Haddleton, D. M. *Journal of Materials Chemistry* **2003**, 13, (11), 2689-2695.

Lee, S. B.; Russell, A. J.; Matyjaszewski, K. *Biomacromolecules* **2003**, 4, (5), 1386-1393.

Li, G. Z.; Wang, L. C.; Ni, H. L.; Pittman, C. U. *Journal of Inorganic and Organometallic Polymers* **2001**, 11, (3), 123-154.

Li, X. F.; Xu, D.; Zhang, G.; Wang, Z.; Zhao, C. J.; Na, H. *Journal of Applied Polymer Science* **2007**, 103, (6), 4020-4026.

Londono, J. D.; Davidson, R. V.; Mazur, S. *Abstracts of Papers of the American Chemical Society* **2001**, 222, 14-PMSE.

Loren, J. C., Krasinski, A., Fokin, V.V., Sharpless, K.B. *Synlett* **2005**, 18, 2847-2850.

Love, J. A.; Morgan, J. P.; Trnka, T. M.; Grubbs, R. H. *Angewandte Chemie-International Edition* **2002**, 41, (21), 4035-4037.

Lu, X.; Zhang, L.; Meng, L.; Liu, Y. *Polymer Bulletin* **2007**, 59, (2), 195-206.

Macdonald, J. R., *Impedance Spectroscopy*. In Wiley: New York, 2005; pp 16-20.

Martwiset, S.; Woudenberg, R. C.; Granados-Focil, S.; Yavuzcetin, O.; Tuominen, M. T.; Coughlin, E. B. *Solid State Ionics* **2007**, 178, (23-24), 1398-1403.

Martwiset, S.; Yavuzcetin, O.; Thorn, M.; Versek, C.; Tuominen, M.; Coughlin, E. B. *Journal of Polymer Science Part A: Polymer Chemistry* **2009**, 47, (1), 188-196.

Mauritz, K. A.; Moore, R. B. *Chemical Reviews* **2004**, 104, (10), 4535-4585.

Meng, Y. Z.; Tjong, S. C.; Hay, A. S.; Wang, S. J. *European Polymer Journal* **2003**, 39, (3), 627-631.

Miyatake, K.; Hay, A. S. *Journal of Polymer Science, Part A: Polymer Chemistry* **2001**, 39, (11), 1854-1859.

Miyatake, K.; Hay, A. S. *Journal of Polymer Science, Part A: Polymer Chemistry* **2001**, 39, (21), 3770-3779.

Munch, W.; Kreuer, K. D.; Silvestri, W.; Maier, J.; Seifert, G. *Solid State Ionics* **2001**, 145, (1-4), 437-443.

Noshay, A.; Robeson, L. M. *Journal of Applied Polymer Science* **1976**, 20, (7), 1885-1903.

Noto, V.; Lavina, S.; Negro, E.; Vittadello, M.; Conti, F.; Piga, M.; Pace, G. *Journal of Power Sources* **2009**, 187, (1), 57-66.

Page, K. A.; Landis, F. A.; Phillips, A. K.; Moore, R. B. *Macromolecules* **2006**, 39, (11), 3939-3946.

Persson, J. C.; Jannasch, P. *Chemistry of Materials* **2003**, 15, (16), 3044-3045.

Persson, J. C.; Jannasch, P. *Chemistry of Materials* **2006**, 18, (13), 3096-3102.

Persson, J. C.; Jannasch, P. *Solid State Ionics* **2006**, 177, (7-8), 653-658.

Phillips, S. H.; Haddad, T. S.; Tomczak, S. J. *Current Opinion in Solid State & Materials Science* **2004**, 8, (1), 21-29.

Przyluski, J.; Dabrowska, A.; Stys, S.; Wieczorek, W. *Solid State Ionics* **1993**, 60, (1-3), 141-146.

Pu, H.; Wu, J.; Wan, D.; Chang, Z. *Journal of Membrane Science* **2008**, 322, (2), 392-399.

Pu, H.; Qin, S.; Yang, Z.; Wan, D.; Yuan, J. *Gongneng Cailiao* **2007**, 38, (9), 1499-1502,1506.

Ratner, M. A., *In Polymer Electrolyte Reviews*, Elsevier Applied Science: New York, 1987; pp 173-235.

Rikukawa, M.; Sanui, K. *Progress in Polymer Science* **2000**, 25, (10), 1463-1502.

Roche, E. J.; Pineri, M.; Duplessix, R. *Journal of Polymer Science, Part B: Polymer Physics* **1982**, 20, (1), 107-116.

Roche, E. J.; Pineri, M.; Duplessix, R.; Levelut, A. M. *Journal of Polymer Science, Part B: Polymer Physics* **1981**, 19, (1), 1-11.

Rostovtsev, V. V.; Green, L. G.; Fokin, V. V.; Sharpless, K. B. *Angewandte Chemie, International Edition in English* **2002**, 41, (14), 2596-2599.

Rusanov, A. L., Likhatchev, D.Y., Mullen, K. *Russian Chem. Rev*. **2002**, 71, (9), 761-774.

Sanghi, S.; Coughlin, E. B. Private communication.

Santore, M. M.; Kozlova, N. *Langmuir* **2007**, 23, (9), 4782-4791.

Sari, H.; Covington, A. K. *Journal of Chemical and Engineering Data* **2005**, 50, (4), 1425-1429.

Savadogo, O. *Journal of New Materials for Electrochemical Systems* **1998**, 1, (1), 47-66.

Scharfenberger, G.; Meyer, W. H.; Wegner, G.; Schuster, M.; Kreuer, K. D.; Maier, J. *Fuel Cells* **2006**, 6, (3-4), 237-250.

Schmidt-Naake, G.; Bohme, M.; Cabrera, A. *Chemical Engineering and Technology* **2005**, 28, (6), 720-724.

Schmidt-Rohr, K.; Chen, Q. *Nature Materials* **2008**, 7, (1), 75-83.

Schneider, H. M.; Granick, S. *Macromolecules* **1992**, 25, (19), 5054-5059.

Schuster, M. E.; Meyer, W. H. *Annual Review of Materials Research* **2003,** 33, 233-261.

Schuster, M. F. H.; Meyer, W. H.; Schuster, M.; Kreuer, K. D. *Chemistry of Materials* **2004**, 16, (2), 329-337.

Schuster, M.; Meyer, W. H.; Wegner, G.; Herz, H. G.; Ise, M.; Schuster, M.; Kreuer, K. D.; Maier, J. *Solid State Ionics* **2001**, 145, (1-4), 85-92.

Schuster, M.; Rager, T.; Noda, A.; Kreuer, K. D.; Maier, J. *Fuel Cells* **2005**, 5, (3), 355-365.

Serpico, J. M.; Ehrenberg, S. G.; Fontanella, J. J.; Jiao, X.; Perahia, D.; McGrady, K. A.; Sanders, E. H.; Kellogg, G. E.; Wnek, G. E. *Macromolecules* **2002**, 35, (15), 5916-5921.

Seurer, B.; Coughlin, E. B. *Macromolecular Chemistry and Physics* **2008**, 209, (12), 1198-1209.

Seurer, B.; Coughlin, E. B. *Macromolecular Chemistry and Physics* **2008**, 209, (19), 2040-2048.

Shin, B. G.; Cho, T. Y.; Yoon, D. Y.; Liu, B. Y. *Macromolecular Research* 2007, 15, (2), 185-190.

Shin, Y.; Roberts, J. E.; Santore, M. M. *Macromolecules* **2002**, 35, (10), 4090-4095.

Steele, B. C. H.; Heinzel, A. *Nature* **2001**, 414, (6861), 345-352.

Steininger, H.; Schuster, M.; Kreuer, K. D.; Maier, J. *Solid State Ionics* **2006**, 177, (26-32), 2457-2462.

Subbaraman, R., Ghassemi, H., Zawodzinski, T.A. *Journal of the American Chemical Society* **2007**, 129, (8), 2238-2239.

Sun, X. G.; Kerr, J. B. *Macromolecules* **2006**, 39, (1), 362-372.

Tabacchi, G.; Gianotti, E.; Fois, E.; Martra, G.; Marchese, L.; Coluccia, S.; Gamba, A. *Journal of Physical Chemistry C* **2007**, 111, (13), 4946-4955.

Tanaka, R.; Yammoto, H.; Kawamura, S.; Iwase, T. *Electrochimica Acta* **1995**, 40, (13-14), 2421-2424.

Thibault, R. J.; Takizawa, K.; Lowenheilm, P.; Helms, B.; Mynar, J. L.; Frechet, J. M. J.; Hawker, C. J. *Journal of the American Chemical Society* **2006**, 128, (37), 12084-12085.

Van der Heijden, P. C.; Rubatat, L.; Diat, O. *Macromolecules* **2004**, 37, (14), 5327-5336.

Victoria D. Bock; Henk Hiemstra; Maarseveen, J. H. v. *European Journal of Organic Chemistry* **2006**, 1, 51-68.

Wainright, J. S.; Wang, J. T.; Weng, D.; Savinell, R. F.; Litt, M. *Journal of the Electrochemical Society* **1995**, 142, (7), L121-L123.

Wang, F.; Hickner, M.; Kim, Y. S.; Zawodzinski, T. A.; McGrath, J. E. *Journal of Membrane Science* **2002**, 197, (1-2), 231-242.

Wei, J.; Stone, C.; Steck, A. E., of Ballard Power Systems, Inc., June 6, 1995; U.S. Patent 5,422,411.

Whittingham, M. S.; Savinell, R. F.; Zawodzinski, T. *Chemical Reviews* **2004**, 104, (10), 4243-4244.

Woudenberg, R. C. Doctoral Thesis. University of Massachusetts, Amherst, MA, 2007.

Woudenberg, R. C.; Yavuzcetin, O.; Tuominen, M.; Coughlin, E. B. *Solid State Ionics* **2007**, 178, 1135-1141.

Wycisk, R.; Pintauro, P. N. *Journal of Membrane Science* **1996**, 119, (1), 155-160.

Xu, H. Y.; Kuo, S. W.; Lee, J. S.; Chang, F. C. *Macromolecules* **2002**, 35, (23), 8788-8793.

Yamada, M.; Honma, I. *Journal of Physical Chemistry B* **2006**, 110, (41), 20486-20490.

Zhang, H. Q.; Klumperman, B.; van der Linde, R. *Macromolecules* **2002**, 35, (6), 2261-2267.

Zhang, M. J.; Flynn, D. L.; Hanson, P. R. *Journal of Organic Chemistry* **2007**, 72, (9), 3194-3198.

Zheng, L.; Farris, R. J.; Coughlin, E. B. *Journal of Polymer Science Part A-Polymer Chemistry* **2001**, 39, (17), 2920-2928.

Zheng, L.; Kasi, R. M.; Farris, R. J.; Coughlin, E. B. *Journal of Polymer Science Part A-Polymer Chemistry* **2002**, 40, (7), 885-891.

Zhou, Z.; Li, S. W.; Zhang, Y. L.; Liu, M. L.; Li, W. *Journal of the American Chemical Society* **2005**, 127, (31), 10824-10825.

Zhou, Z.; Liu, R.; Wang, J. H.; Li, S. W.; Liu, M. L.; Bredas, J. L. *Journal of Physical Chemistry A* **2006**, 110, (7), 2322-2324.